PLANE-STRAIN VISIOPLASTICITY FOR DYNAMIC AND QUASI-STATIC DEFORMATION PROCESSES

by

SURENDRA NATH DWIVEDI

M.E., University of Roorkee, 1971

A THESIS SUBMITTED IN PARTIAL FULFILLMENT OF
THE REQUIREMENTS FOR THE DEGREE OF
MASTER OF APPLIED SCIENCE

in

THE FACULTY OF GRADUATE STUDIES

(Department of Mechanical Engineering)

We accept this thesis as conforming
to the required standard

THE UNIVERSITY OF BRITISH COLUMBIA

November, 1978

Department of Mechanical Engineering
The University of British Columbia
2075 Wesbrook Place
Vancouver, B.C., Canada
V6T 1W5

Date: 30/11/78

ABSTRACT

The visioplasticity approach is developed to enable the complete stress history of any steady or non-steady, quasi-static or impact, plane strain plastic deformation process to be determined from a record of the deformation pattern. The velocity field is determined experimentally and for dynamic conditions high speed photographs are taken of a grid pattern marked on the end surface of the specimen. Digitization of the instantaneous grid node positions allows the velocity fields to be obtained at predetermined time intervals throughout the transient deformation period. Hence, the strain-rate, equivalent strain rate, equivalent strain and finally stress fields can all be obtained.

A three dimensional surface fitting procedure, using fourth order polynomials, is used to smooth the scalar component of the experimentally determined velocity field. The condition of continuity ($\dot{\varepsilon}_x=-\dot{\varepsilon}_y$ for plane strain) is imposed on both surfaces thereby reducing the number of independent parameters from 30 to 10. Besides smoothing the experimental points this procedure has the distinct advantage that the polynomials can be readily differentiated for determining strain-rates and that deformation can be referred to a master reference grid that is fixed with respect to time.

Plane-strain upsetting tests, conducted at a speed of 0.02 ft/min give results that agree closely with the well docu-

mented 'friction hill' type of normal stress distribution for quasi-static rates of strain. However, with the specimen deformed at a speed of 15.7 ft/sec the normal stress distribution is radically different exhibiting a saddle type distribution. The effect of strain rate on the interface and body stresses will have significant bearing on a number of metal forming operations.

ACKNOWLEDGEMENTS

The author sincerely thanks the thesis supervisor, Professor G.W. Vickers for his unending words of encouragement and whose amiable attitude made this work a pleasant experience.

Sincere thanks must also go to the other members of the thesis committee i.e., Professor H. Ramsey, I.S. Gartshore, N.G. Ely, R.E. McKechnie and Norman Franz for their time to time fruitful discussions and expert opinions.

The author is most grateful to all the other members of the department for their inspiring interest and assistance.

Thanks are also due to my wife Shashi for some typing help and for her moral support.

Above all, I thank God for giving me the opportunity to better myself academically and spirtually during the course of the research.

TABLE OF CONTENTS

Page

LIST OF FIGURES

Page

NOMENCLATURE

μ	the component of velocity in x-direction
v	the component of velocity in y-direction
w	the component of velocity in z-direction
$\dot{\varepsilon}_x$	strain rate along x-direction
$\dot{\varepsilon}_y$	strain rate along y-direction
$\dot{\gamma}_{xy}$	shear strain-rate
$\dot{\bar{\varepsilon}}$	effective strain-rate
$\bar{\varepsilon}$	total effective strain
$\bar{\sigma}$	effective stress
σ_x	normal stress along x-direction
σ_y	normal stress along y-direction
σ_z	normal stress along z-direction
τ_{xy}	shear stress
ρ	the density of the material
V	the volume of the plastically deforming body
$\dot{\varepsilon}_v$	volumetric strain-rate
$\tilde{F}$	the traction on the part of surface S_F
$\tilde{U}$	the velocity presented on the remainder surface S_U
λ	Lagrange multiplier
α	the penalty function
$\emptyset$	the angle made by the driving arm with vertical

C H A P T E R   O N E

INTRODUCTION

&

LITERATURE SURVEY

CHAPTER ONE

INTRODUCTION

The mechanism of plastic deformation plays a vital role in many industrial metal-working processes. However, it has not proved possible to analyse completely many of these processes using the general basic equations derived from the theory of plasticity. This is primarily due to unclearly defined boundary conditions; for example, the actual frictional conditions present at the metal-die interface are frequently unknown.

Many simplified alternative methods have been developed and used to study certain of the metal forming process. In these analyses certain assumptions and simplifications are made regarding the processes and the behaviour of the materials during deformation. However, in spite of these idealizations the solutions often lack uniqueness and completeness.

One approach called visioplasticity has been used with some success to determine the complete stress picture throughout the deformation zone in certain steady-state extrusion and forging operations. It requires that the velocity field be determined experimentally and hence the strain-rates and finally stress fields can all be obtained. This method has been shown to give realistic solutions and its application has been extended during the last decade.

In this work the visioplasticity approach has been used to study material deformation in dynamic and non-steady conditions. The relevant equations and procedure have been embodied into a specially developed computer program, so that the complete stress history of any steady or non-steady, quasi-static or impact plane strain, deformation can be determined from a record of the deformation pattern. Special attention has been given in this work to smoothing the experimentally determined velocity fields, a point which has caused some difficulty in the past. Results from this work have been suitably compared with previous steady-state results for verification purposes.

1.1. PLASTICITY IN METAL-WORKING

While the analyses of metal-working processes has been restricted by the complexities involved, some approaches have been made. A number of these in common use are the slab (or equilibrium) method, uniform deformation energy method, slip line solutions, upper and lower bound solutions, finite difference and finite element methods. For completeness a brief description of these common approaches is given below.

1.1.1. Slab or Equilibrium Method.

The method introduced by Sachs (1) in 1931, consists of isolating a small elemental volume of the material undergoing deformation and observing the behaviour of this element as it moves through the working zone. Since this element is an integral part of the material, it should always be in a state of equilibrium. The assumption is made that stresses on a plane surface perpendicular to the direction of the flow are principal stresses and that these do not vary on this plane.

Analysis of the equilibrium condition results in one or more differential equations which together with the necessary boundary conditions, give the deformation stresses.

Since the effect of redundancy, friction and pattern of flow are not considered, this method gives an underestimate of the deformation stresses. However, the analysis is straightforward and it has been widely used in wire and tube drawing problems as well as hot and cold rolling of strip and sheet (1).

1.1.2. Uniform Deformation Energy Method:

Siebel (2) proposed this approach in 1932 in which the amount of deformation is determined by considering the shape of an element of material before and after deformation. It hence gives only the average forming pressure as a function of specific internal energy and is generally used for steady-state metal-working processes.

1.1.3. Slip Line Method:

Hencky(3) introduced the slip line theory in 1923. It can be used for determining the local stress and velocity distribution during deformation, although it is restricted to plane strain conditions and requires a predetermined pattern of flow.

The slip line solution consists of families of curvilinear or straight lines, which are perpendicular to each other and correspond to the directions of maximum and minimum constant shear stress. These lines satisfy the static equilibrium condition, yield condition and the pattern of flow everywhere in the plastic zone of the material. These shear or slip lines are known as characteristics of the differential equations of equilibrium. In the slip line method the forming tool and the material outside the slip line are considered as rigid (i.e. the metal ahead and behind the plastic zones and the tool material have an infinite modulus of elasticity). The slip line solution is not optimal or unique and also gives values higher than the true solution.

This method has been widely used for the study of many metal deformation processes (4-14), some of the latest work has involved slip line solutions for anisotropic materials (15, 16) and has taken account of friction on the die-workpiece interface (17, 18). Also Ewing (19) and later Collins (20) have produced slip line solution using numerical computation by power series and by matrix operational methods.

1.1.4. Limit Analysis:

The mathematical model of limit analysis places upper and lower estimates on the load required for deformation. This limit analysis is based on two extremum theorems put forward by Prager and Hodge (8), and Drucher and Prager (21). Hill (7) gave the mathematical proof of these theorems, which are based on the assumption that the material is rigid and perfectly plastic. They can be stated as:

a) Upper Bound Theorem. If a kinematically admissible velocity field exists, the loads required to be applied to cause the velocity field to operate constitute an upper bound solution.

b) Lower Bound Theorem. If a statically admissible stress field exists such that the stresses are everywhere just below those necessary to cause yielding, then the loads associated with that field constitute a lower bound solution.

These techniques have been used extensively (22-39) to study metal-working processes, such as forging, extrusion, wire drawing and tube drawing.

1.1.5. Finite Element Method:

The finite element method is one of the most powerful techniques for solving two dimensional problems in metal-working but at present has a limited potential for complex problems due to economic constraints. This method was introduced by Argyris (40) in 1954. In this approach, the deforming area or continuum is subdivided into an equivalent system of elements, known as finite elements. The finite elements may be triangles, group of triangles, quadrilateral etc. for two dimensional studies and tetrahedra, rectangular prisms or hexahedra etc. for three dimensional studies. Once a displacement model is selected, an element stiffness matrix is derived using variational principles. The algebraic equations for the whole continuum are then assembled and solutions for unknown displacements at the nodal points can be obtained. By use of the computed displacements and the stress and strain relations, the stresses at the nodal points may be determined. The solution is based on extremum principle according to which the actual solution minimizes the functional ϕ , where

$$\phi = \int \bar{\sigma} \; \dot{\bar{\varepsilon}} \, dV - \int_{S_F} \tilde{F} \cdot \tilde{\mu} \, dS$$

with the constraint that

$$\dot{\varepsilon}_V = 0$$

where V = volume of the plastically deforming body

$\bar{\sigma}$ = effective stress

$\dot{\bar{\varepsilon}}$ = effective strain rate

$\dot{\varepsilon}_V$ = volumetric strain rate

$\tilde{F}$ = the traction of the part of surface S_F

and $\tilde{u}$ = the velocity prescribed on the remainder surface S_u

A modified functional has been given by Lee & Kobayashi (41) using the Lagrange multiplier so that

$$\phi = \int_V \bar{\sigma}\,\dot{\bar{\varepsilon}}\,dV + \int_V \lambda\,\dot{\varepsilon}_V\,dV - \int_{S_F} \tilde{F}\cdot\tilde{u}\,dS$$

where λ = the Lagrange multiplier. While Godbole and Zienkiewicz (42) have suggested that the functional be modified using a penalty function, α, as follows:

$$\phi = \int_V \bar{\sigma}\,\dot{\bar{\varepsilon}}\,dV + \int \frac{\alpha}{2}\,(\dot{\varepsilon}_V)^2\,dV - \int_{S_F} \tilde{F}\cdot\tilde{u}\,dS$$

where α = very large number.

By use of above functionals, many metal-working processes such as upsetting drawing, piercing etc. (40-57) have been studied.

1.1.6. <u>Finite Difference Method</u>:

This method is one of the most recent techniques to be used for the study of metal-working processes. It requires that the continuum be divided into a number of grids and that 'difference' (i.e. finite) quantities are substituted for differential quantities across the grids. Thus for a given differential equation with boundary conditions a set of simultaneous equations can be substituted, which can be solved numerically using a computer. The size of the grid spacing determines the accuracy of the solution. The finer the grid, the better is the accuracy obtained, but this at the expense of computer cost.

Studies which describe the application of this technique to forging, extrusion and sheet-metal processes are given in references (58-64).

1.2. VISIOPLASTICITY

The visioplasticity was introduced by Thomsen (56, 66, 67) and later developed and extended by Shabaik, Kobayashi et al. (68, 69, 70, 71, 72). In this method, the grid line patterns are photographed for each incremental step of deformation and thus the movement of grid points can be determined. From enlarged photographs of consecutive grid patterns the instantaneous velocities of all grid node across the surfaces can be found. The strains, strain rates, total effective strain can thus be determined for all points in the deformation region and finally the stress field and forming loads may be found.

In this method the instantaneous flow field is an actual one and gives information of all strains and stresses over the entire deformation region. It may be used for both work-hardening and non-workhardening materials.

Details of the basic equations used in visioplasticity are given in the next chapter.

The visioplasticity method has been applied to forging and axisymmetric and plane strain extrusion and rolling processes. (Reference 68 to 76). Recently it has been used for investigating the relationship between strain and microhardness (77), crack propagation and for the derivation of criteria for ductile rupture of fully plastic notched bars (78).

C H A P T E R   T W O

NON-STEADY PLANE-STRAIN DYNAMIC AND QUASI-STATIC VISIOPLASTICITY

CHAPTER TWO

NON-STEADY PLANE-STRAIN DYNAMIC AND QUASI-STATIC VISIOPLASTICITY

2.1. EQUATIONS FOR QUASI-STATIC VISIOPLASTICITY

2.1.1 Equations for Three Dimensional Non Steady State Quasi-static Visioplasticity

The following equations in three dimensions are used to describe the mechanism of plastic deformation of an isotropic solid.

The strain rate $\dot{\varepsilon}_x$, $\dot{\varepsilon}_y$, $\dot{\gamma}_{xy}$ can be given terms of velocity components as follows:

$$\dot{\varepsilon}_x = \frac{\partial u}{\partial x}, \qquad \dot{\varepsilon}_y = \frac{\partial v}{\partial y}, \qquad \dot{\varepsilon}_z = \frac{\partial w}{\partial z};$$

$$\dot{\gamma}_{xy} = \frac{\partial u}{\partial y} + \frac{\partial v}{\partial x}, \qquad \dot{\gamma}_{yz} = \frac{\partial w}{\partial y} + \frac{\partial v}{\partial z} \text{ and}$$

$$\dot{\gamma}_{zx} = \frac{\partial u}{\partial z} + \frac{\partial w}{\partial x} \tag{2.1}$$

where u, v, w are the components of velocity in the x, y and z directions respectively. The equations of static equilibrium, neglecting all body forces are:

$$\frac{\partial \sigma_x}{\partial x} + \frac{\partial \tau_{xy}}{\partial y} + \frac{\partial \tau_{xz}}{\partial z} = 0$$

$$\frac{\partial \tau_{xy}}{\partial x} + \frac{\partial \sigma_y}{\partial y} + \frac{\partial \tau_{yz}}{\partial z} = 0$$

$$\frac{\partial \tau_{xz}}{\partial x} + \frac{\partial \tau_{yz}}{\partial y} + \frac{\partial \sigma_z}{\partial z} = 0$$

The Levy-Von Mises stress and strain rate relationships (or flow rule) is given by

$$\frac{\dot{\varepsilon}_x}{\sigma_x + p} = \frac{\dot{\varepsilon}_y}{\sigma_y + p} = \frac{\dot{\varepsilon}_z}{\sigma_z + p} = \frac{\dot{\gamma}_{xy}}{2\tau_{xy}} = \frac{\dot{\gamma}_{yz}}{2\tau_{yz}} = \frac{\dot{\gamma}_{zx}}{2\tau_{zx}} = \dot{\lambda} \qquad (2.3)$$

where $p = -\frac{1}{3}(\sigma_x + \sigma_y + \sigma_z)$,

$\dot{\lambda} = \frac{3}{2}\left[\frac{\dot{\bar{\varepsilon}}}{\bar{\sigma}}\right]$,

$\dot{\bar{\varepsilon}}$ = effective strain rate, and

$\bar{\sigma}$ = effective stress.

The Von Mises yield condition is

$$(\sigma_x - \sigma_y)^2 + (\sigma_y - \sigma_z)^2 + (\sigma_z - \sigma_x)^2 + 6(\tau_{xy}^2 + \tau_{zy}^2 + \tau_{zx}^2) = 2\bar{\sigma}^2 \qquad (2.4)$$

The above equation (2.4) can be expressed in terms of principal stresses σ_1, σ_2 and σ_3 as

$$(\sigma_1 - \sigma_2)^2 + (\sigma_2 - \sigma_3)^2 + (\sigma_3 - \sigma_1)^2 = 2\bar{\sigma}^2$$

where $\bar{\sigma}$ = effective stress, which is constant for perfectly plastic materials

$\bar{\sigma} = \bar{\sigma}(\dot{\bar{\varepsilon}})$, for non-workhardening plastic material

$\bar{\sigma} = \bar{\sigma}(\bar{\varepsilon})$, for workhardening plastic material

$\bar{\sigma} = (\bar{\varepsilon}, \dot{\bar{\varepsilon}}, T)$, for material which is affected by strain rate, strain and temperature.

From equation (2.3), we may write

$$\dot{\varepsilon}_x = \frac{3\dot{\bar{\varepsilon}}}{2\bar{\sigma}} (\sigma_x + p) = \dot{\lambda}(\sigma_x + p)$$

$$\dot{\varepsilon}_y = \frac{3\dot{\bar{\varepsilon}}}{2\bar{\sigma}} (\sigma_y + p) = \dot{\lambda}(\sigma_y + p)$$

$$\dot{\varepsilon}_z = \frac{3\dot{\bar{\varepsilon}}}{2\bar{\sigma}} (\sigma_z + p) = \dot{\lambda}(\sigma_z + p)$$

$$\dot{\gamma}_{xy} = \frac{3\dot{\bar{\varepsilon}}}{2\bar{\sigma}} 2\tau_{xy} = 2\dot{\lambda}\tau_{xy}$$

$$\dot{\gamma}_{yz} \; 3\frac{\dot{\bar{\varepsilon}}}{\bar{\sigma}} \tau_{yz} = 2\dot{\lambda}\tau_{yz}$$

$$\dot{\gamma}_{zx} = 3\frac{\dot{\bar{\varepsilon}}}{\bar{\sigma}} \tau_{zx} = 2\dot{\lambda}\tau_{zx} \tag{2.5}$$

Now subtracting the second equation (2.5) from first equation (2.5) gives

$$\dot{\varepsilon}_x - \dot{\varepsilon}_y = \frac{3\dot{\bar{\varepsilon}}}{2\bar{\sigma}} (\sigma_x - \sigma_y)$$

and similarly for the other equations (2.5)

$$\dot{\varepsilon}_y - \dot{\varepsilon}_z = \frac{3\dot{\bar{\varepsilon}}}{2\bar{\sigma}} (\sigma_y - \sigma_z)$$

$$\dot{\varepsilon}_z - \dot{\varepsilon}_x = \frac{3\dot{\varepsilon}}{2\bar{\sigma}} (\sigma_z - \sigma_x)$$

$$\sqrt{\frac{3}{2}}\dot{\gamma}_{xy} = \frac{3\dot{\varepsilon}}{2\bar{\sigma}} \times 2\tau_{xy}\sqrt{\frac{3}{2}}$$

$$\sqrt{\frac{3}{2}}\dot{\gamma}_{yz} = \frac{3\dot{\varepsilon}}{2\bar{\sigma}} \times 2\tau_{yz}\sqrt{\frac{3}{2}}$$

$$\sqrt{\frac{3}{2}}\dot{\gamma}_{zx} = \frac{3\dot{\bar{\varepsilon}}}{2\bar{\sigma}} \times 2\tau_{zx}\sqrt{\frac{3}{2}} \tag{2.6}$$

Squaring the left hand side and right hand side of all the equations (2.6) and adding, we get

$$(\dot{\varepsilon}_x - \dot{\varepsilon}_y)^2 + (\dot{\varepsilon}_y - \dot{\varepsilon}_z)^2 + (\dot{\varepsilon}_z - \dot{\varepsilon}_x)^2 + \frac{3}{2}(\dot{\gamma}_{xy}{}^2 + \dot{\gamma}_{yz}{}^2 + \dot{\gamma}_{zx}{}^2)$$

$$= \left(\frac{3}{2}\frac{\dot{\bar\varepsilon}}{\bar\sigma}\right)^2 \left\{(\sigma_x - \sigma_y)^2 + (\sigma_y - \sigma_z)^2 + (\sigma_z - \sigma_x)^2 + 6\tau_{xy}^2 + 6\tau_{yz}^2 + 6\tau_{zx}^2\right\} \tag{2.7}$$

Combining equation (2.4) and (2.7) gives

$$(\dot\varepsilon_x - \dot\varepsilon_y)^2 + (\dot\varepsilon_y - \dot\varepsilon_z)^2 + (\dot\varepsilon_z - \dot\varepsilon_x)^2 + \frac{3}{2}(\dot\gamma_{xy}^2 + \dot\gamma_{yz}^2 + \dot\gamma_{zx}^2)$$

$$= \left[\frac{3\dot{\bar\varepsilon}}{2\bar\sigma}\right]^2 \times 2\bar\sigma^2 = \frac{9}{2}\dot{\bar\varepsilon}^2$$

So that the equivalent strain rate may be given as

$$\dot{\bar\varepsilon} = \left[\sqrt{\frac{2}{9}}\left\{(\dot\varepsilon_x - \dot\varepsilon_y)^2 + (\dot\varepsilon_y - \dot\varepsilon_z)^2 + (\dot\varepsilon_z - \dot\varepsilon_x)^2 + \frac{3}{2}\left(\dot\gamma_{xy}^2 + \dot\gamma_{yz}^2 + \dot\gamma_{zx}^2\right)\right\}\right]^{\frac{1}{2}}$$

$$= \left[\frac{4}{9}\left\{\frac{(\dot\varepsilon_x - \dot\varepsilon_y)^2 + (\dot\varepsilon_y - \dot\varepsilon_z)^2 + (\dot\varepsilon_z - \dot\varepsilon_x)^2}{2} + \frac{3}{4}(\dot\gamma_{xy}^2 + \dot\gamma_{yz}^2 + \dot\gamma_{zx}^2)\right\}\right]^{\frac{1}{2}}$$

$$= \frac{2}{3}\left[\frac{(\dot\varepsilon_x - \dot\varepsilon_y)^2 + (\dot\varepsilon_y - \dot\varepsilon_z)^2 + (\dot\varepsilon_z - \dot\varepsilon_x)^2}{2} + \frac{3}{4}\left(\dot\gamma_{xy}^2 + \dot\gamma_{yz}^2 + \dot\gamma_{zx}^2\right)\right]^{\frac{1}{2}} \tag{2.8}$$

2.1.2. Equations for Plane Strain Non-Steady State Quasi-Static Visioplasticity

For the plane strain condition, ε_z, $\dot\varepsilon_z$, γ_{yz}, γ_{zx}, $\dot\gamma_{yz}$, $\dot\gamma_{zx}$, τ_{yz} and $\tau_{zx} = 0$, also $\mu = \frac{1}{2}$ (for a rigid perfectly plastic material). Hence the basic equations for plane strain are given as follows: (2.9)

The equation for static equilibrium from equation (2.2) is

$$\frac{\partial\sigma_x}{\partial x} + \frac{\partial\tau_{xy}}{\partial y} = 0$$

$$\frac{\partial\tau_{xy}}{\partial x} + \frac{\partial\sigma_y}{\partial y} = 0 \tag{2.10}$$

The flow rule from equation (2.3) now becomes

$$\frac{\dot{\varepsilon}_x}{\sigma_x+p} = \frac{\dot{\varepsilon}_y}{\sigma_y+p} = \frac{\dot{\gamma}_{xy}}{2\tau_{xy}} = \dot{\lambda} \qquad (2.11)$$

where $\dot{\lambda} = \frac{3}{2}\left(\frac{\dot{\bar{\varepsilon}}}{\bar{\sigma}}\right)$

Von Mises yield criteria from equation (2.4) becomes

$$(\sigma_x-\sigma_y)^2+[\sigma_y-\tfrac{1}{2}(\sigma_x+\sigma_y)]^2+[\tfrac{1}{2}(\sigma_x+\sigma_y)-\sigma_x]^2$$

$$+6(\tau_{xy}^2+0+0) = 2\bar{\sigma}^2$$

or $\bar{\sigma} = [\frac{3}{4}(\sigma_x-\sigma_y)^2+3\tau_{xy}^2]^{\frac{1}{2}}$ (2.12)

The effective strain rate can be written from equation (2.8) as

$$\dot{\bar{\varepsilon}} = \frac{2}{3}[3\dot{\varepsilon}_x^2+\frac{3}{4}\dot{\gamma}_{xy}^2]^{\frac{1}{2}} \qquad (2.13)$$

2.1.3. Determination of the stress field from the strain field

Once all the normal and shear strains are known throughout the deforming region from equation (2.1) the stresses may be calculated. To determine the stress field from the strain field, the following steps are required.

From equation (2.3)

$$\dot{\varepsilon}_x - \dot{\varepsilon}_y = \frac{3\dot{\bar{\varepsilon}}}{2\bar{\sigma}}(\sigma_x+p-\sigma_y-p) = \frac{3\dot{\bar{\varepsilon}}}{2\bar{\sigma}}(\sigma_x-\sigma_y)$$

or $(\sigma_x-\sigma_y) = \frac{2\bar{\sigma}}{3\dot{\bar{\varepsilon}}}(\dot{\varepsilon}_x-\dot{\varepsilon}_y)$

$$\sigma_y = \sigma_x - \frac{2\bar{\sigma}}{3\dot{\bar{\varepsilon}}}(\dot{\varepsilon}_x - \dot{\varepsilon}_y) = \sigma_x - \frac{\dot{\varepsilon}_x - \dot{\varepsilon}_y}{\dot{\lambda}} \tag{2.14}$$

Differentiate equation (2.14) with respect to x gives

$$\frac{\partial \sigma_y}{\partial x} = \frac{\partial \sigma_x}{\partial x} - \frac{\partial}{\partial x}\left[\frac{\dot{\varepsilon}_x - \dot{\varepsilon}_y}{\dot{\lambda}}\right] \tag{2.15}$$

From the equilibrium equation (2.10)

$$\frac{\partial \sigma_x}{\partial x} = -\frac{\partial \tau_{xy}}{\partial y}$$

Substituting in equation (2.15) we get

$$\frac{\partial \sigma_y}{\partial x} = -\frac{\partial \tau_{xy}}{\partial y} - \frac{\partial}{\partial x}\left[\frac{\dot{\varepsilon}_x - \dot{\varepsilon}_y}{\dot{\lambda}}\right] \tag{2.16}$$

From equation (2.10)

$$\frac{\partial \sigma_y}{\partial y} = -\frac{\partial \tau_{xy}}{\partial x} \tag{2.17}$$

Using equation (2.16) and (2.17) with the known value of $\sigma(x,y)$ at $x = 0$ and $y = a$ i.e. $\sigma(o,a)$ we get,

$$\sigma_y(x,y) = \sigma_y(0,a) - \int_a^y \frac{\partial \tau_{xy}}{\partial x}\,dy - \int_0^x \left[\frac{\partial \tau_{xy}}{\partial y} + \frac{\partial}{\partial x}\left(\frac{\dot{\varepsilon}_x - \dot{\varepsilon}_y}{\dot{\lambda}}\right)\right]_{y=a} dx \tag{2.18}$$

From equation (2.14)

$$\sigma_x = \sigma_y + \frac{\dot{\varepsilon}_x - \dot{\varepsilon}_y}{\dot{\lambda}} \tag{2.19}$$

and from equation (2.11)

$$\tau_{xy} = \frac{\dot{\gamma}_{xy}}{2\dot{\lambda}} \tag{2.20}$$

where

$$\dot{\lambda} = \frac{3}{2}\frac{\dot{\bar{\varepsilon}}}{\bar{\sigma}} \tag{2.21}$$

2.2 EQUATIONS FOR DYNAMIC VISIOPLASTICITY

2.2.1 Equations for Three Dimensional Non-Steady State Dynamic Visioplasticity

For the case of dynamic deformation the Levy-Von Mises stress and strain rate relationship and Von Mises yield criteria are similar to the three dimensional non-steady quasi-static case. However, the static equilibrium equation is replaced by the equation of motion.

The equation of motion is obtained by considering a generic elemental cube subject to three normal and three independent shear stresses as shown in Fig. (2.1). If x,y are the current coordinates of a particle then

$$x = x(x_o, y_o, t)$$

$$y = y(x_o, y_o, t)$$

where x_o, y_o are the initial coordinates at time $t = 0$. The components of velocity along the x, y, z axes are given by u, v, W respectively.

Writing the equation of motion along x axis gives

$$(\sigma_{xx} + \frac{\partial \sigma_x}{\partial x} dx)\ dy\ dz - \sigma_x\ dy\ dz + (\tau_{yx} + \frac{\partial \tau_{yx}}{\partial y} dy) dz\ dx$$

$$- \tau_{yx}\ dz\ dx + (\tau_{zx} + \frac{\partial \tau_{zx}}{\partial z} dz)\ dx\ dy - \tau_{zx} dx\ dy$$

$$= (dx\ dy\ dz) \frac{\partial}{\partial t} \{\rho u\} \qquad (2.22)$$

Dividing throughout by dx dy dz

$$\frac{\partial \sigma_{xx}}{\partial x} + \frac{\partial \tau_{yx}}{\partial y} + \frac{\partial \tau_{zx}}{\partial z} = \frac{\partial}{\partial t}(\rho u) \qquad (2.23)$$

Similarly equation of motion along y and z directions we get

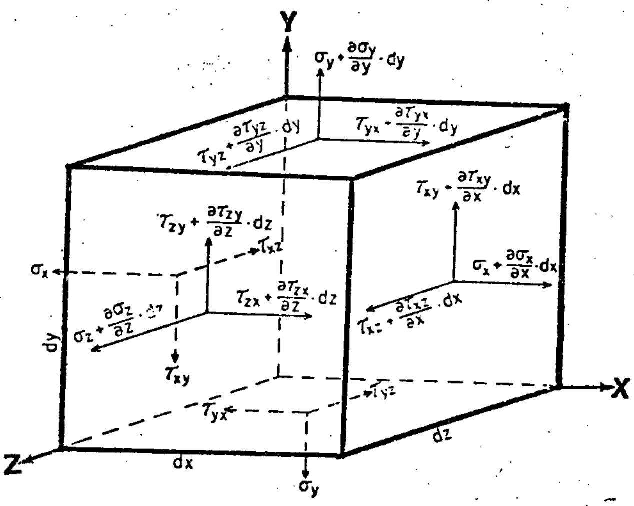

FIG. 2.1 ELEMENTAL CUBE FOR DERIVATION OF THE EQUATION OF MOTION

$$\frac{\partial \tau_{yx}}{\partial x} + \frac{\partial \sigma_{yy}}{\partial y} + \frac{\partial \tau_{yz}}{\partial z} = \frac{\partial}{\partial t}(\rho v) \qquad (2.24)$$

and

$$\frac{\partial \tau_{zx}}{\partial x} + \frac{\partial \tau_{zy}}{\partial y} + \frac{\partial \sigma_{zz}}{\partial z} = \frac{\partial}{\partial t}(\rho w) \qquad (2.25)$$

Considering ρ as constant, we get

$$\frac{\partial \sigma_{xx}}{\partial x} + \frac{\partial \tau_{yx}}{\partial y} + \frac{\partial \tau_{zx}}{\partial z} = \rho \frac{\partial u}{\partial t}$$

$$\frac{\partial \tau_{yx}}{\partial x} + \frac{\partial \sigma_{yy}}{\partial y} + \frac{\partial \tau_{yz}}{\partial z} = \rho \frac{\partial v}{\partial t} \qquad (2.26)$$

$$\frac{\partial \tau_{zx}}{\partial x} + \frac{\partial \tau_{zy}}{\partial y} + \frac{\partial \sigma_{zz}}{\partial z} = \rho \frac{\partial w}{\partial t}$$

2.2.2. Equations for Plane Strain Non-Steady State Dynamic Visioplasticity

For the plane strain condition $\tau_{zx} = \tau_{zy} = \frac{\partial w}{\partial t} = 0$,

so that the equation of motion (2.26) can be written as

$$\frac{\partial \sigma_{xx}}{\partial x} + \frac{\partial \tau_{xy}}{\partial y} = \rho \frac{\partial u}{\partial t} \qquad (2.27)$$

$$\frac{\partial \tau_{yx}}{\partial x} + \frac{\partial \sigma_{yy}}{\partial y} = \rho \frac{\partial v}{\partial t}$$

2.2.3. Determination of the Stress Field from the Strain Field

Proceeding in the same way as in the case of quasi-static visioplasticity method, the equation (2.15) can be written as

$$\frac{\partial \sigma_y}{\partial x} = \frac{\partial \sigma_x}{\partial x} - \frac{\partial}{\partial x}\left(\frac{\dot{\varepsilon}_x - \dot{\varepsilon}_y}{\dot{\lambda}}\right) \qquad (2.15)$$

Now from the equation of motion (2.27) we get

$$\frac{\partial \sigma_x}{\partial x} = - \frac{\partial \tau_{xy}}{\partial y} + \rho \frac{\partial u}{\partial t} \tag{2.28}$$

Substituting in equation (2.15) gives

$$\frac{\partial \sigma_y}{\partial x} = - \frac{\partial \tau_{xy}}{\partial y} + \rho \frac{\partial u}{\partial t} - \frac{\partial}{\partial x} \left[\frac{\dot{\varepsilon}_x - \dot{\varepsilon}_y}{\dot{\lambda}} \right] \tag{2.29}$$

Similarly from the equation of motion (2.27)

$$\frac{\partial \sigma_y}{\partial y} = - \frac{\partial \tau_{xy}}{\partial x} + \rho \frac{\partial v}{\partial t} \tag{2.30}$$

Using equation (2.29) and (2.30) with the known values of $\sigma(x,y)$ at x=o and y=a, i.e. $\sigma(o,a)$ we get

$$\sigma_y(x,y) = \sigma_y(o,a) - \int_a^y \left(\frac{\partial \tau_{xy}}{\partial x} + \rho \frac{\partial v}{\partial t} \right) dy$$

$$- \int_o^x \left[\frac{\partial \tau_{xy}}{\partial y} - \frac{\partial}{\partial x} \left\{ \frac{\dot{\varepsilon}_x - \dot{\varepsilon}_y}{\dot{\lambda}} \right\} + \rho \frac{\partial u}{\partial t} \right] dx \quad y = a \tag{2.31}$$

From equation (2.14)

$$\sigma_x = \sigma_y + \frac{\dot{\varepsilon}_x - \dot{\varepsilon}_y}{\dot{\lambda}} \tag{2.32}$$

and from equation (2.11)

$$\tau_{xy} = \frac{\dot{\gamma}_{xy}}{2\dot{\lambda}} \tag{2.33}$$

where $\dot{\lambda} = \frac{3\bar{\dot{\varepsilon}}}{2\bar{\sigma}}$ (2.34)

2.3. GENERAL PROCEDURE FOR THE STUDY OF DEFORMATION USING VISIOPLASTICITY

The instantaneous grid velocities are determined from experimental data and thus the strain rates, equivalent strain rates and finally stresses can be determined.

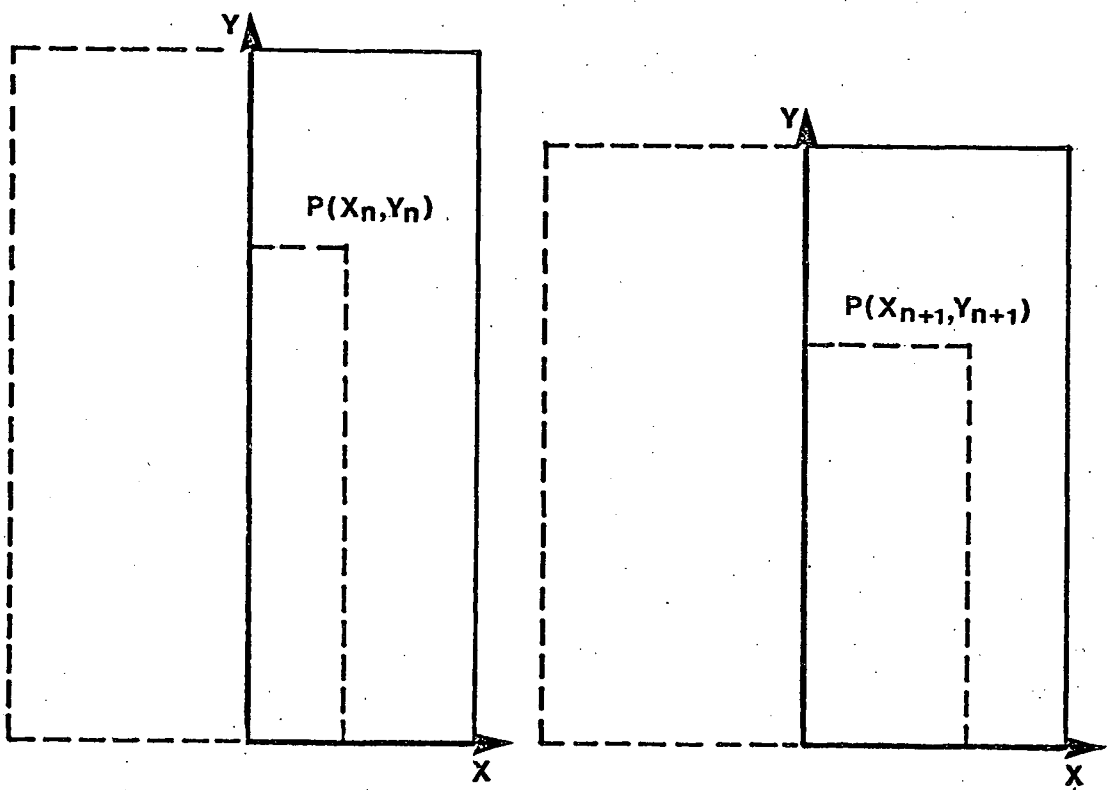

FIG. 2.2 POSITIONS OF POINT P AT INSTANCES T_n AND T_{n+1}

Grid lines are marked on an end face of the specimen, which is deformed at a predetermined speed. The deforming grid pattern is photographed using a high speed camera. The grid points at all stages of deformation are digitized from enlarged photographs and the digital positional data used as input to determine the instantaneous grid nodes velocities. The procedure is illustrated in Fig. (2.2), where a grid point formed by I row and J column has coordinates x_n, y_n at a particular instant of time t_n and grid-coordinates of x_{n+1}, y_{n+1} at the instant t_{n+1}. The instantaneous horizontal velocity u and the vertical velocity v is then given by

$$u_{ij} = \frac{x_{n+1}-x_n}{t_{n+1}-t_n} = \frac{\Delta x}{\Delta t}$$

$$v_{ij} = \frac{y_{n+1}-y_n}{t_{n+1}-t_n} = \frac{\Delta y}{\Delta t} \qquad (2.35)$$

Since the above components of velocity are obtained from the digitized coordinates of experimental grid points an efficient smoothing procedure is required. The smoothing procedure mentioned by Shabaik (71) is based on a simple averaging of the points. This procedure has caused difficulties in the past in treating data which is ill-defined and also tends to be time consuming in operation. Further for non-steady state conditions a reference grid is needed, which can be fixed with respect to time (called a master grid). The simple averaging technique gives grid node positions that continually change with time. In order to surmount these difficulties a number of alternate methods were considered and finally a three dimensional surface smoothing procedure was adopted, which treats x, y and u and also x, y and v as separate surfaces and fits a complete fourth order polynomial through the experimental points i.e. smoothing is done in three dimensions to a surface formed from the scaler components of the vector field. The condition of continuity (i.e. $\dot{\varepsilon}_x = -\dot{\varepsilon}_y$ or $\frac{\partial u}{\partial x} = -\frac{\partial v}{\partial y}$ for plane strain) can also be imposed within the surface fitting procedure, thereby reducing the number of independent parameters from 15 for each surface (a total of 30) to 10 for both surfaces. The smoothing procedure mentioned by Shabaik (71) does not take account of continuity and merely checks to see if the error is less than 15%.

Besides fitting a smooth surface, the polynomials have the distinct advantage that they can be readily differentiated for determining strains rates, and that the deformation can be automatically referred to a master reference grid. This means that strains and stresses can be determined for fixed points within the non-steady deformation zone. Also stresses can be evaluated directly at any position of x and y purely by substituting the coordinates of a point (not necessarily a grid point) required, whereas the simple averaging technique requires an incremental evaluation of stresses over contiguous grid points until the required grid point is reached.

After calculating $\dot{\varepsilon}_x$ and $\dot{\varepsilon}_y$ using equation (2.1), the effective strain rates at all grid points for all instances of deformation can calculated from the equation (2.13).

In order to calculate τ_{xy} (equation 2.33), σ_y (equation 2.31) and σ_x (equation 2.32) the value of $\dot{\lambda}$ is required. For non-workhardening materials the value of $\dot{\lambda}$ is purely a function of effective strain rate ($\dot{\bar{\varepsilon}}$) as effective stress ($\bar{\sigma}$) is constant. For a workhardening material the value of $\bar{\sigma}$ must be obtained from experimental $\bar{\sigma}$ vs $\bar{\varepsilon}$ material data taken at the relevant strain rate conditions. It is normal to fit a curve such as $\bar{\sigma} = c\,\bar{\varepsilon}^n$ where c and n are material constants. Thus if $\dot{\bar{\varepsilon}}$ is known at all instances of time, the value of equivalent strain $\bar{\varepsilon}$ at any deformation time t and hence $\bar{\sigma}$ may be determined incrementally (assuming small intervals of time) from the expression

$$\bar{\varepsilon}_{ij} = \int_o^t \dot{\bar{\varepsilon}}_{ij} \quad dt \qquad (2.36)$$

where $\dot{\bar{\varepsilon}}_{ij}$ is the effective strain rate of a particular grid point as it moves along its deformation path.

2.4. GENERALIZED EQUATIONS FOR PLANE-STRAIN VISIOPLASTICITY FOR COMPUTATIONAL PURPOSES

The equations in a form suitable for the development of the computer program are given below.

The calculation of u and v is done using equation (2.35).

$$u_{ij} = \frac{x_{n+1}-x_n}{t_{n+1}-t_n} = \frac{\Delta x}{\Delta t}$$

$$v_{ij} = \frac{y_{n+1}-y_n}{t_{n+1}-t_n} = \frac{\Delta y}{\Delta t}$$

Curve fitting of the velocities is done by a library subroutine called DLSQHS. This fits a complete fourth order polynomial in x and y and determines the 15 parameters (constants) for u and v for the equations given below. The equations used for computational purposes can be given as

$$u(x,y) = a_1+a_2x+a_3x^2+a_4x^3+a_5x^4$$
$$+a_6y+a_7y^2+a_8y^3+a_9y^4+a_{10}xy$$
$$+a_{11}xy^2+a_{12}xy^3+a_{13}x^2y+a_{14}x^2y^2$$
$$+a_{15}x^3y \qquad (2.37)$$

Similarly:

$$v(x,y) = b_1+b_2x+b_3x^2b_4x^3+b_5x^4$$
$$+b_6y+b_7y^2+b_8y^3+b_9y^4$$
$$+b_{10}xy+b_{11}xy^2+b_{12}xy^3$$
$$+b_{13}x^2y+b_{14}x^2y^2+b_{15}x^3y \qquad (2.38)$$

Thus the velocity component u anv v can be expressed separately and the calculation for strain rates $\dot{\varepsilon}\ x$, $\dot{\varepsilon}\ y$, $\dot{\gamma}_{xy}$ and can be done as follows:

$$\dot{\varepsilon}_x = \frac{\partial u}{\partial x} = a_2+2a_3x+3a_4x^2+4a_5x^3+a_{10}y$$
$$+a_{11}y^2+a_{12}y^3+2a_{13}xy+2a_{14}xy^2$$
$$+3a_{15}x^2y \qquad (2.39)$$

$$\dot{\varepsilon}_y = \frac{\partial v}{\partial y} = b_6+2b_7y+3b_8y^2+4b_9y^3+b_{10}x$$
$$+2b_{11}xy+3b_{12}xy^2+b_{13}x^2$$
$$+2b_{14}x^2y+b_{15}x^3 \tag{2.40}$$

and
$$\dot{\gamma}_{xy} = \frac{\partial u}{\partial y} + \frac{\partial v}{\partial x} = a_6+2a_7y+3a_8y^2+4a_9y^3$$
$$+a_{10}x+2a_{11}xy+3a_{12}xy^2$$
$$+a_{13}x^2+2a_{14}x^2y+a_{15}x^3$$
$$+b_2+2b_3x+3b_4x^2+4b_5x^3$$
$$+b_{10}y+b_{11}y^2+b_{12}y^3$$
$$+2b_{13}xy+2b_{14}xy^2+3b_{15}x^2y \tag{2.41}$$

The condition of continuity ($\dot{\varepsilon}_x = - \dot{\varepsilon}_y$ or $\frac{\partial u}{\partial x} = -\frac{\partial v}{\partial y}$) is imposed on the curve fitting by requiring the coefficients to be related as follows.

$$a_2 = - b_6$$
$$2a_3 = - b_{10}$$
$$3a_4 = - b_{13}$$
$$4a_5 = - b_{15}$$
$$a_{11} = - 3b_8 \tag{2.42}$$
$$3a_{15} = -2b_{14}$$

$$a_{12} = -4b_9$$

$$a_{10} = -2b_7$$

$$2a_{13} = -2b_{11}$$

$$2a_{14} = -3b_{12}$$

The partial derivative of $\dot{\gamma}_{xy}$ with respect to x and y is given by

$$\frac{\partial \dot{\gamma}_{xy}}{\partial x} = a_{10}+2a_{11}y+3a_{12}y^2+2a_{13}x+4a_{14}xy$$
$$+3a_{15}x^2+2b_3+6b_4x+12b_5x^2$$
$$+2b_{13}y+2b_{14}y^2+6b_{15}xy \qquad (2.43)$$

and hence

$$\int \frac{\partial \dot{\gamma}_{xy}}{\partial x}\, dy = (a_{10}+2b_3)y + (a_{11}+b_{13})y^2 + \frac{(3a_{12}+2b_{14})y^3}{3}$$
$$+(2a_{13}+6b_4)xy + \frac{(4a_{14}+6b_{15})xy^2}{2}$$
$$+(3a_{15}+12b_5)x^2y \qquad (2.44)$$

Similarly

$$\frac{\partial \dot{\gamma}_{xy}}{\partial y} = 2a_7+6a_8y+12a_9y^2+2a_{11}x+6a_{12}xy$$
$$+2a_{14}x^2+b_{10}+2b_{11}y+3b_{12}y^2$$
$$+2b_{13}x+4b_{14}xy+3b_{15}x^2 \qquad (2.45)$$

and $$\int \frac{\partial \dot{\gamma}_{xy}}{\partial y}\,dx = (2a_7+b_{10})\ x + (6a_8+2b_{11})xy$$

$$+ (a_{11}+b_{13})\ x^2 + \frac{(2a_{14}+3b_{15})}{3}\ x^3$$

$$+ (12a_9+3b_{12})\ y^2x$$

$$+ (3a_{12}+2b_{14})x^2y \qquad (2.46)$$

Further equation (2.36) can be expressed as

$$\bar{\varepsilon}_{i+1} = \frac{(\dot{\bar{\varepsilon}}_i + \dot{\bar{\varepsilon}}_{i+1})}{2}\Delta t + \bar{\varepsilon}_i \qquad (2.47)$$

The normal stress σ_y can be calculated using equation (2.31), i.e.

$$\sigma_y = \sigma_y(o,a) - \int_a^y \left(\frac{\partial \tau_{xy}}{\partial x} + \rho\frac{\partial v}{\partial t}\right)dy - \int_o^x \left[\frac{\partial \tau_{xy}}{\partial y} - \frac{\partial}{\partial x}\left\{\frac{\dot{\varepsilon}_x - \dot{\varepsilon}_y}{\dot{\lambda}}\right\} + \rho\frac{\partial u}{\partial t}\right]_{y=a} dx \qquad (2.31)$$

The terms for this equation may be calculated separately. The first term $\sigma_y\ (o,a)$ is determined experimentally at each interval of time. The second term can be calculated from the equation.

$$\tau_{xy} = \frac{\dot{\gamma}_{xy}}{2\dot{\lambda}} \qquad (2.33)$$

so that

$$\frac{\partial \tau_{xy}}{\partial x} = \frac{\partial}{\partial x}\left(\frac{\dot{\gamma}_{xy}}{2\dot{\lambda}}\right) = \frac{\partial}{\partial x}\left[\frac{\dot{\gamma}_{xy}}{\frac{3\dot{\bar{\varepsilon}}}{\bar{\sigma}}}\right]$$

$$= \frac{1}{3}\frac{\partial}{\partial x}\left[\frac{\dot{\gamma}_{xy}\ c\ \bar{\varepsilon}^{n}}{\dot{\bar{\varepsilon}}}\right]$$

$$= \frac{c}{3}\frac{\partial}{\partial x}\left[\frac{\dot{\gamma}_{xy}\,\bar{\varepsilon}^{n}}{\dot{\bar{\varepsilon}}}\right]$$

$$= \frac{c}{3}\left[\frac{\dot{\gamma}_{xy}}{\dot{\bar{\varepsilon}}}\frac{\partial}{\partial x}(\bar{\varepsilon})^{n} + \frac{\left\{\frac{\partial\dot{\gamma}_{xy}}{\partial x}\dot{\bar{\varepsilon}} - \dot{\gamma}_{xy}\frac{\partial\dot{\bar{\varepsilon}}}{\partial x}\right\}\bar{\varepsilon}^{n}}{\dot{\bar{\varepsilon}}^{2}}\right]$$

$$= \frac{c}{3}\left[\left(n\frac{\dot{\gamma}_{xy}}{\dot{\bar{\varepsilon}}}\bar{\varepsilon}^{n-1}\frac{\partial\bar{\varepsilon}}{\partial x}\right) + \frac{\bar{\varepsilon}^{n}}{\dot{\bar{\varepsilon}}}\frac{\partial\dot{\gamma}_{xy}}{\partial x} - \frac{(\bar{\varepsilon})^{n}\dot{\gamma}_{xy}}{(\dot{\bar{\varepsilon}})^{2}}\frac{\partial}{\partial x}(\dot{\bar{\varepsilon}})\right] \tag{2.48}$$

Similarly

$$\frac{\partial\tau_{xy}}{\partial y} = \frac{c}{3}\left[n\frac{\dot{\gamma}_{xy}}{\dot{\bar{\varepsilon}}}\bar{\varepsilon}^{n-1}\frac{\partial}{\partial y}\bar{\varepsilon} + \frac{\bar{\varepsilon}^{n}}{\dot{\bar{\varepsilon}}}\frac{\partial\dot{\gamma}_{xy}}{\partial y} - \frac{(\bar{\varepsilon})^{n}\dot{\gamma}_{xy}}{(\dot{\bar{\varepsilon}})^{2}}\frac{\partial}{\partial y}(\dot{\bar{\varepsilon}})\right] \tag{2.49}$$

Using equation (2.1), the third term of equation (2.31) can be computed as

$$\frac{\partial}{\partial x}\left(\frac{\dot{\varepsilon}_x - \dot{\varepsilon}_y}{\dot{\lambda}}\right) = -\frac{\dot{\varepsilon}_x - \dot{\varepsilon}_y}{\dot{\lambda}^{2}}\frac{\partial\dot{\lambda}}{\partial x} + \frac{1}{\dot{\lambda}}\frac{\partial}{\partial x}(\dot{\varepsilon}_x - \dot{\varepsilon}_y)$$

$$= -\frac{(\dot{\varepsilon}_x - \dot{\varepsilon}_y)}{\dot{\lambda}^{2}}\frac{\partial}{\partial x}\left(\frac{3\dot{\bar{\varepsilon}}}{2c\bar{\varepsilon}^{n}}\right) + \frac{1}{\dot{\lambda}}\left[\frac{\partial}{\partial x}(\dot{\varepsilon}_x - \dot{\varepsilon}_y)\right] \tag{2.50}$$

But $\frac{\partial}{\partial x}\left(\frac{3\dot{\bar{\varepsilon}}}{2c\bar{\varepsilon}^{n}}\right) = \frac{3}{2c}\frac{\partial}{\partial x}\left[\dot{\bar{\varepsilon}}(\bar{\varepsilon})^{-n}\right]$

$$= \frac{3}{2c}\left[\left\{-n\,\dot{\bar{\varepsilon}}\,(\bar{\varepsilon})^{-n-1}\right\}\frac{\partial\bar{\varepsilon}}{\partial x} + (\bar{\varepsilon})^{-n}\frac{\partial}{\partial x}(\dot{\bar{\varepsilon}})\right]$$

$$= -\frac{3}{2c}n\frac{\dot{\bar{\varepsilon}}}{(\bar{\varepsilon})^{n}}\frac{1}{\bar{\varepsilon}}\frac{\partial\bar{\varepsilon}}{\partial x} + \frac{3}{2c}\frac{\dot{\bar{\varepsilon}}}{(\bar{\varepsilon})^{n}}\frac{1}{\dot{\bar{\varepsilon}}}\frac{\partial}{\partial x}(\dot{\bar{\varepsilon}})$$

$$= -\frac{n\dot{\lambda}}{\bar{\varepsilon}}\frac{\partial\bar{\varepsilon}}{\partial x} + \frac{\dot{\lambda}}{\dot{\bar{\varepsilon}}}\frac{\partial\dot{\bar{\varepsilon}}}{\partial x}$$

$$= \dot{\lambda}\left[-\frac{n}{\bar{\varepsilon}}\frac{\partial\bar{\varepsilon}}{\partial x} + \frac{1}{\dot{\bar{\varepsilon}}}\frac{\partial\dot{\bar{\varepsilon}}}{\partial x}\right] \tag{2.51}$$

differentiating equation (2.13) with respect to x, we get

$$\frac{\partial\dot{\bar{\varepsilon}}}{\partial x} = \frac{\partial}{\partial x}\left[\frac{2}{3}\left(3\dot{\varepsilon}_x^{2} + \frac{3}{4}\dot{\gamma}_{xy}^{2}\right)^{\frac{1}{2}}\right]$$

$$= \frac{1}{3} \left[\left(3 \dot{\varepsilon}_x^{\,2} + \frac{3}{4} \dot{\gamma}_{xy}^{\,2}\right)^{-\frac{1}{2}} \left(6 \dot{\varepsilon}_x \frac{\partial \dot{\varepsilon}_x}{\partial x} + \frac{3}{4} \times 2 \dot{\gamma}_{xy} \frac{\partial \dot{\gamma}_{xy}}{\partial x}\right) \right.$$

$$= \left(3 \dot{\varepsilon}_x^{\,2} + \frac{3}{4} \dot{\gamma}_{xy}^{\,2}\right)^{-\frac{1}{2}} \left[2 \dot{\varepsilon}_x \frac{\partial \dot{\varepsilon}_x}{\partial x} + \frac{1}{2} \dot{\gamma}_{xy} \frac{\partial \dot{\gamma}_{xy}}{\partial x} \right] \tag{2.52}$$

So that the third term of equation (2.31), using equations (2.50-2.52) can be computed as

$$\frac{\partial}{\partial x} \left(\frac{\dot{\varepsilon}_x - \dot{\varepsilon}_y}{\dot{\lambda}}\right) = \frac{1}{\dot{\lambda}} \left[(\dot{\varepsilon}_y - \dot{\varepsilon}_x) \left\{ \frac{-n}{\bar{\varepsilon}} \frac{\partial \bar{\varepsilon}}{\partial x} + \frac{1}{\dot{\bar{\varepsilon}}} \frac{\partial \dot{\bar{\varepsilon}}}{\partial x} \right\} + \frac{\partial}{\partial x} (\dot{\varepsilon}_x - \dot{\varepsilon}_y) \right] \tag{2.53}$$

Thus the normal stresses σ_y and σ_x can be computed using equations (2.31, 2.32, 2.48, 2.49, 2.50, 2.51, 2.52 and 2.53) with the known values of $\sigma(o,a)$.

2.5 COMPUTER PROGRAM

The flow chart of the computer program developed for plane-strain dynamic and quasi-static visioplasticity is given in Fig. (2.4) and a listing of the program is given in Appendix I.

The running instructions and the main steps in the program are described below:

(1) Input all data required for the calculations

(a) Read

IX = No. of experimental grid lines parallel to y axis

IY = No. of experimental grid lines parallel to x axix

The above are given in FORMAT (3I2)

IT = No. of the time steps

DT = Time interval between two consecutive photographs (this need not be constant time interval)

FORMAT (8F10.0)

NIX = No. of grid lines parallel to y axis in master grid

NIY = No. of grid lines parallel to x axis in master grid

Both in FORMAT (3I2)

CA = Constant a used for σ (o,a)

CC = Constant used in true stress and true strain relation

CN = Constant (or index) for workhardening

SIGOA = σ (o, a), known value of y at x = o and y = a

All above in FORMAT (8F10.0)

(b) Read, the instantaneous coordinates of the grid points of consecutive photograph. The format is given as FORMAT (5X, 2F6.3, 1X, 2F6.3, 1X, 2F6.3, 1X, 2F6.3, 1X, 2F6.3)

(2) Calculate the values of horizontal velocity u and vertical velocity v at each grid point using equation (2.35)

(3) Fit a 4th degree polynomial through the three dimensional curves for u and v as a function of x and y using the computer library routine called 'DLSQHS'.
This program provides a least square fit to a linear function of M parameters (i.e. M independent variables) and N data points by the Householder transformation techniques.

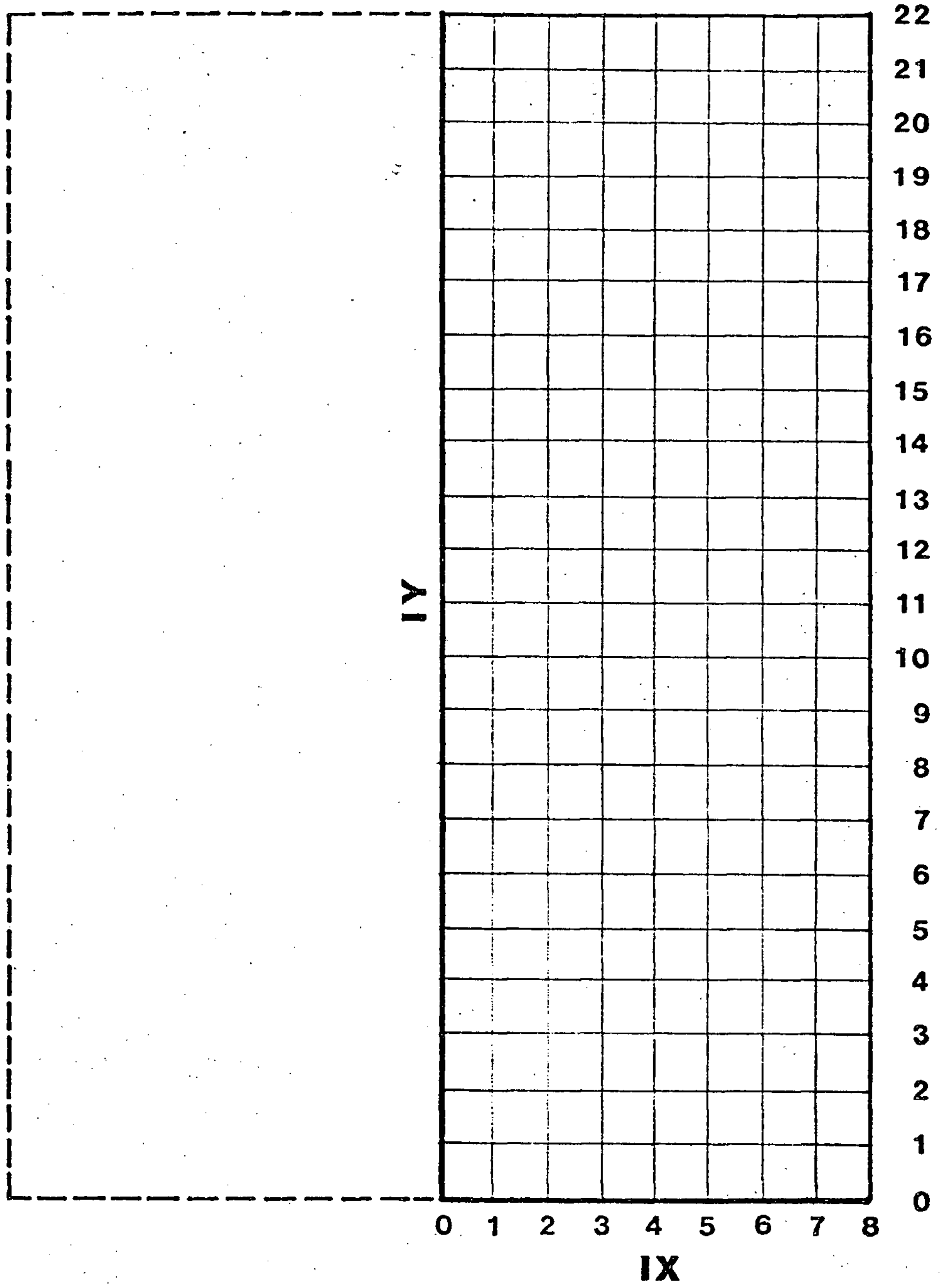

FIG. 2.3. GRID LINES ON THE SPECIMEN

FLOW CHART OF COMPUTER PROGRAM

Read IX, IY, IT, DT, NIX, NIY, CA, CC, CN and (o,a)

↓

Read (x,y), the grid points at each time interval. Plot them

↓

Calculate component velocities u and v for each time increment using the equations

$$u_{ij} = \frac{x_{n+1} - x_n}{t_{n+1} - t_n}$$

$$v_{ij} = \frac{y_{n+1} - y_n}{t_{n+1} - t_n} \qquad \text{(equ. 2.35)}$$

↓

Fit the curves to the u and v values with complete fourth degree polynomial in x and y (Subroutine DLSQHS)

↓

Calculate and store strain-rates for all points, using subroutine DERIV

$$\dot{\varepsilon}_x = \frac{\partial u}{\partial x} \qquad \text{(equ. 2.1, 2.13, 2.38, 2.39, 2.40)}$$

$$\dot{\varepsilon}_y = \frac{\partial v}{\partial y}$$

$$\dot{\gamma}_{xy} = \frac{\partial u}{\partial y} + \frac{\partial v}{\partial x}$$

$$\dot{\bar{\varepsilon}} = \frac{2}{3}(3\dot{\varepsilon}_x + \frac{3}{4}\dot{\gamma}_{xy}{}^2)^{\frac{1}{2}}$$

↓

Calculate and store the total effective strain at all specified node points

↓

(i) Set Master Grid for final plot and further calculations

(ii) Fill zero for the points, outside the boundary of the deforming zone by use of subroutine FILL

↓

Plot:

$u = f(x,y)$,

$v = f(x,y)$,

$\dot{\varepsilon}_x = f(x,y)$,

$\dot{\varepsilon}_y = f(x,y)$,

$\dot{\bar{\varepsilon}} = f(x,y)$,

(a) in two dimensional form using subroutine PLOT, PLOTAND & SYMBOL

(b) in three dimensional form using subroutine PERS

↓

Calculate normal & shear stress using equation 2.1, 2.13, 2.38, 2.39, 2.40

↓

Plot:

(i) σ_y as a function of x and y

(ii) σ_x as a function of x and y

(iii) τ_{xy} as a function of x and y

(a) in two dimensional form using subroutine PLOT, PLOTAND & SYMBOL

(b) in three dimensional form using subroutine PERS

↓

STOP

FIG. 2.4

That is it minimises

$$\sum_{i=1}^{N} \left(y_i - \sum_{j=1}^{M} a_i x_{ji}\right)^2$$

DLSQHS transforms the matrix X to an upper triangular form via Householder transformations, and then solves the system by backward substitution. If the command REFINE is defined by 'TRUE': a correction vector is computed from the residual errors between the dependent variables and the fitted values. Correction vectors are then applied to the solution and re-computed iteratively until convergence is obtained. DLSQHS is most effective for problems, where the correction of the matrices is unknown and the scale of different variables varies widely.

(4) Impose the condition of continuity i.e. $\dot{\varepsilon}_x = -\dot{\varepsilon}_y$ or $\frac{\partial u}{\partial x} = -\frac{\partial v}{\partial y}$

(5) Calculate the strain-rates $\dot{\varepsilon}_x$, $\dot{\varepsilon}_y$,shear strain-rate $\dot{\gamma}_{xy}$ and effective strain-rate using equations (2.39),(2.40),(2.41) and (2.73) ,are combined into a 'DERIV' (details are given in Appendix) .

(6) Calculate the total effective strain by integrating along the path of particular particle or grid node (refer equations 2.36 and 2.47).

(7) Calculate shear stress τ_{xy} using equations (2.33, 2.34 and 2.41).

(8) Calculate independently the terms from equations (2.31), (2.48), (2.49), (2.50), (2.51), (2.52), and (2.53) and thereby calculate σ_y using the computer library subroutine 'DQUANK'. This subroutine integrates a function f(x) when the limits a and b are given. i.e. $I = \int_a^b f(x)\,dx$. It is basically based on Simpon's three points integration & improved by using an adjustment term of fifth degree in place of the three degree term.
The absolute error can be limited to any arbitrarily specified value.
Calculate stresses σ_x using equations (2.31) and (2.31).

(9) Plot the different quantities, u, v, $\dot{\varepsilon}_x$, $\dot{\varepsilon}_y$, $\dot{\gamma}_{xy}$, $\dot{\bar{\varepsilon}}$, $\bar{\varepsilon}$, σ_y, σ_x, τ_{xy}, etc. for different x, y values. The plotting vectors are taken at defined master grid node points. Any point within the master grid but outside the deformation zone are given zero values by the subroutine 'FILL'.

(a) These values can be plotted in two dimensions either as a function of x or a function of y. For this purpose the subprogram 'PLOT' can be used. Thus subprogram is the basic plot subroutine. It generates the pen movement required to move the pen in a straight line from its present position to the position indicated in the call. It is also used to relocate the origin of the plotter coordinate system in the X direction. To ensure that plotting is complete, a second subprogram 'PLOTND' is used. For clear distinction of different lines in a plot, a third subprogram 'SYMBOL' can be used. This plots alphanumeric characters and special symbols.

(10) Three dimensional orthographic displays can be made using the subroutine 'PERS'. The above values are taken as 'Z' values and are plotted in three dimensional form as a function of x, and y.

C H A P T E R   T H R E E

VARIABLE SPEED, CONTROLLED VELOCITY PROFILE, SINGLE CYCLE, IMPACTING PRESS

CHAPTER THREE

VARIABLE SPEED, CONTROLLED VELOCITY PROFILE, SINGLE CYCLE IMPACTING PRESS

3.1 DESCRIPTION OF EQUIPMENT

3.1.1. Background Information

For experimental investigation of forging operations such as heading and upsetting, where strain-rate, forming-speed and forming load are important, a device with special requirements is needed.

Obviously as wide a range of impact speed as possible is required together with a velocity profile which is sensibly independent of forming load and which may be adjusted to suit circumstances.

The commercial alternatives that are available have been developed for specific applications and of necessity have a limited flexibility. For example, the crank press, used in many forging operations has a variable stroke and maximum velocity and has a well controlled velocity profile, which is sensibly independent of forming load. However, the maximum velocity is limited to approximately 15 to 20 ft./sec.. With the drop hammer and high velocity forming machines (such as the petroforge) a higher velocity can be reached (15-30 ft./sec. for the drophammer, 90-100 ft./sec. for the petroforge) but the stroke and velocity profile during deformation are determined purely by the resistance of the workpiece. That is the high

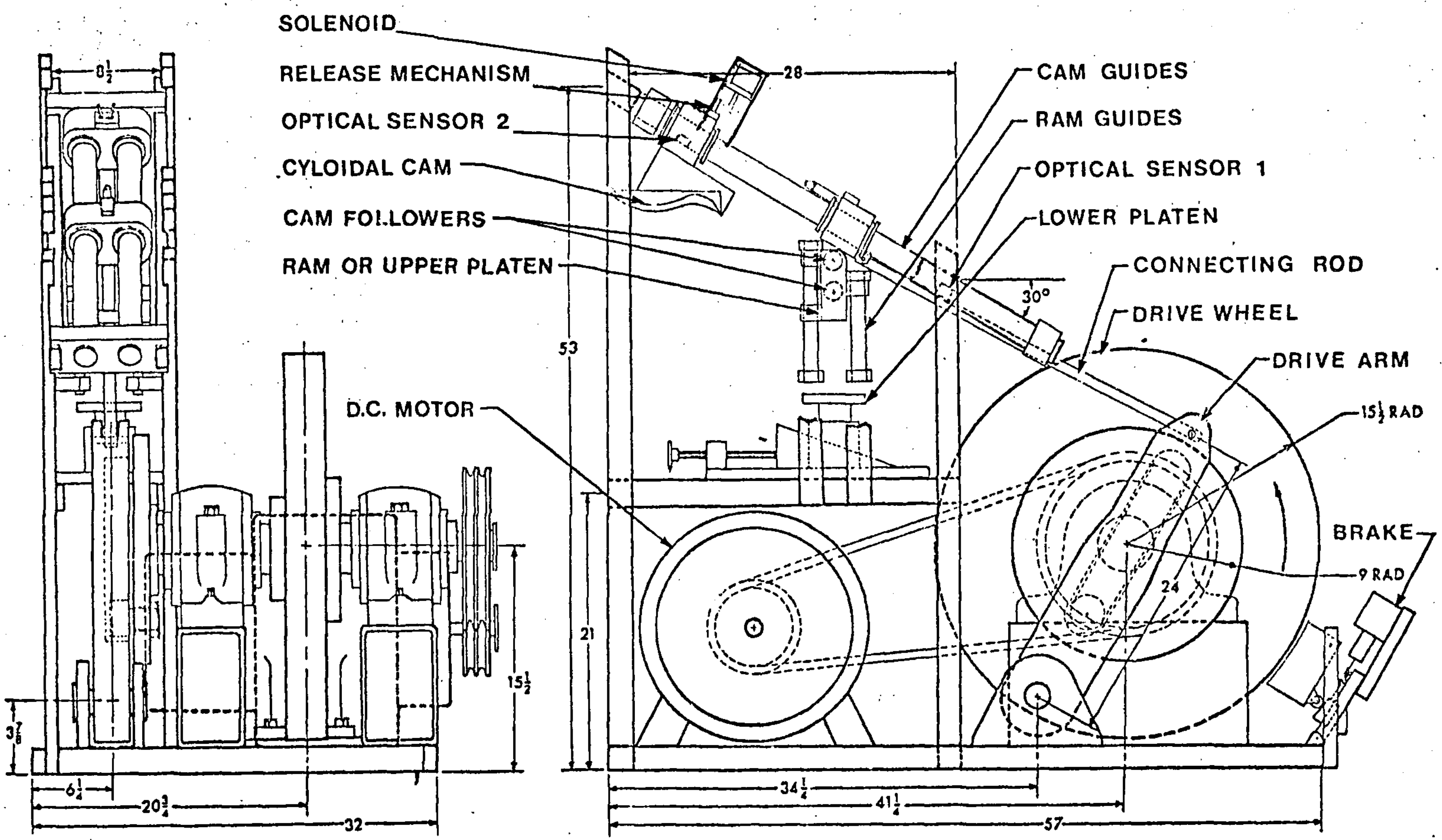

FIG 3.1 VARIABLE SPEED, CONTROLLED VELOCITY PROFILE, SINGLE CYCLE IMPACTING PRESS

velocity results in high energy and with low strength targets very little of the energy is absorbed in plastic work. Further the high velocity devices cannot be used for low velocity work.

With these design criteria in mind a variable speed, controlled velocity profile, single cycle, impacting press was designed and built within the department.

3.1.2 Description of the Press:

A diagram of the impacting press is shown in Fig. 3.1. The drive comprises a modified Whitworth quick-return mechanism consisting of a crank and a drive arm together with a variable speed D.C. motor, a flywheel, bearings etc. The end of the drive arm is attached by a connecting rod to a cycloidal cam. In single cycle operation, the cam is made to engage with an upper platen (or ram) which impacts the workpiece. The upper platen and cam are both mounted on multirod supports with linear ball bushings. A brake is provided on the flywheel for emergency purposes.

3.1.3 Operation of the Press:

The drive wheel is rotated at a particular speed by adjustment of the D.C. motor controller causing the drive arm to oscillate about its lower pivot. The single cycle tripping mechanism connects the drive arm with the cam and the cam engages with the cam followers on the upper-platen. The upper-platen is thus forced down towards the workpiece. The platen achieves a maximum velocity when the drive arm is in a central position after which time the platen is brought to rest. On the return stroke of the cam the platen is returned to its initial position. The tripping mechanism then disengages the connecting rod from the cam and the drive arm continues to oscillate freely about its lower pivot.

The stroke, velocity and acceleration profile of the upper-platen are determined solely by the cam contour and the speed setting of the D.C. motor. A cycloidal cam is used for high velocity work to minimise excessive wear, through shock and vibration.

The lower platen height can be adjusted relative to the upper platen thereby determining the working portion of the stroke.

3.2 KINEMATIC ANALYSIS OF THE MECHANISM

3.2.1. Derivation of Expressions for Velocity and Acceleration:

The drive mechanism is shown schematically in Fig. (3.2.). The centre line of the drive arm is indicated by line AB, where point A denotes the fixed lower pivot. The path of B is indicated by the dotted line with B' and B", showing the extreme points. The point C is the centre of rotation of the drivewheel, a distance P above the fixed pivot of the drive arm. The eccentricity of point E, the cam follower, about C is given by a distance Q. The line CD is a reference for angle θ. The length of AB is L. The path of point F denoting the cam position, is shown by dotted line. The length of connecting rod, BF = R and the distance of cam position F from line AC (or AH) be X. The angle made by AB with line AC is ϕ

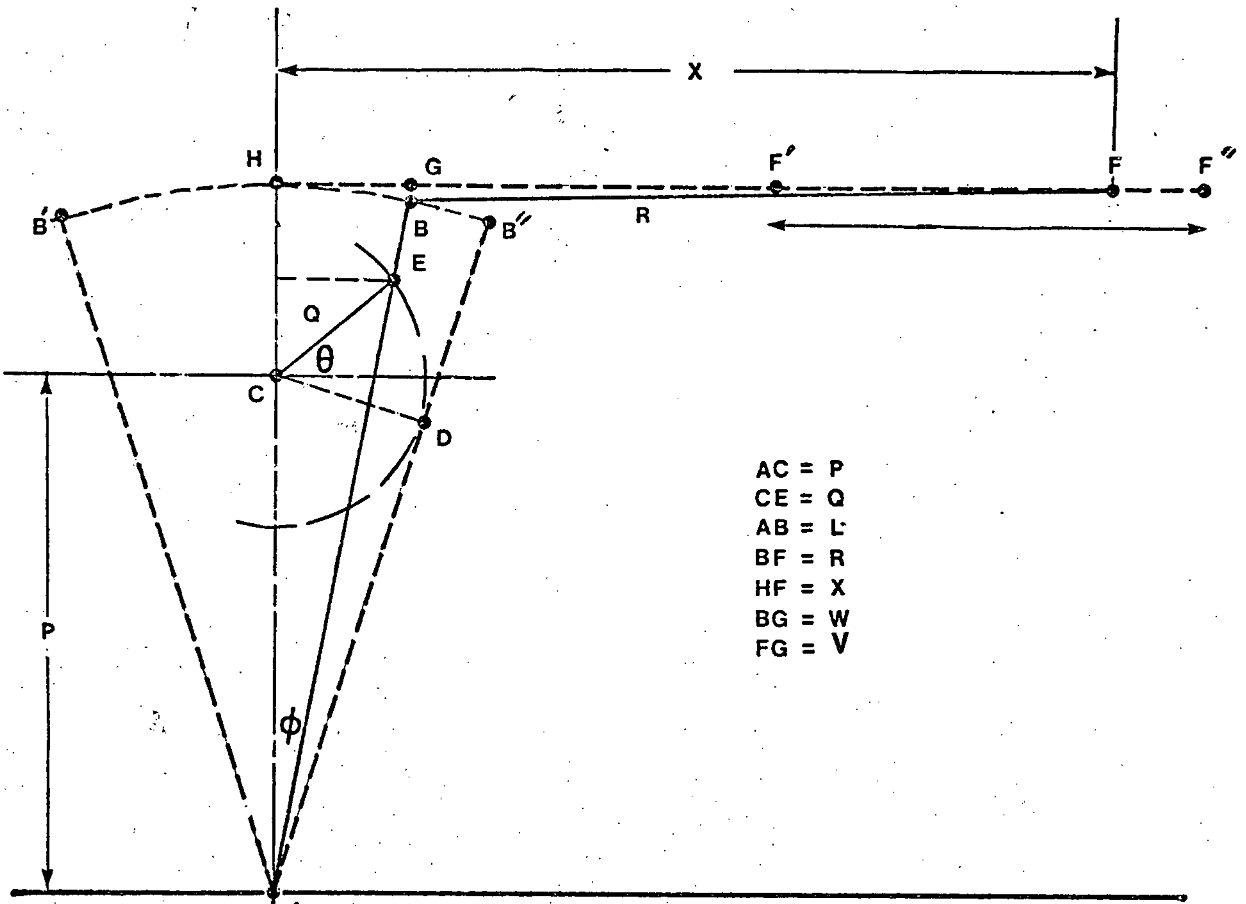

FIG. 3.2 DRIVE MECHANISM OF IMPACTING PRESS

Then from geometry

$$\phi = \arctan \frac{Q\cos\theta}{P+Q\sin\theta} \tag{3.1}$$

Differentiate ϕ with respect to t, we get

$$\frac{d\phi}{dt} = - \frac{PQ\sin\theta+Q^2}{P^2+2PQ\sin\theta+q^2} \frac{d\theta}{dt} \tag{2.3}$$

Differentiating again, we get

$$\frac{d^2\phi}{dt^2} = - \left(\frac{d\theta}{dt}\right)^2 PQ \cos\theta \left[\frac{P^2 - Q^2}{(P^2+2PQ\sin\theta+Q^2)^2}\right] \tag{3.3}$$

Now from Fig. (3.2) $\quad HF = HG + GF = L \sin\phi + GF = X$

but $GF = [(BF^2 - BG^2)]^{\frac{1}{2}} = [R^2 - \{L(1-\cos\phi)\}^2]^{\frac{1}{2}}$

Hence, $X = L \sin\phi + [R^2 - \{L(1-\cos\phi)\}^2]^{\frac{1}{2}}$

Differentiating with respect to t, we get

$$\frac{dx}{dt} = L \frac{d\phi}{dt}\left[\cos\phi - \frac{L(1-\cos\phi)}{[R^2-\{L(1-\cos\phi)\}^2]^{\frac{1}{2}}} \sin\phi\right]$$

$$= L \frac{d\phi}{dt} [\cos\phi - \frac{W}{V} \sin\phi] \tag{3.4}$$

where $W = L(1-\cos\phi)$

and $V = [(R^2 - W^2)]^{\frac{1}{2}}$

Differentiating again and rearranging the terms, we get

$$\frac{d^2x}{dt^2} = L \frac{d^2\phi}{dt^2} (\cos\phi + \frac{W}{V}) - L \left(\frac{d\phi}{dt}\right)^2 [(\sin\phi + \frac{L\sin\phi}{V} (\frac{W^2}{V^2} + 1) + \frac{W}{V}\cos\phi)] \tag{3.5}$$

3.2.2. Maximum Velocity and Acceleration of the Mechanism:

The press has following dimensions:-

P = 14 inch.

Q = 6 inch.

L = 24 inch.

R = 26 inch.

Ratio of driver to driven pulley dia. = 0.573

For a flywheel speed of 250 RPM, (i.e. a motor speed of 434.4 rpm) the angular velocity of the flywheel = $\frac{2 \times 250}{60}$ = 15 rad/sec. (3.6)

The position of the maximum velocity of the ram (hence the upper-platen) occurs when $\phi = o$ or $\theta = -90°$.

Hence from equation (3.2) we get

$$\frac{d\phi}{dt} = - \frac{d\theta}{dt} \frac{PQ \text{ Sin } \theta + Q^2}{P^2+2PQ\text{Sin}\theta+Q^2}$$

$$= (-\omega) \frac{(14x6)\ (-1)+(6x6)}{(14x14)+(2x14x6(-1))+(6x6)}$$

$$= 0.75\,\omega \quad \text{(omega)}$$

From equation (3.4)

$$\frac{dx}{dt} = L\frac{d\phi}{dt} \left(\text{Cos } \phi - \frac{W}{V} \text{ Sin } \phi\right); \text{ here } \phi = o$$

$$= L\frac{d\phi}{dt} \left(1 - \frac{W}{V} x\ o\right) = L\frac{d\phi}{dt}$$

$$= \frac{24}{12}\frac{d\phi}{dt} = 2 \times .75\,\omega = 1.5\,\omega \text{ (ft./sec.)} \quad (3.7$$

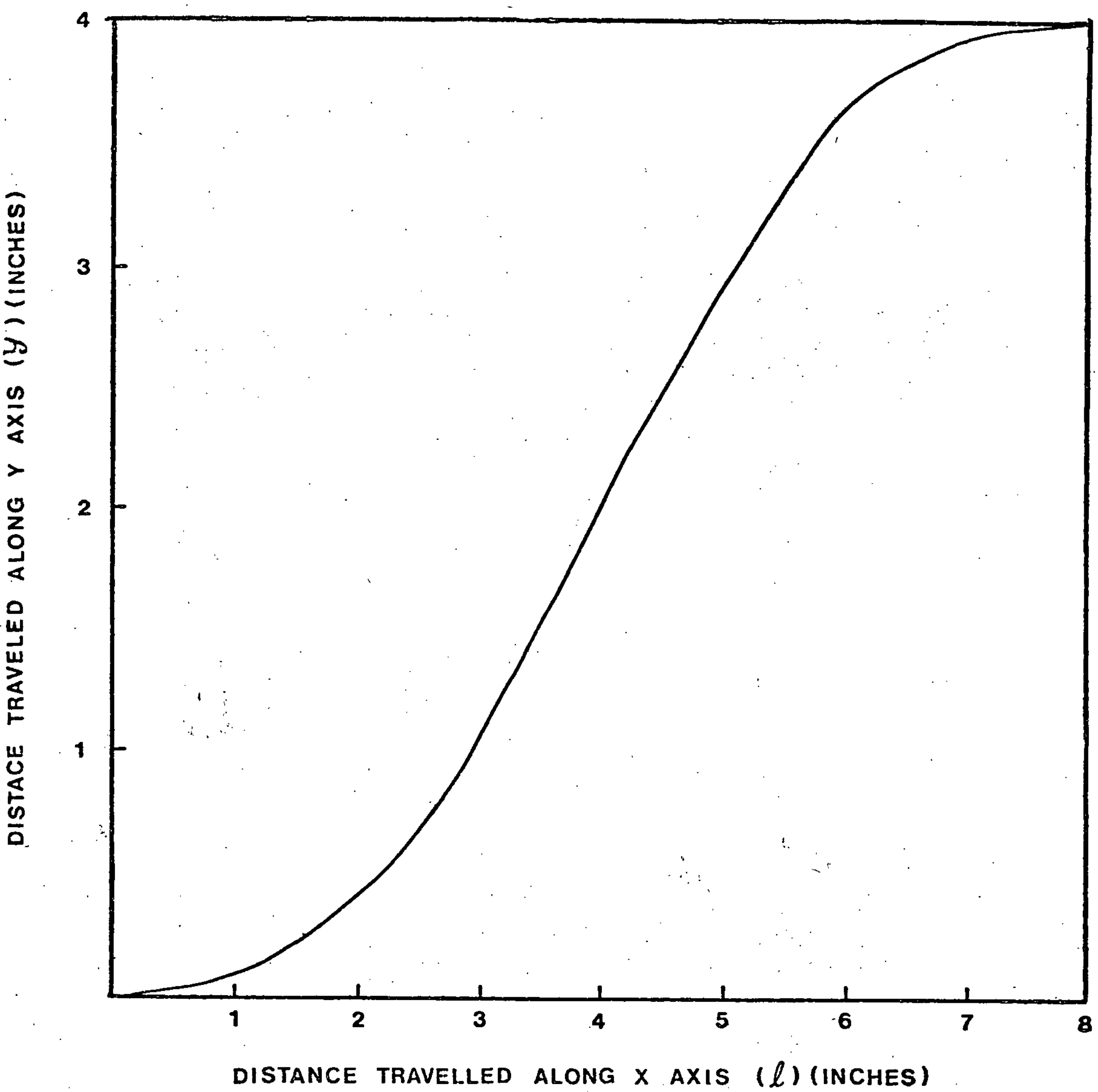

FIG. 3.3 MOTION OF THE CYCLOIDAL CAM

Now the displacement of platen, y, in relation to the cycloidal cam (refer. Fig. 3.3) is given by

$$y = \frac{h}{\pi}\left(\frac{\pi\ell}{L'} - \frac{1}{2}\,\mathrm{Sin}\,\frac{2\pi\ell}{L'}\right) \tag{3.8}$$

where ℓ = distance travelled along x axis at a particular time

L' = length of cycloidal cam in x direction

h = maximum distance travelled by upper-platen or follower in the y direction

Velocity of follower i.e. platen is given as

$$v = \frac{h\left(\frac{d\ell}{dt}\right)}{L'}\left(1 - \frac{\mathrm{Cos}2\pi\ell}{L'}\right) \tag{3.9}$$

$$v_{max} = \frac{2h\frac{d\ell}{dt}}{L'} \tag{3.10}$$

Similarly the equation for acceleration of the upper-platen, a, is given by

$$a = \ddot{y} = \frac{2h\,\pi\left(\frac{d\ell}{dt}\right)^2}{L'^2}\,\mathrm{Sin}\,\frac{2\pi\ell}{L'} + \frac{h}{L'}\left(1 - \frac{\mathrm{Cos}2\pi\ell}{L'}\right)\frac{d^2\ell}{dt^2} \tag{3.11}$$

For the present cam, h = 4.0 inch. and L'= 8", so that

$$v_{max} = \frac{2x4.0x\left(\frac{d\ell}{dt}\right)}{8} = \frac{2x4.0x\left(\frac{dx}{dt}\right)}{8}$$

$$= \frac{2x4.0x1.5\,\omega}{8}$$

$$= 1.5\,\omega$$

Using the value of ω = 15 rad./sec. from equation (3.6)

v_{max} = 22.5 ft./sec.

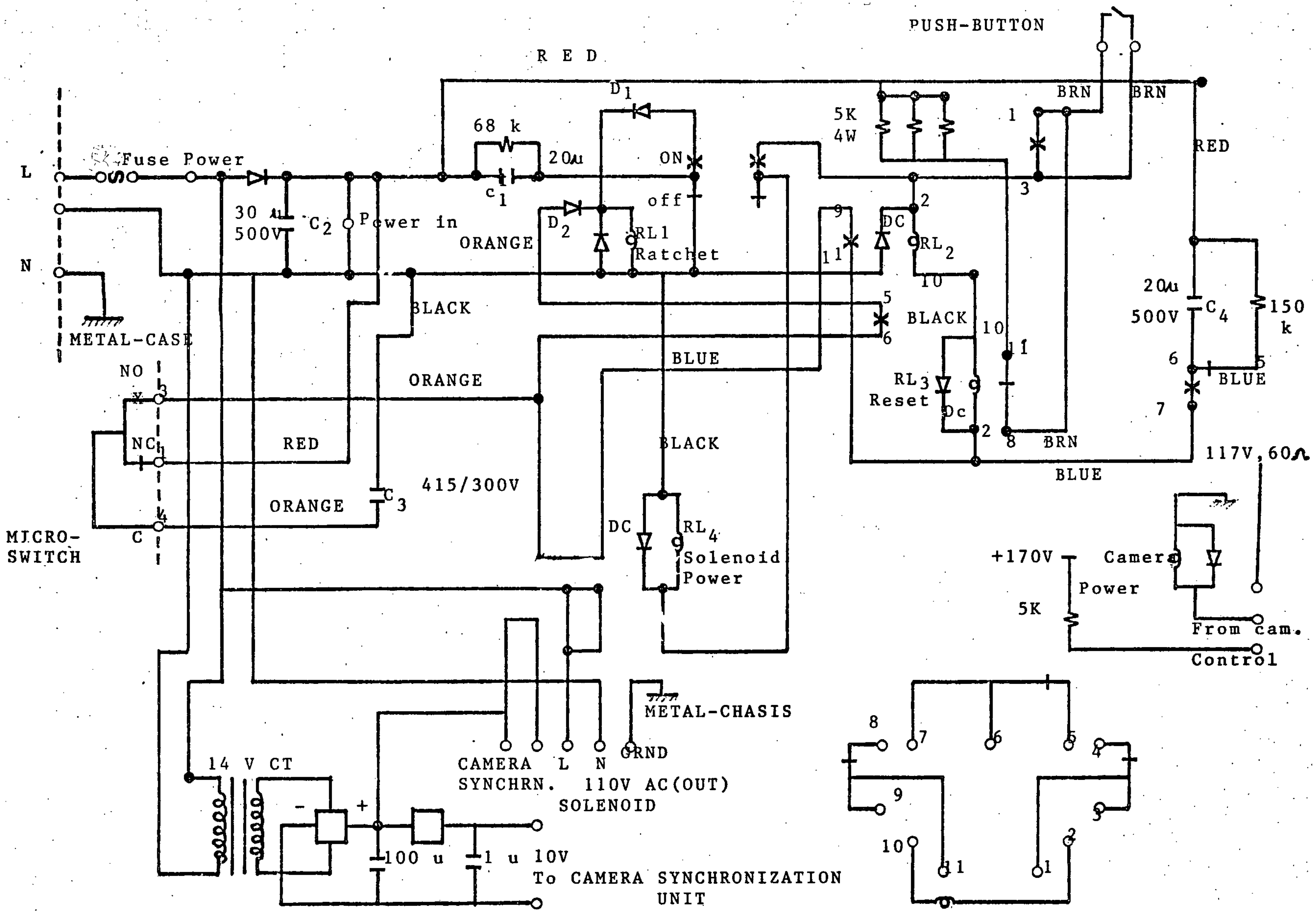

FIG. 3.4 ELECTRICAL CIRCUIT FOR SINGLE - CYCLE OPERATION CONTROL

3.3 CONTROL

With single cycle operation it is essential that engagement of the drive arm with the cam occur at the correct point in the cycle and have sufficient time to engage properly. This is achieved by requiring that a sensing device placed at the extreme point of the drive arm motion be actuated in conjunction with a push-button start switch before engagement occurs. A solenoid then retracts and allows the maximum time for the two parts to engage.

Synchronization of the high speed camera with the specimen deformation is also accomplished using the signal from the remote sensing switch. A time delay device is used to vary the start of filming so that different impact speeds can be accommodated. A further sensing device placed at the opposite extreme of the drive arm movement indicates when the event is completed and triggers the magnetic camera brake.

Details of the electronic circuitry for engagement and disengagement of the drive arm and for sychronization of the high speed camera are given in the following sections.

3.3.1. Control for Single Cycle Operation:

The electrical circuit used for controlling the engagement of the driving arm of the cam is given in Fig. (3.4) and the flow diagram of the relay sequence is given in Fig. (3.5). The sequence of events is as follows:

(i) Single cycle start switch (push button) is pressed which sets the latch relay (RL2) through reset relay (RL3), normally

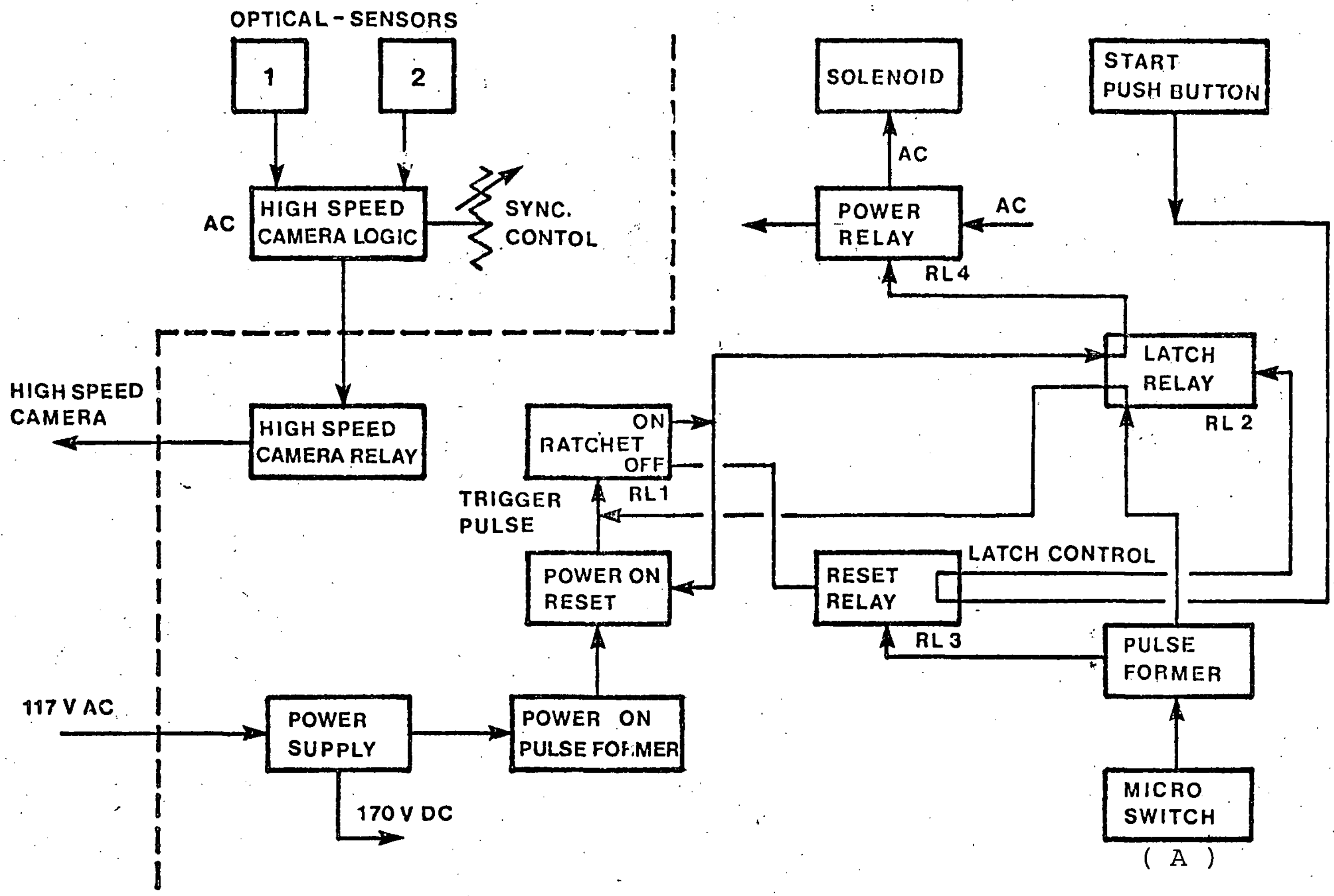

FIG. 3.5 FLOW DIAGRAM FOR RELAY SEQUENCE FOR SINGLE CYCLE CONTROL

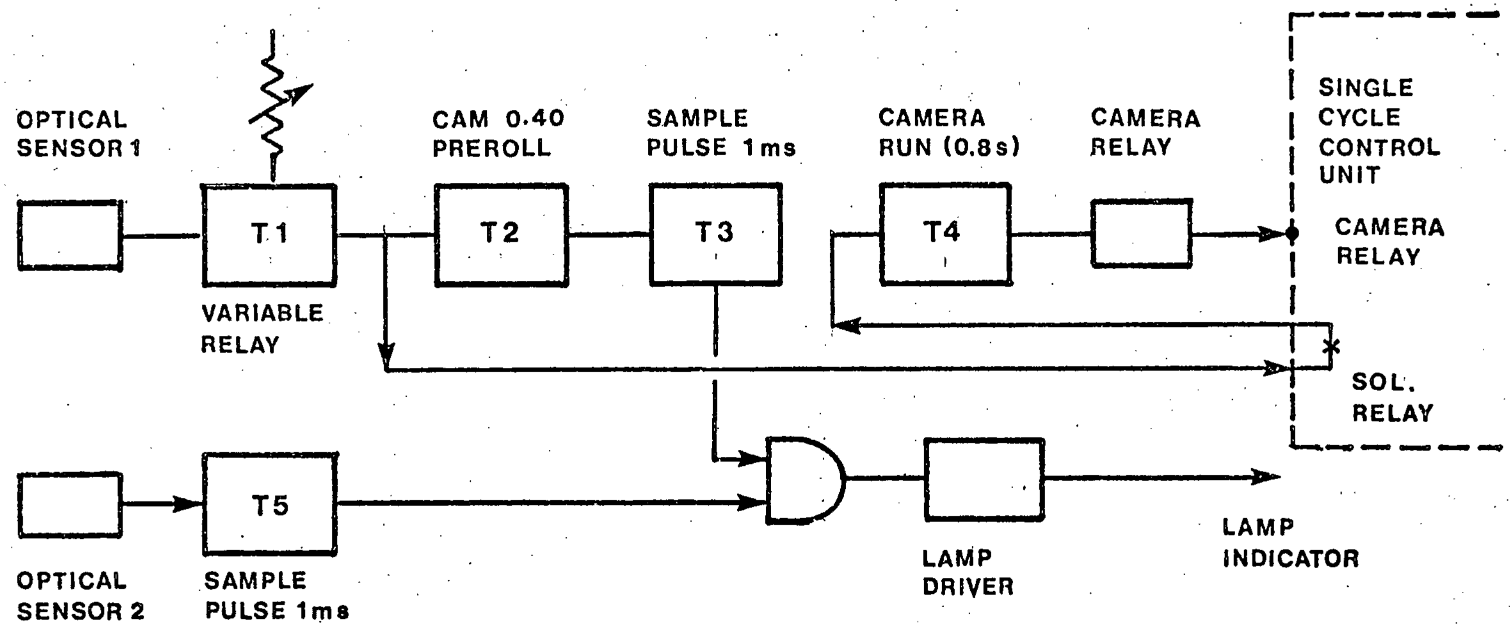

FIG. 3.6 CIRCUIT OPERATION BLOCK DIAGRAM FOR HIGH SPEED CAMERA SYNC.

closed contact position).

(iii) The ratchet relay steps to 'ON' as the drive arm contacts the micro switch (A) at the bottom of the stroke. This puts a signal on the solenoid relay (RL4) through the latch relay (RL2), and energizes the solenoid and hence the trippling mechanism.

(iv) When the drive arm contacts the micro switch (B) for the second time the ratchet relay steps to the 'OFF' position. The reset relay (RL) momentarily energizes and the latch relay (RL2) deenergizes via RL3.

3.3.2 Control for Synchronizing the High Speed Camera:

The block diagram of the sychronization control of high speed camera is given in Fig. (3.6). It consists of an optical sensor microswitch (A) to initiate a filming signal and an integrated circuit timers type 556 to give a variable time delay to the actuation of the camera relay and hence the camera.

Reference pulses of 1 m.sec duration are compared with the pulses received from the optical sensor no. 2. (in Fig. (3.6)) and when these correspond, a lamp indicator is triggered showing correct synchronization.

CHAPTER FOUR

EXPERIMENTAL PROCEDURE AND DISCUSSIONS

4.1. EXPERIMENTAL PROCEDURE

A plane strain upset compression test was made at an impact speed 15.7 ft./sec. The plane-strain specimen was made from plasticine using a metal mould. The specimen measuring 1"x1-1/2"x2" was cut with a fine wire and a lubricant of silicone grease was used to prevent the specimen from sticking in the mould.

The end surface of the specimen was sprayed with black paint and a square grid pattern was made by spraying white paint on the black surface through a wire mesh grid (14 mesh, inch.). The use of black and white paint gave good contrast for high speed photography.

Plane-strain conditions were obtained by placing the specimen on the lowest platen of the high speed impacting press between two parallel lubricated pexiglas plates (called a Kudo apparatus). The upper platen of the ram was adjusted to impact the specimen at the maximum velocity in the cycle and all controls and filming synchronization (as discussed in Chapter 3) appropriately set. The height of the camera was kept, such that the objective lens of the camera was on the same height as that of the specimen and the plane of specimen was parallel to the plane of the lens.(see Fig. A)

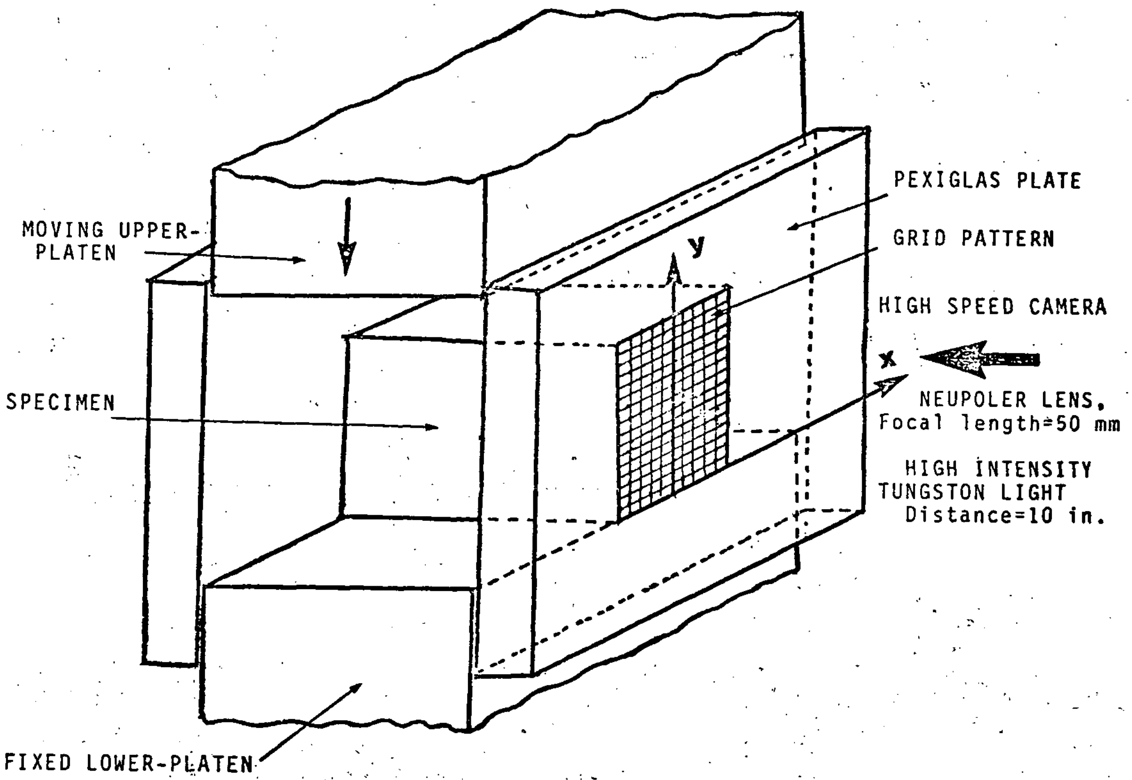

FIG. (A) LOCATION OF THE SPECIMEN IN KUDO APPARATUS

4.2. DISCUSSION

The grid points, for the dynamic plane strain upset compression test, were digitized at 0.00133 second time intervals (every 4th frame of the high speed film). Also results from a quasi-static plane-strain compression test done by Shabaik (71) (see Fig. 15) at a speed of 0.02 ft./min. were digitized. The digitized grid points are plotted for the four steps of quasi-static deformation in Fig. 4.1 and 4.2 and in Figs. 4.3 to 4.9 for the seven steps of dynamic deformation. The movement of certain grid-node points during deformation is plotted in Figs. 4.10 and 4.11.

The smoothed horizontal velocity (u) and vertical velocity (v) are given as a function of x and y in Figs. 4.12 to 4.15 for last time interval in both static and dynamic tests.

Plots of effective strain rate ($\dot{\bar{\varepsilon}}$) are given in Figs. 4.16 and 4.17, while total effective strain accumulated incrementally for all time intervals for the 0.02 ft./min. and for 15.7 ft./sec. deformation speeds are shown in Figs. 4.18 and 4.19.

The normal and shear stresses (σ_y, σ_x, τ_{xy}) are plotted as functions of x and y for the 0.02 ft./min. deformation speed in Figs. 4.20, 4.21 and 4.22, and for the 15.7 ft./sec. deformation speed in Figs. 4.23, 4.24 and 4.25. The values of σ (o,a) for 0.02 ft./min. deformation speed was taken from reference (71) as 31000 psi at the origin with the relationship between effective stress and strain as $\bar{\sigma} = 31000\ \bar{\varepsilon}^{\,0.25}$. The values of σ (o,a) for the plasticine specimen was taken as 20 psi at the origin from reference (79). The stresses σ_x and τ_{xy} are also plotted as a function of x for the 0.02 ft./min. deformation speed in Figs. 4.26 and 4.27 and for 15.7 ft./sec. deformation speed in Figs. 4.28 and 4.29.

The results from the specimen deformed at 0.02 ft./min. agree closely with well documented results for quasi-static deformation showing a'friction hill' type of normal (σ_y) interface stress distribution with maximum stress occurring at the central portion of the specimen. The normal stress distribution for the specimen deformed at 15.7 ft/sec is radically different, showing a saddle type distribution of normal stress, with the maximum stress occurring near the periphery of the contact zone. The interface shear stress distributions also change form with strain rate.

The dramatic change of normal stress distribution with strain rate is totally at variance with currently held views and furthermore it occurs at quite moderate velocities which are certainly well within the range of those encountered in many metal forming operations.

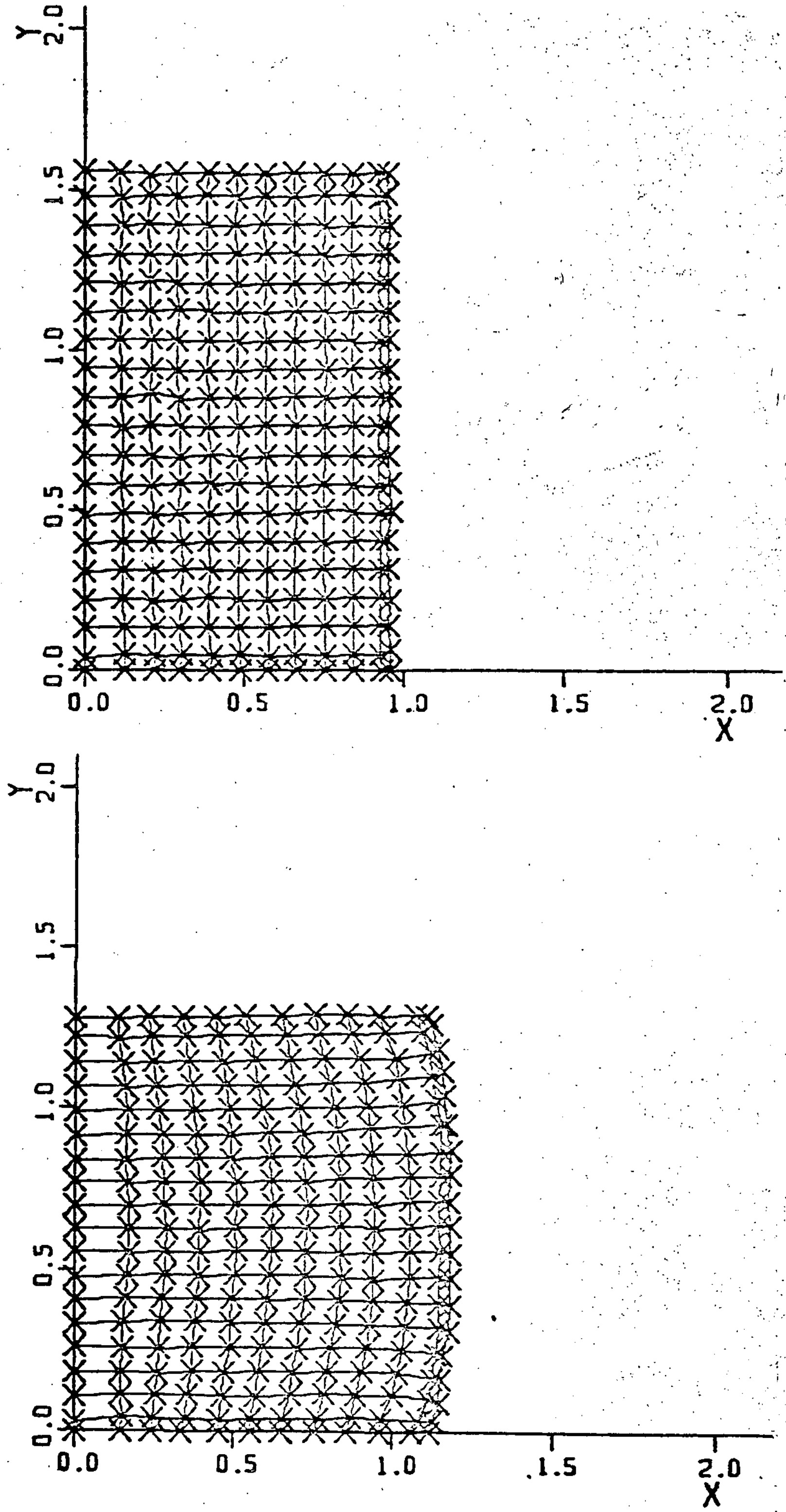

FIG.4.1 DISTORTION OF GRID LINES DURING DEFORMATION FOR 0.02 FT./MIN. DEFORMATION SPEED.

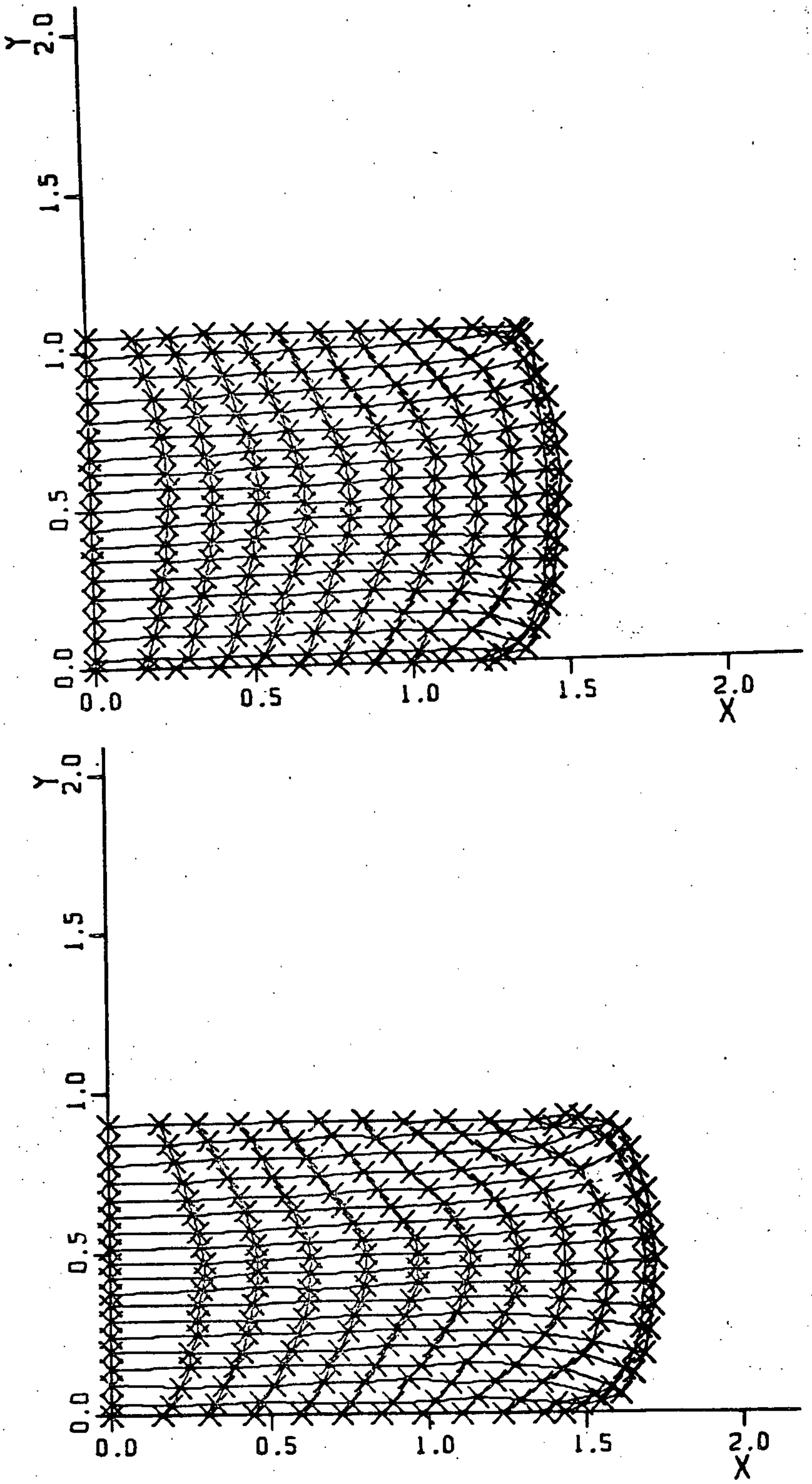

FIG. 4.2 DISTORTION OF GRID LINES DURING DEFORMATION FOR 0.02 FT./MIN DEFORMATION SPEED.

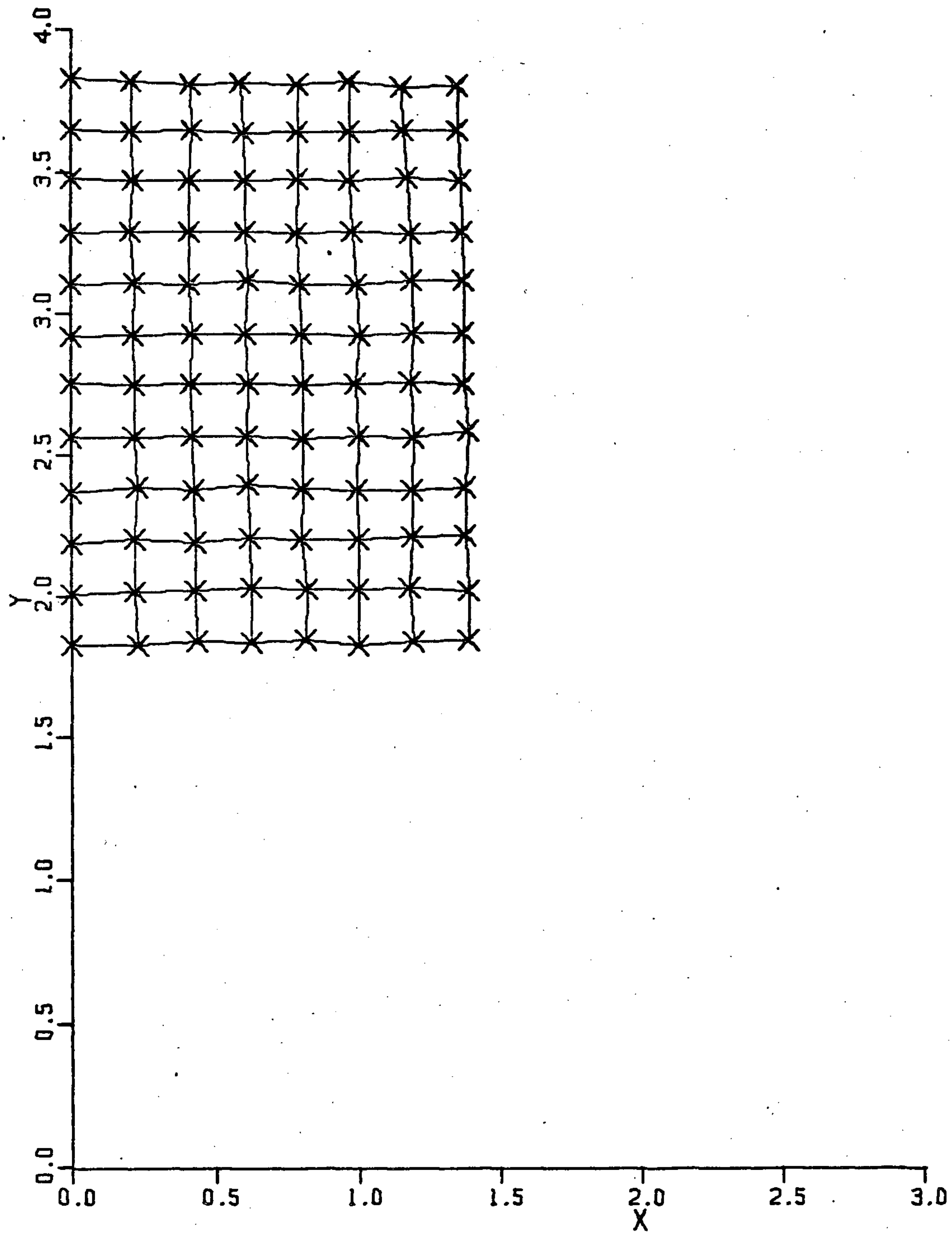

FIG.4.3 DISTORTION OF GRID LINES DURING DEFOMATION FOR 15.7 FT./SEC. DEFORMATION SPEED.

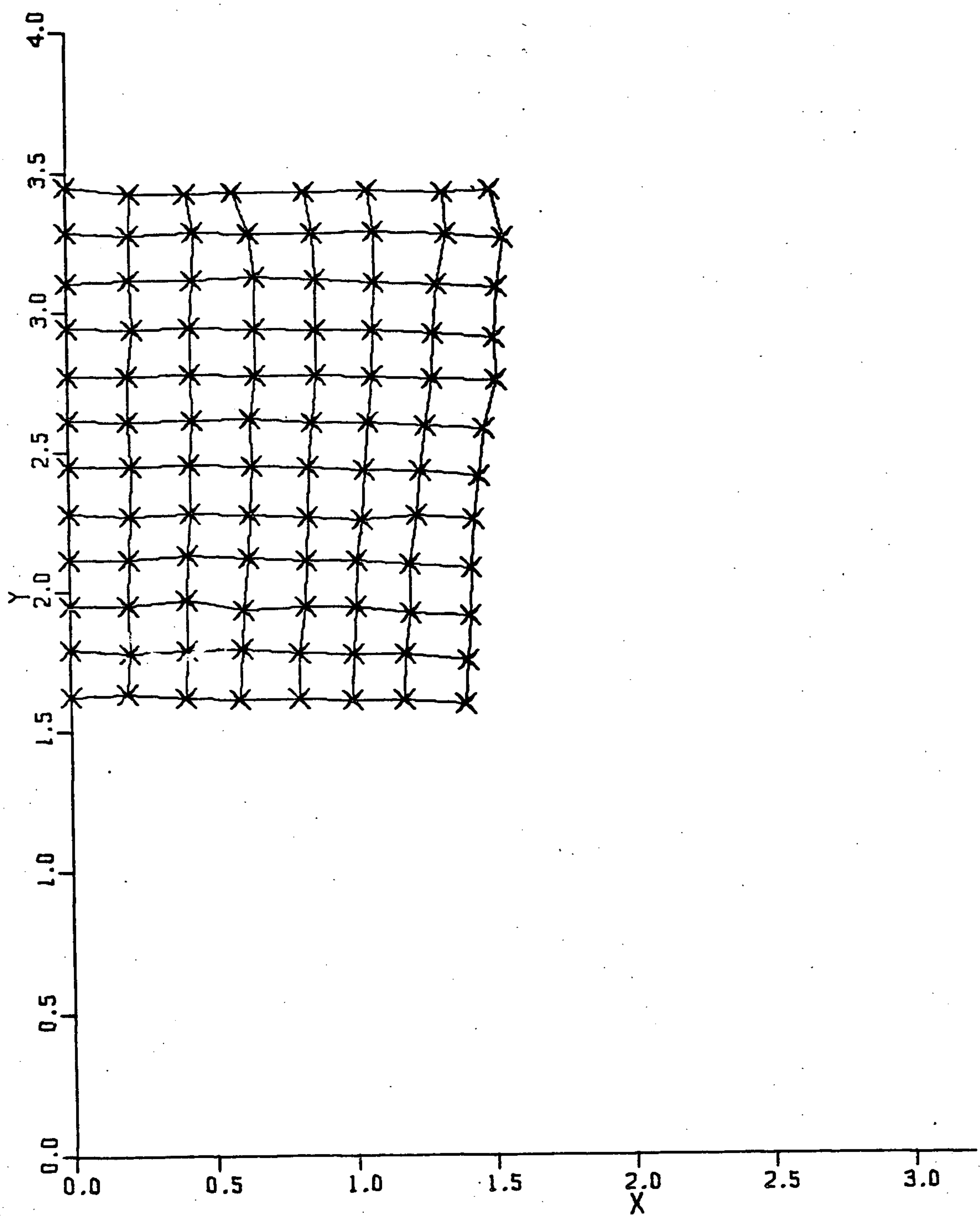

FIG.4.4 DISTORTION OF GRID LINES DURING DEFOMATION FOR 15.7 FT./SEC. DEFORMATION SPEED.

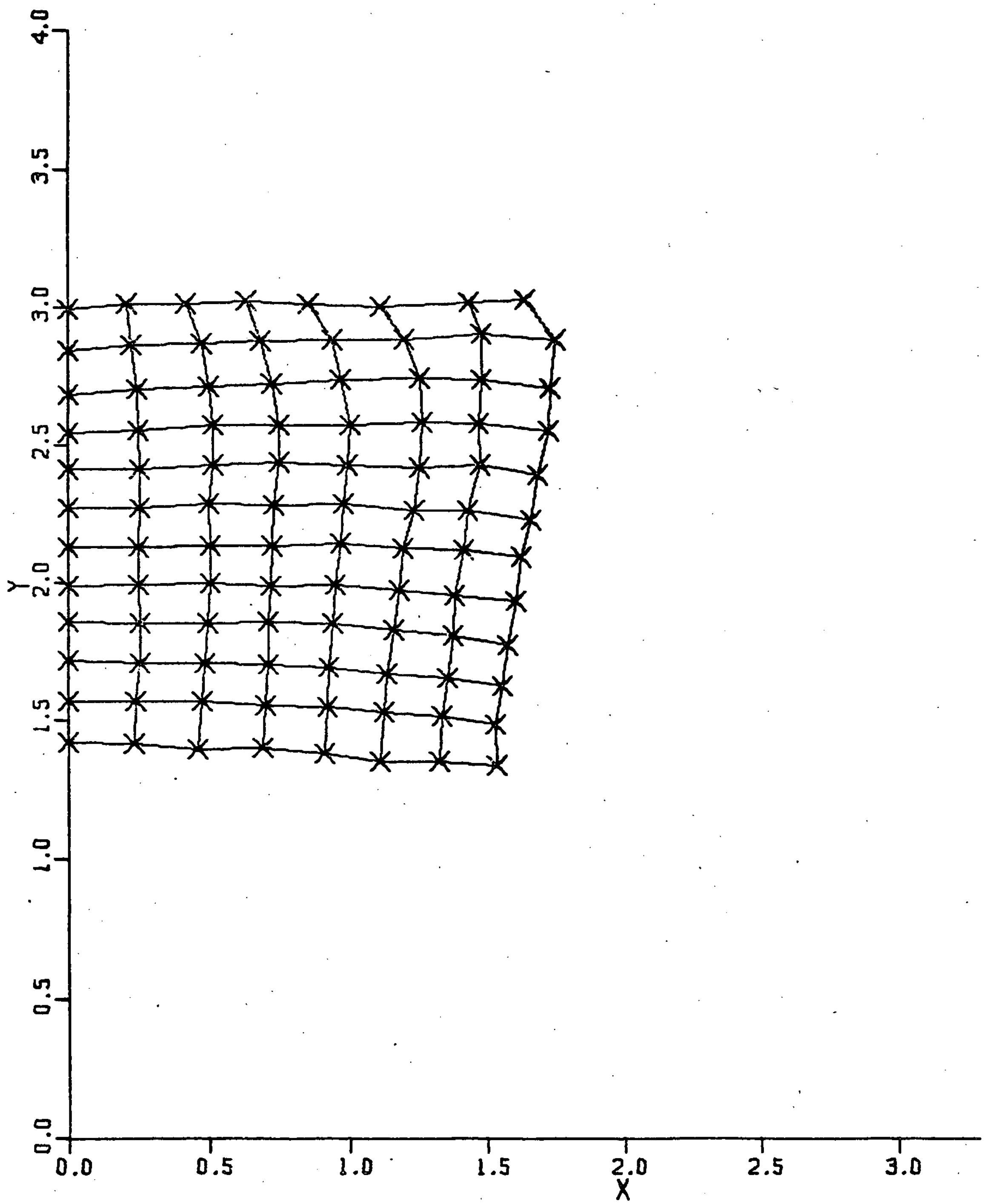

FIG.4.5 DISTORTION OF GRID LINES DURING DEFOMATION FOR 15.7 FT./SEC. DEFORMATION SPEED.

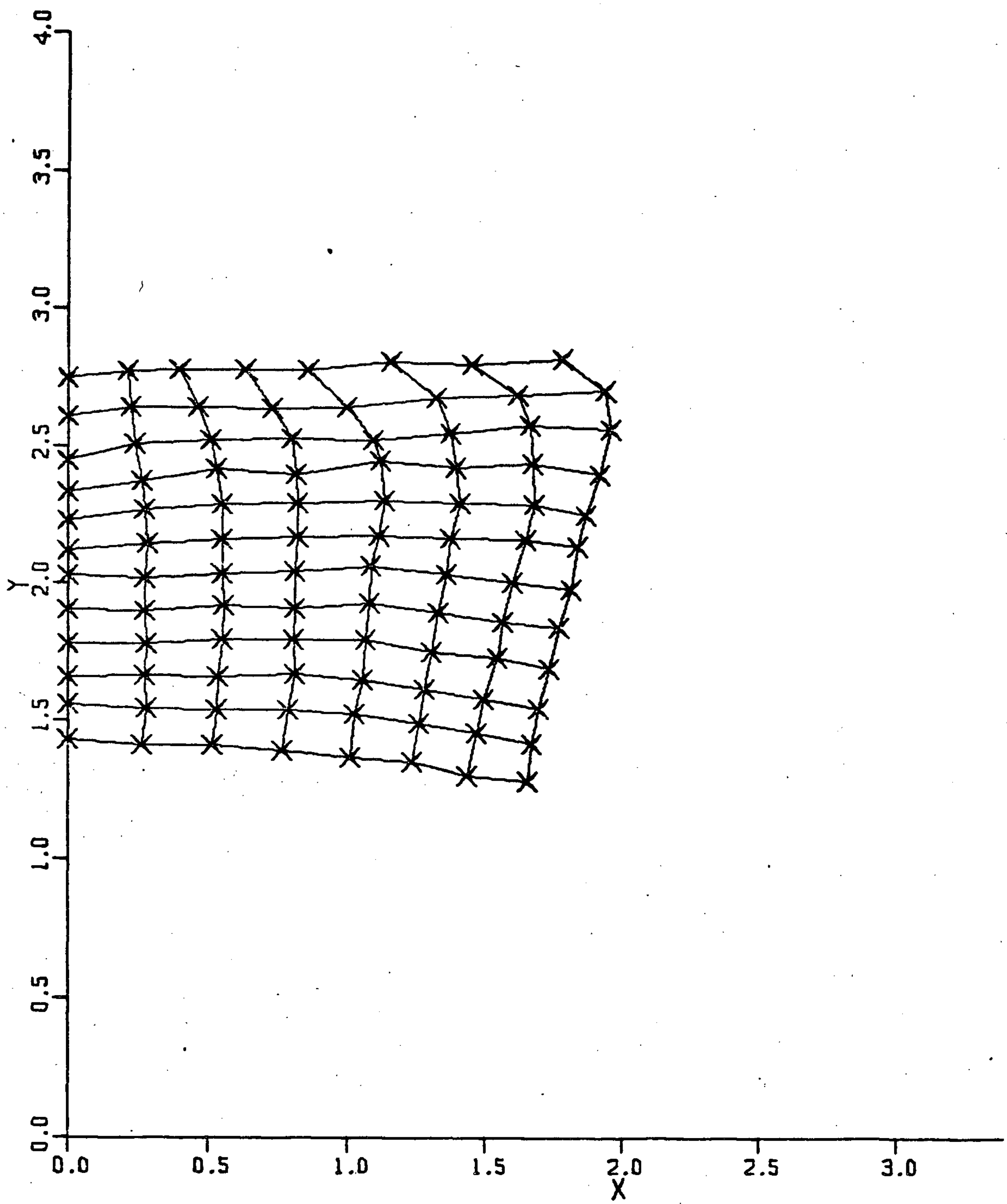

FIG. 4.6 DISTORTION OF GRID LINES DURING DEFOMATION FOR 15.7 FT./SEC. DEFORMATION SPEED.

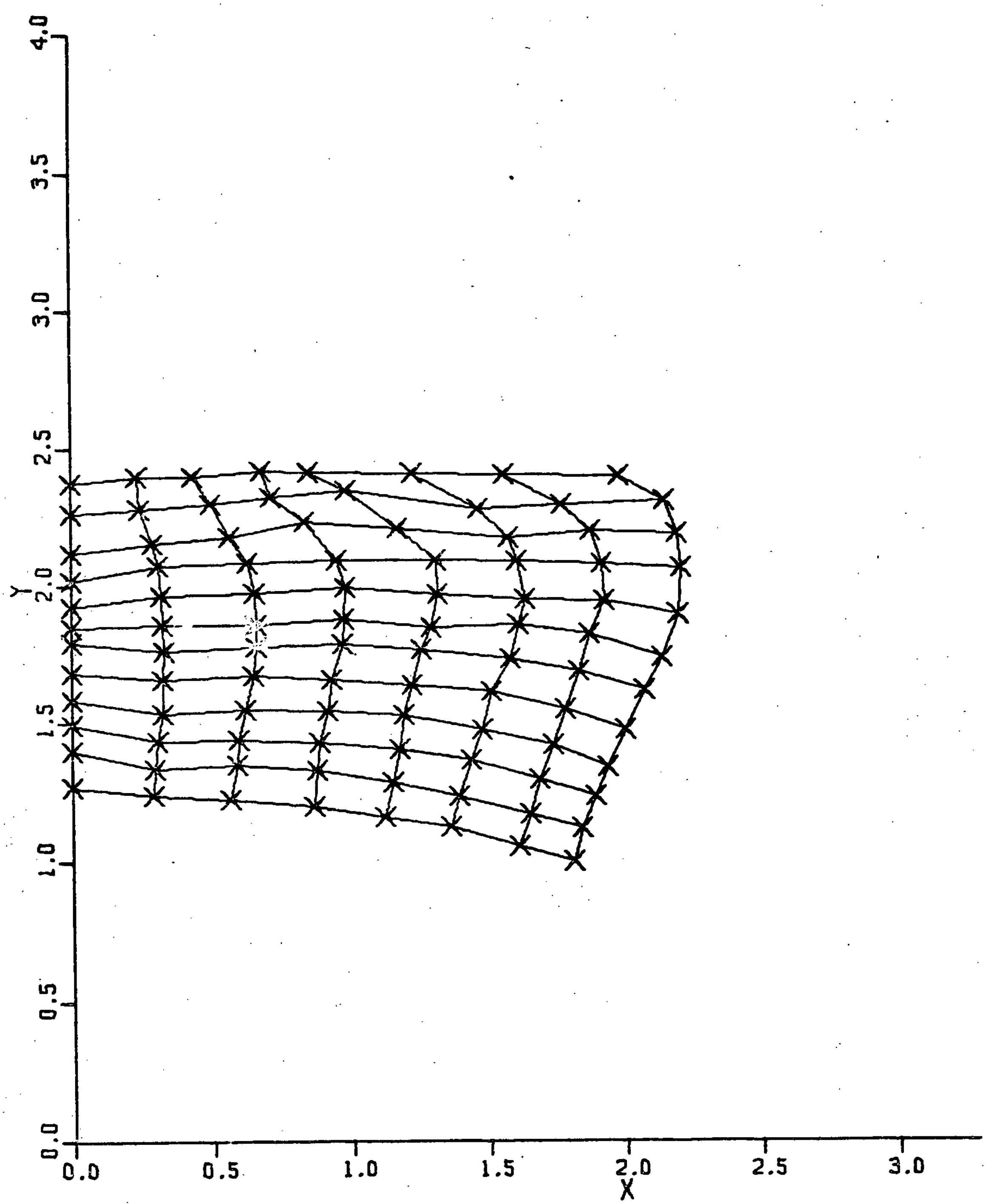

FIG.4.7 DISTORTION OF GRID LINES DURING DEFOMATION FOR 15.7 FT./SEC. DEFORMATION SPEED.

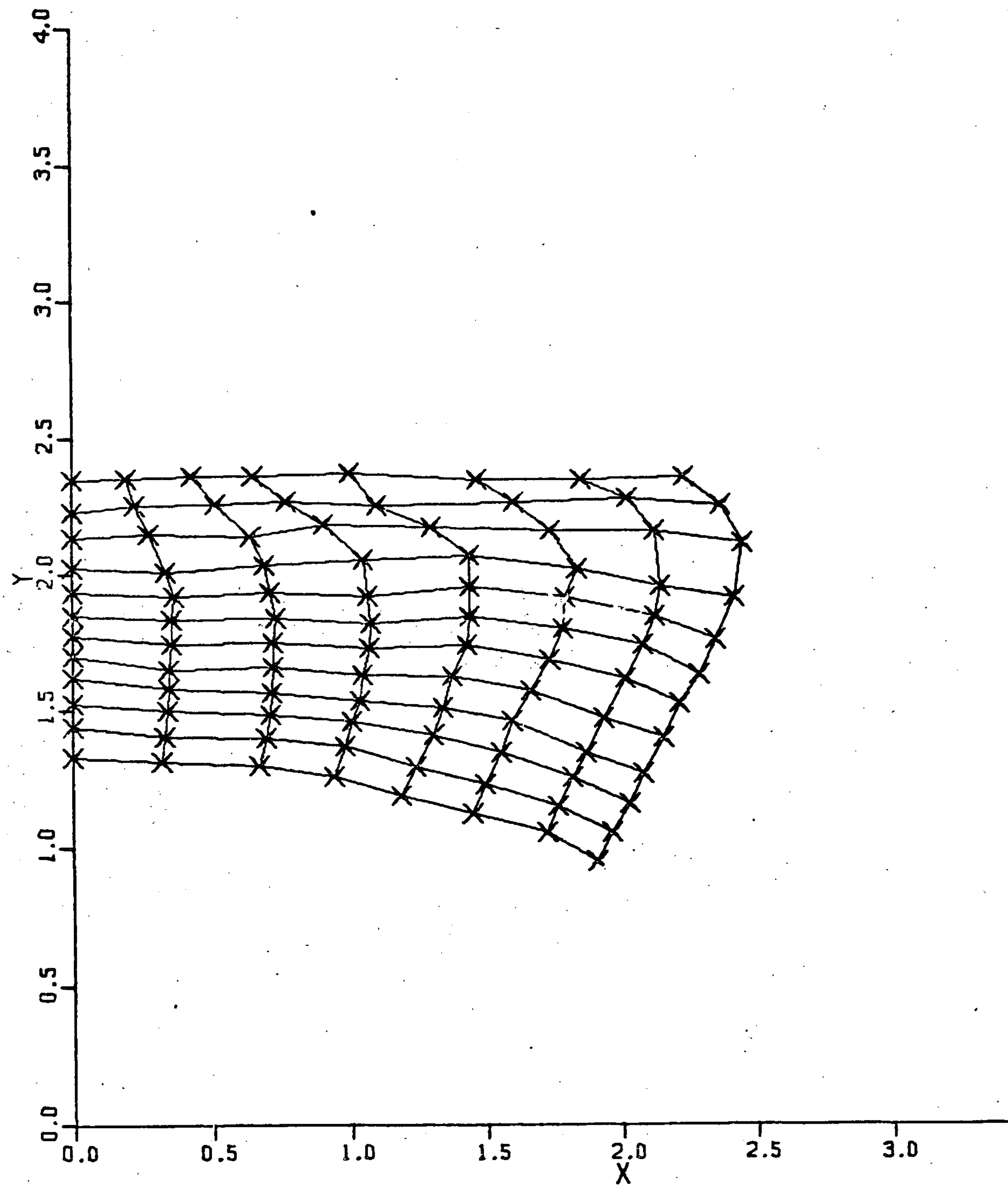

FIG.4.8 DISTORTION OF GRID LINES DURING DEFOMATION FOR 15.7 FT./SEC. DEFORMATION SPEED.

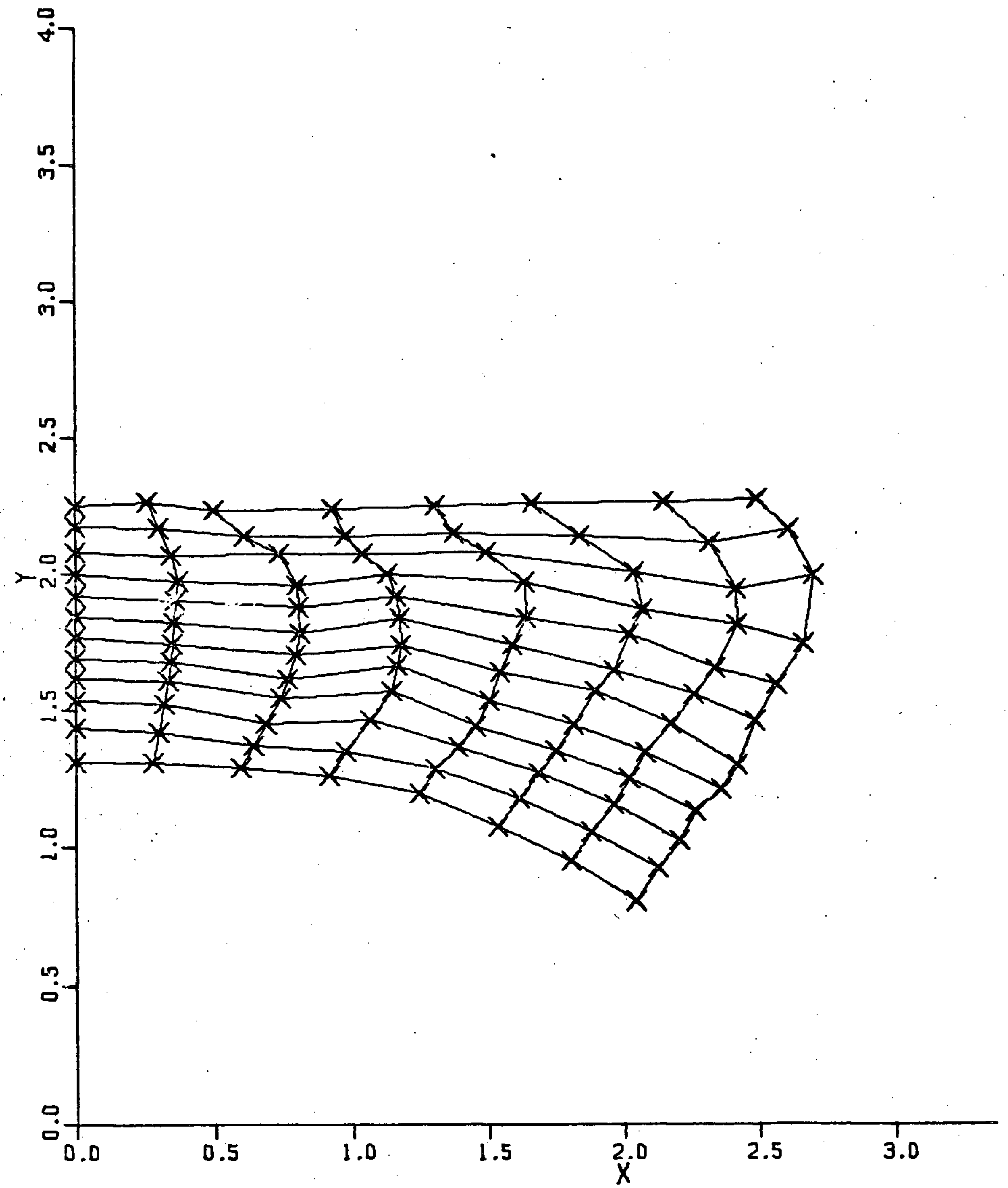

FIG.4.9 DISTORTION OF GRID LINES DURING DEFOMATION FOR 15.7 FT./SEC. DEFORMATION SPEED.

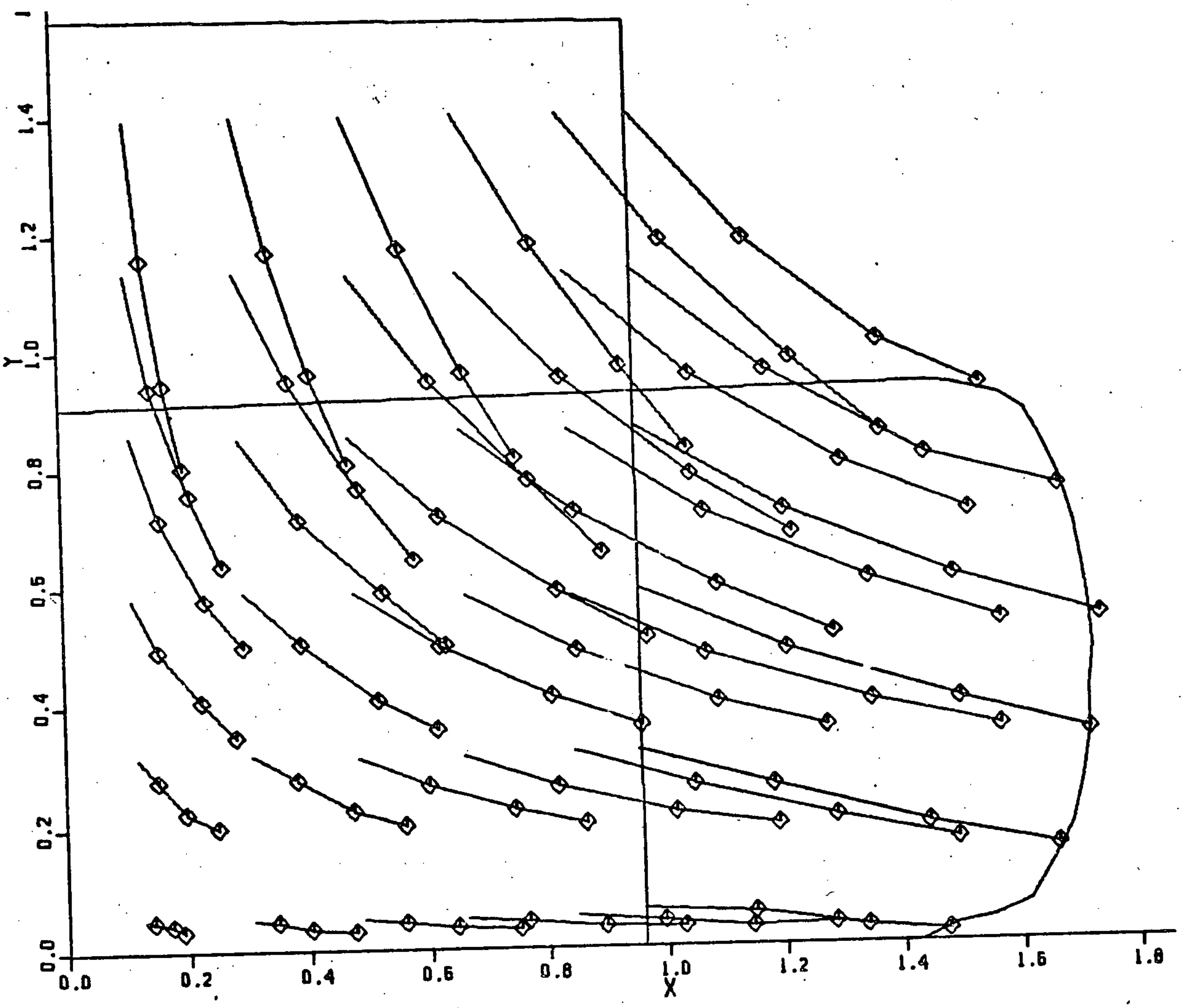

FIG.4.10 GRID NODE POINT MOVEMENT DURING DEFORMATION FOR 0.02 FT/MIN DEFORMATION SPEED.

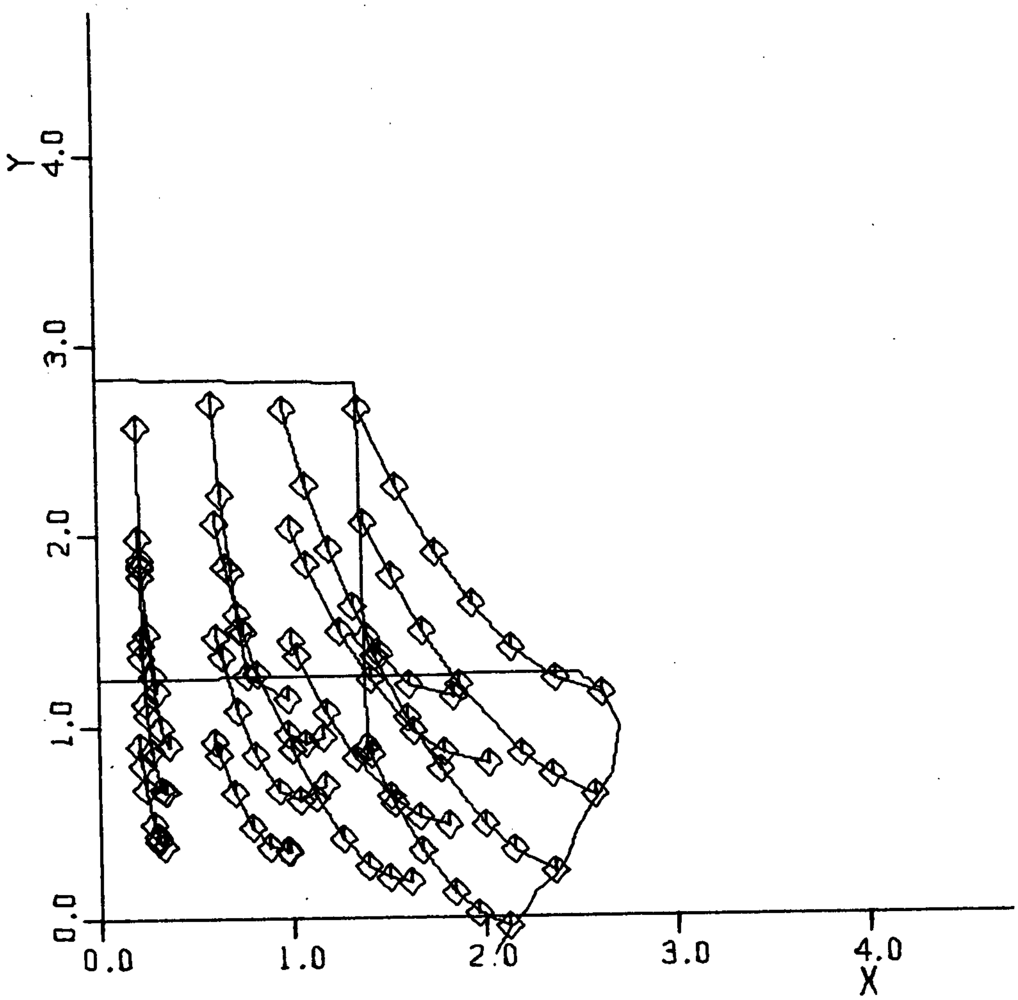

FIG.4.11 GRID NODE POINT MOVEMENT DURING DEFORMATION FOR 15.7 FT/SEC. DEFORMATION SPEED.

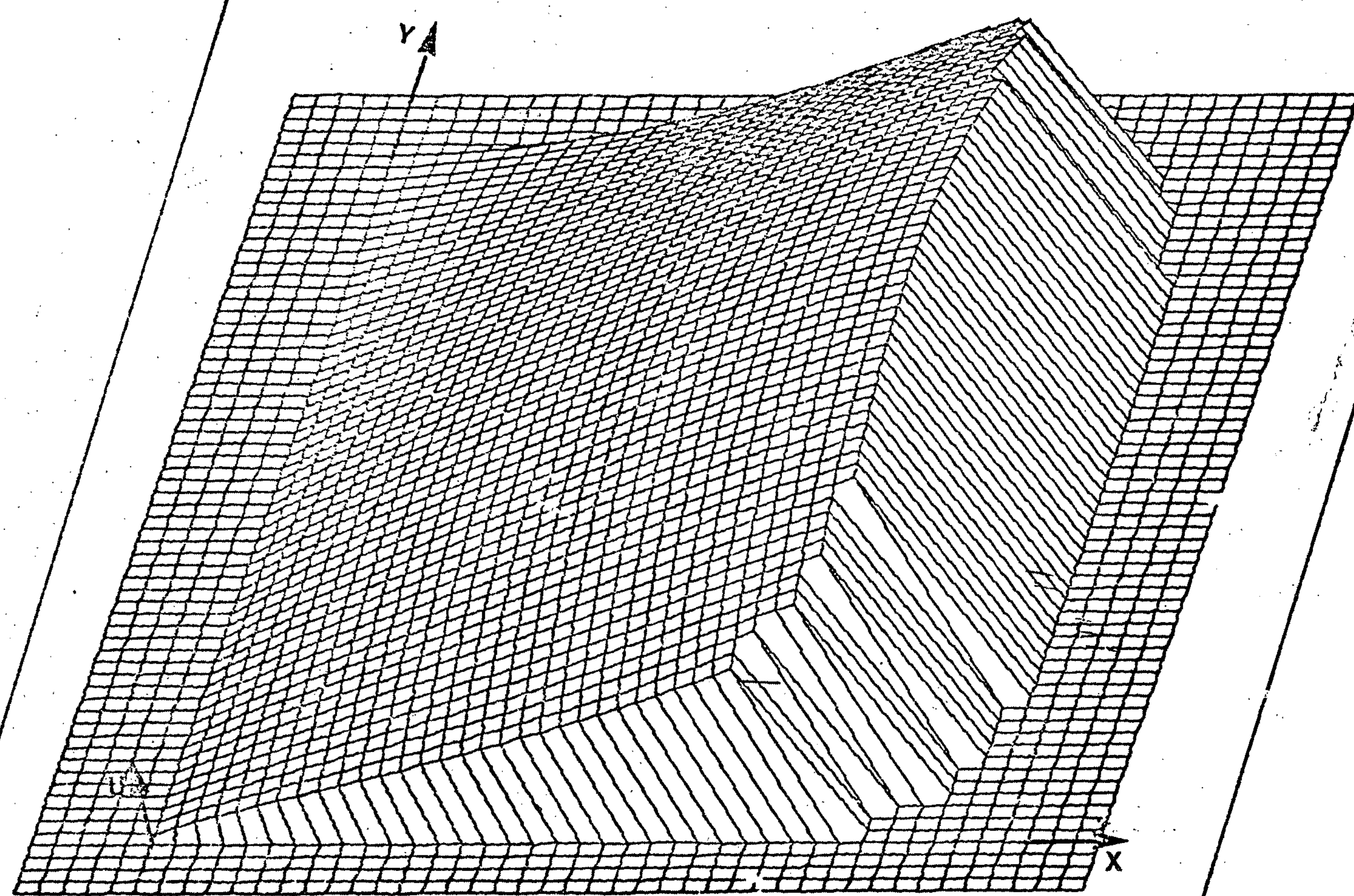

FIG.4.1 2 THREE DIMENSIONAL PLOT OF HORIZONTAL VELOCITY (**u**) AS A FUNCTION OF X AND Y FOR 0.02 FT./MIN DEFORMATION SPEED.

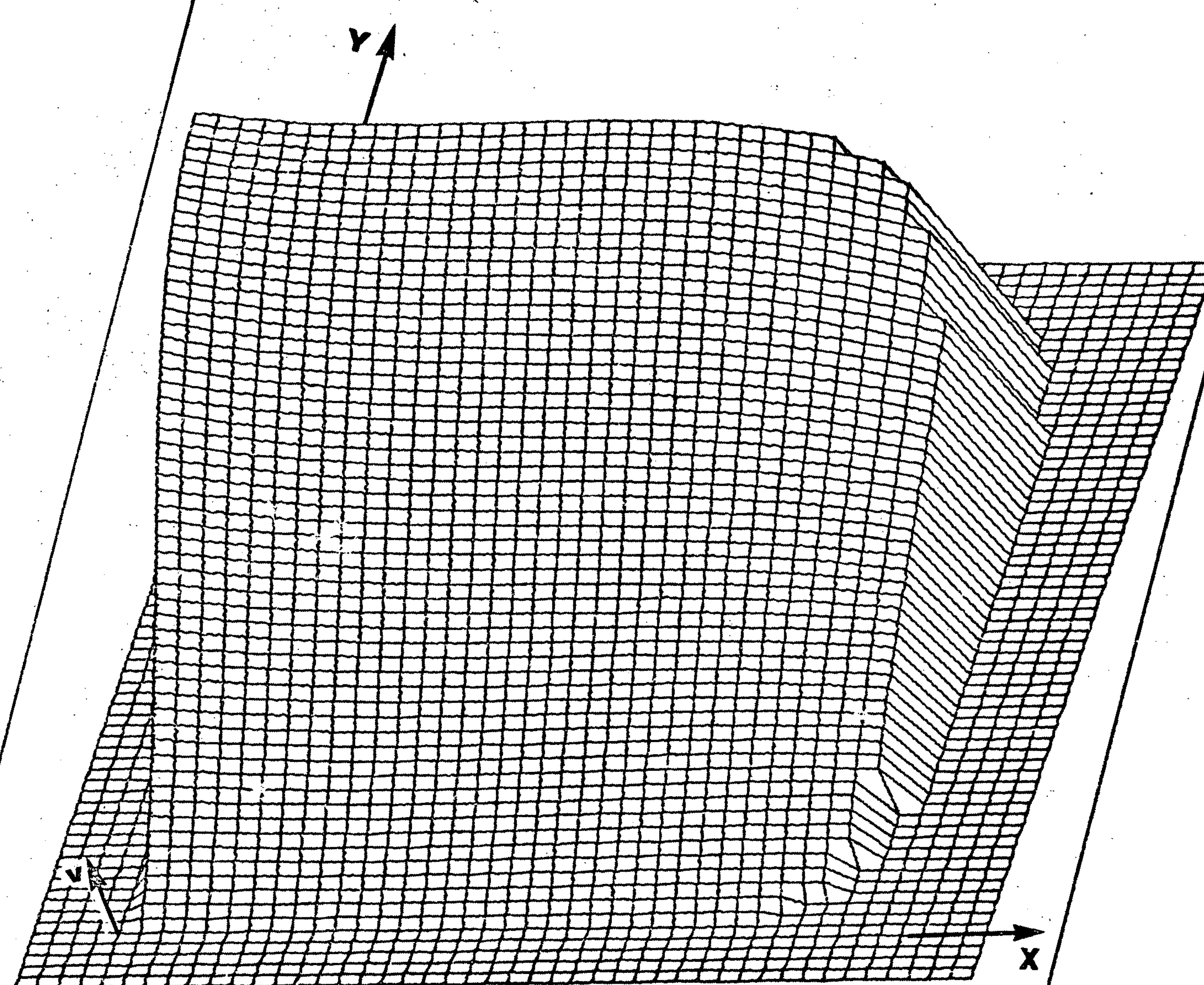

FIG4.13 THREE DIMENSIONAL PLOT OF VERTICAL VELOCITY (v) AS FUNCTION OF X AND Y FOR 0.02 FT./MIN. DEFORMATION SPEED.

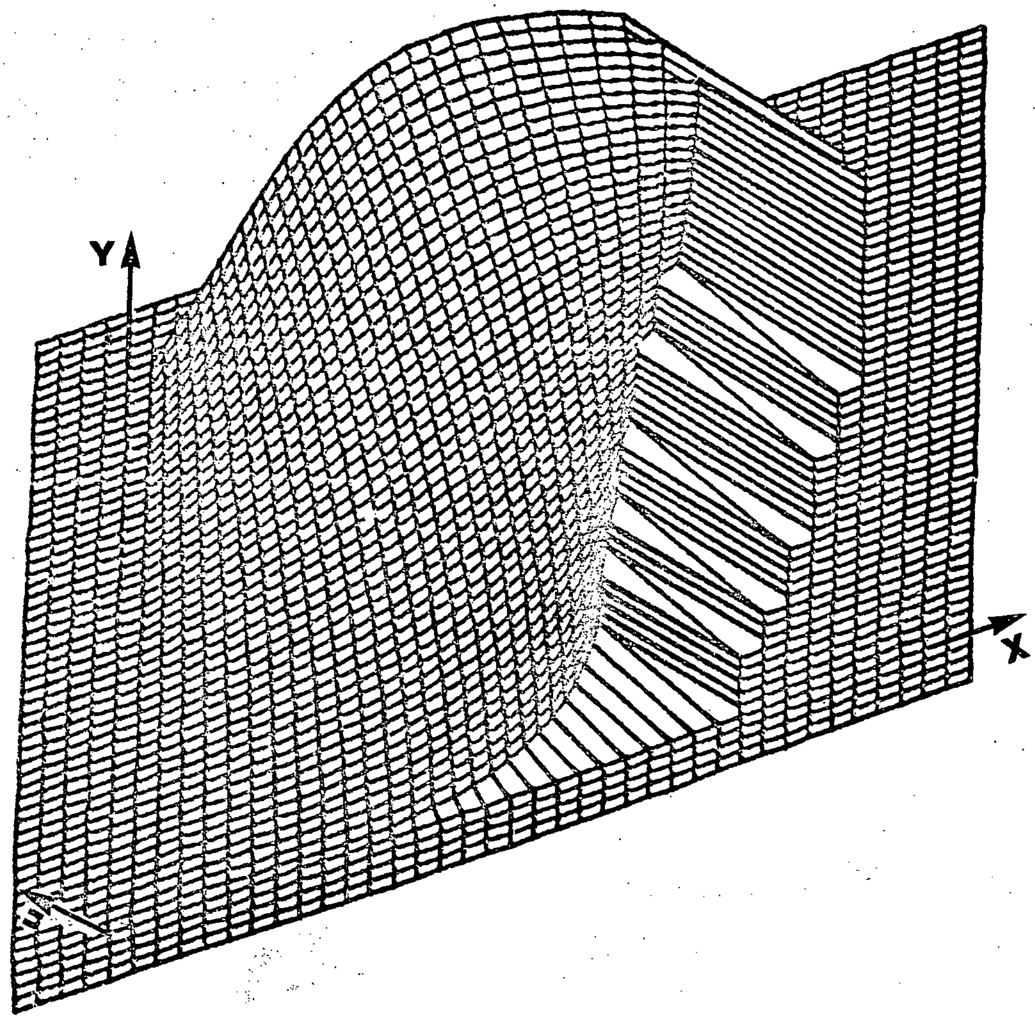

FIG.4.14 THREE DIMENSIONAL PLOT OF HORIZONTAL VELOCITY (u) AS A FUNCTION OF X AND Y FOR 15.7 FT./SEC. DEFORMATION SPEED.

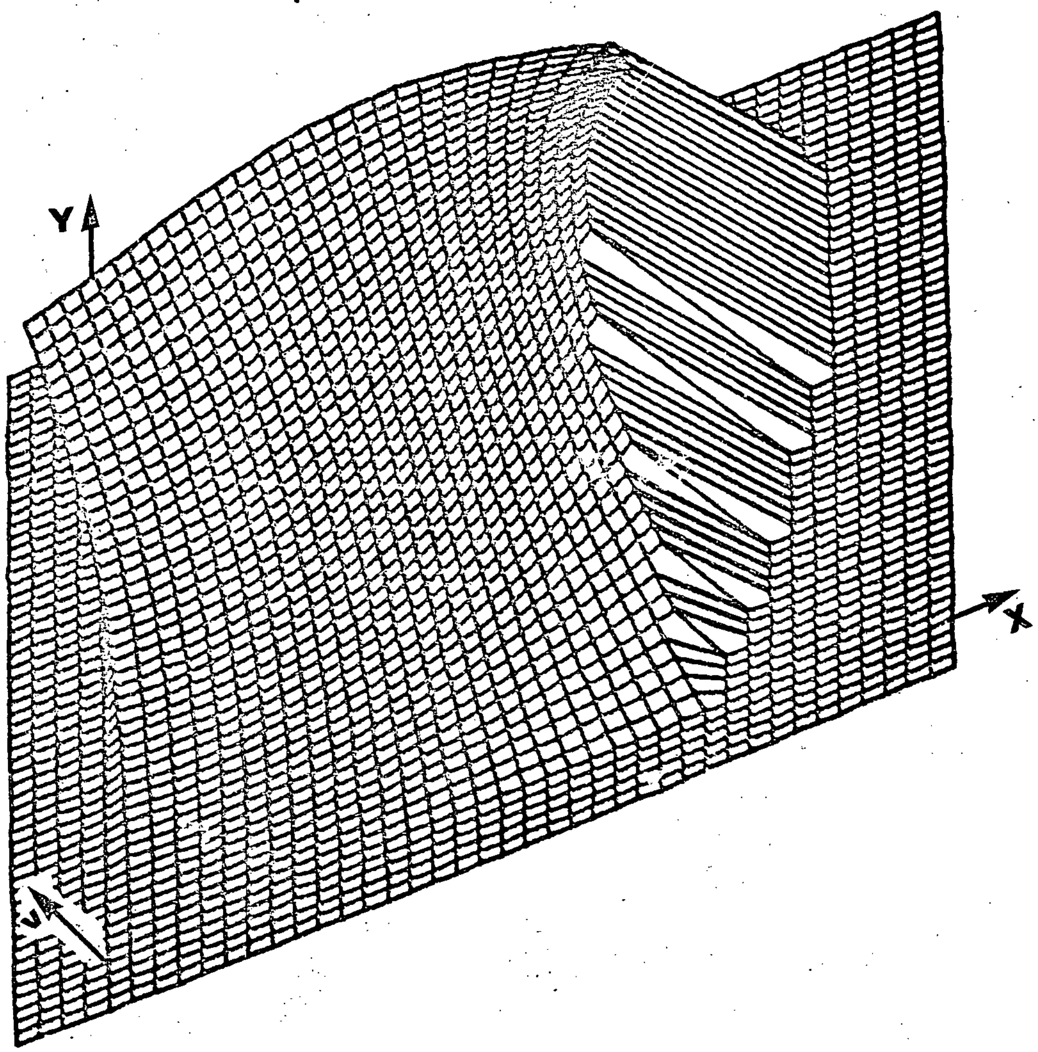

FIG. 4.15 THREE DIMENSIONAL PLOT OF VERTICAL VELOCITY (V) AS A FUNCTION OF X AND Y FOR 15.7 FT./SEC. DEFORMATION SPEED.

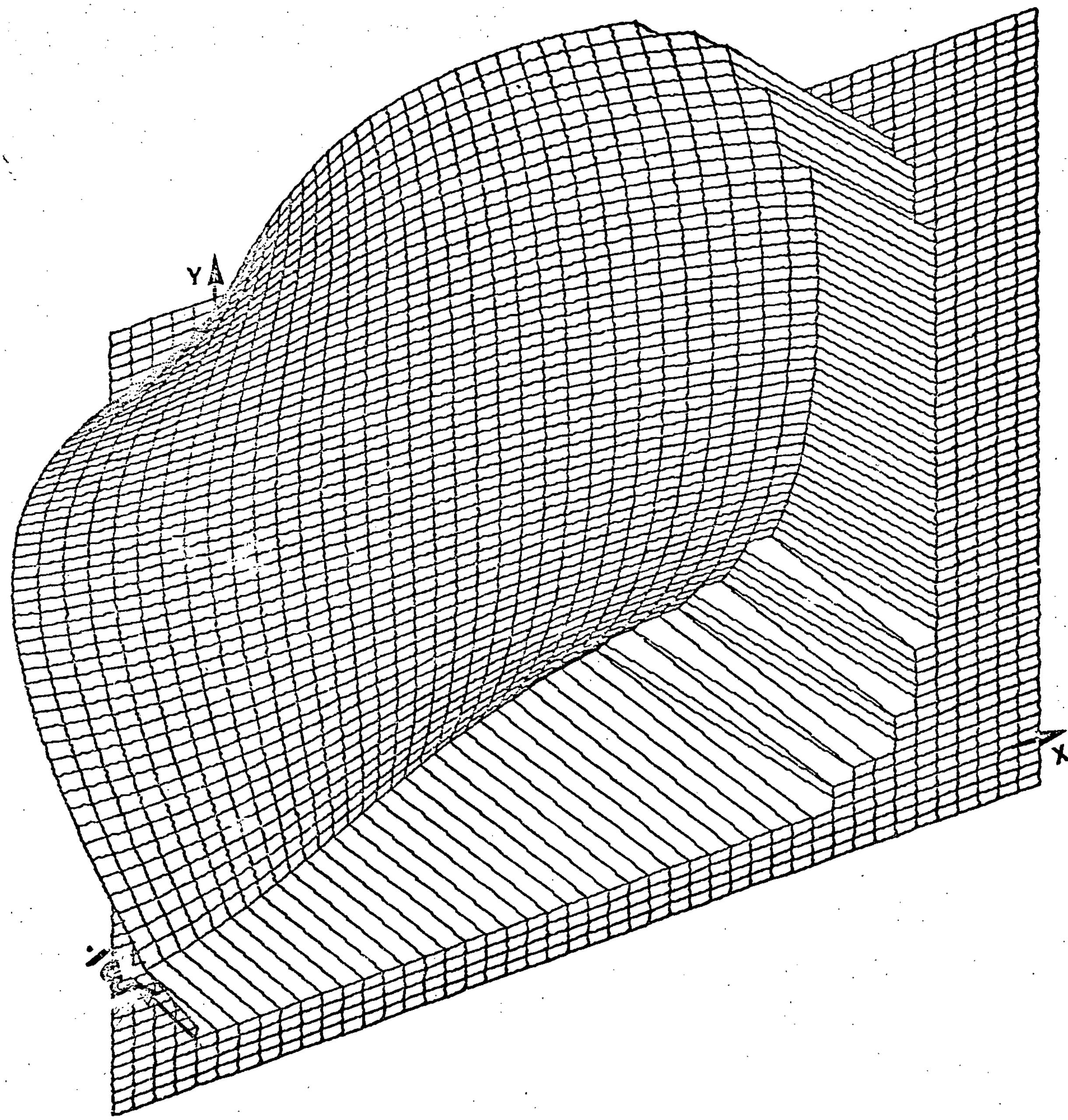

FIG.4.16 THREE DIMENSIONAL PLOT OF EFFECTIVE STRAIN-RATE ($\dot{\bar{\varepsilon}}$) AS FUNCTION OF X AND Y FOR 0.02 FT./MIN DEFORMATION SPEED.

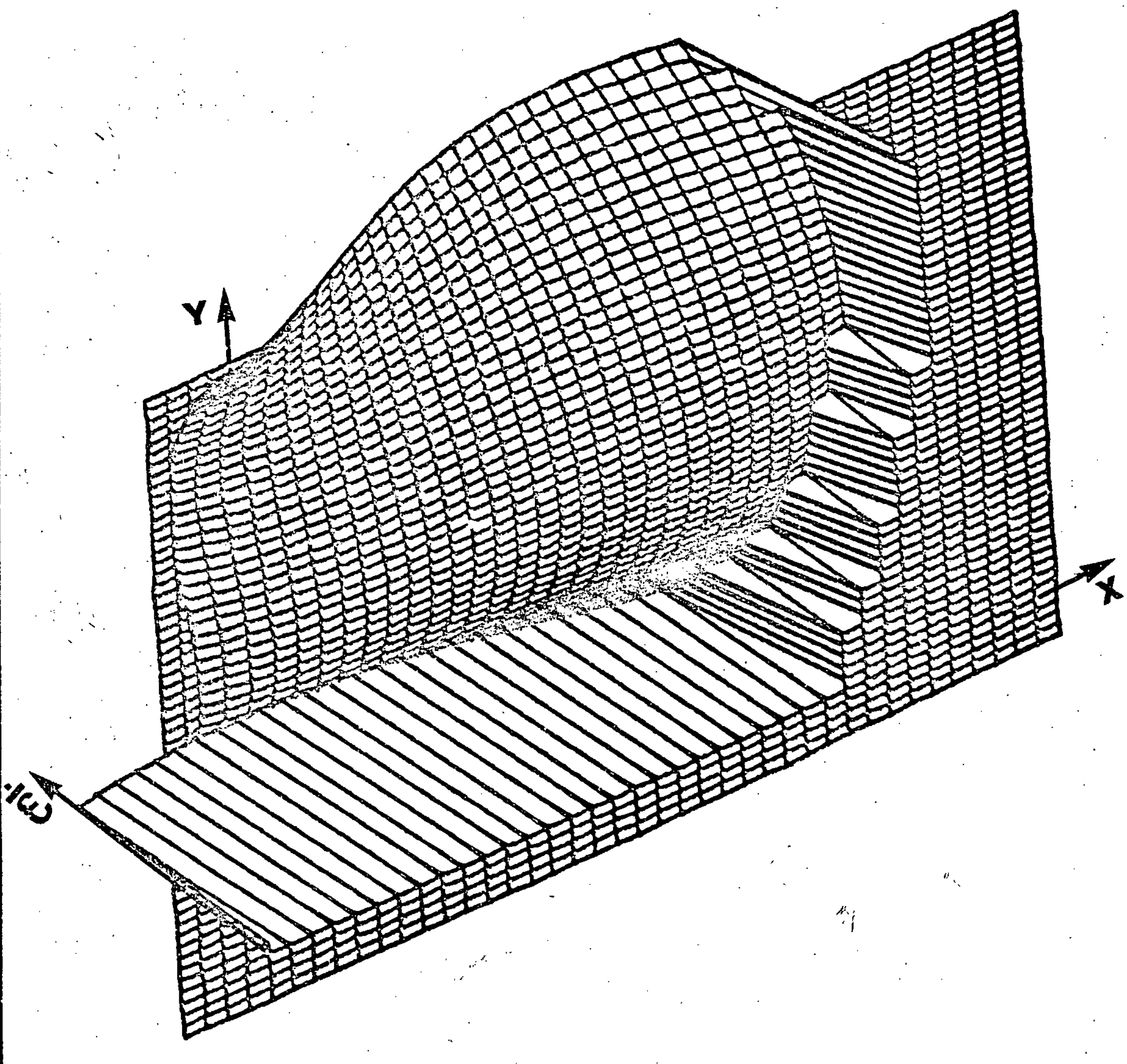

FIG. 4.17 THREE DIMENSIONAL PLOT OF EFFECTIVE STRAIN-RATE ($\dot{\bar{\varepsilon}}$) AS FUNCTION OF X AND Y FOR 15.7 FT./SEC. DEFORMATION SPEED.

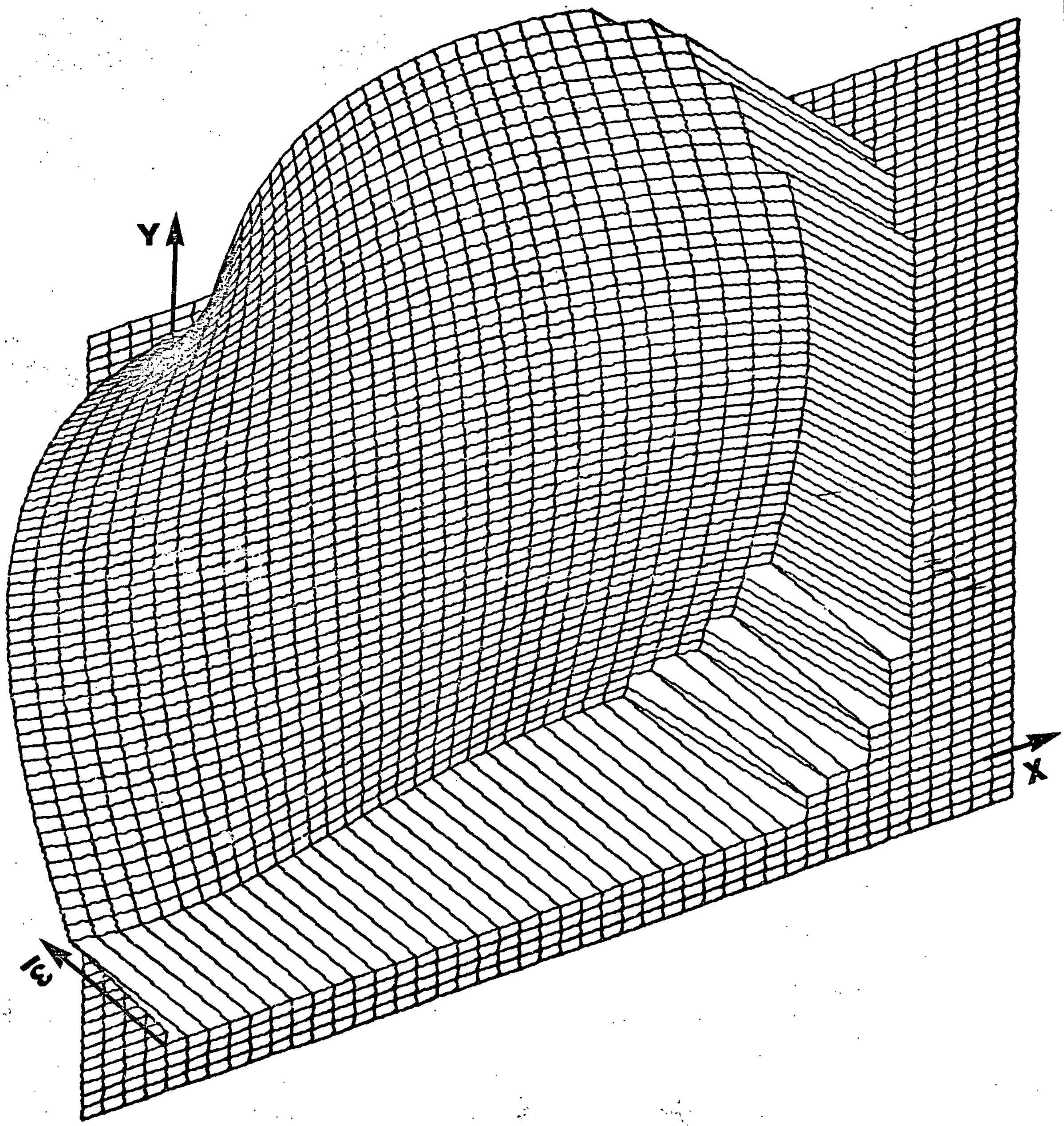

FIG.4.18 THREE DIMENSIONAL PLOT OF TOTAL EFFECTIVE STRAIN ($\bar{\varepsilon}$) AS FUNCTION OF X AND Y FOR DEFORMATION SPEED OF 0.02 FT./MIN.

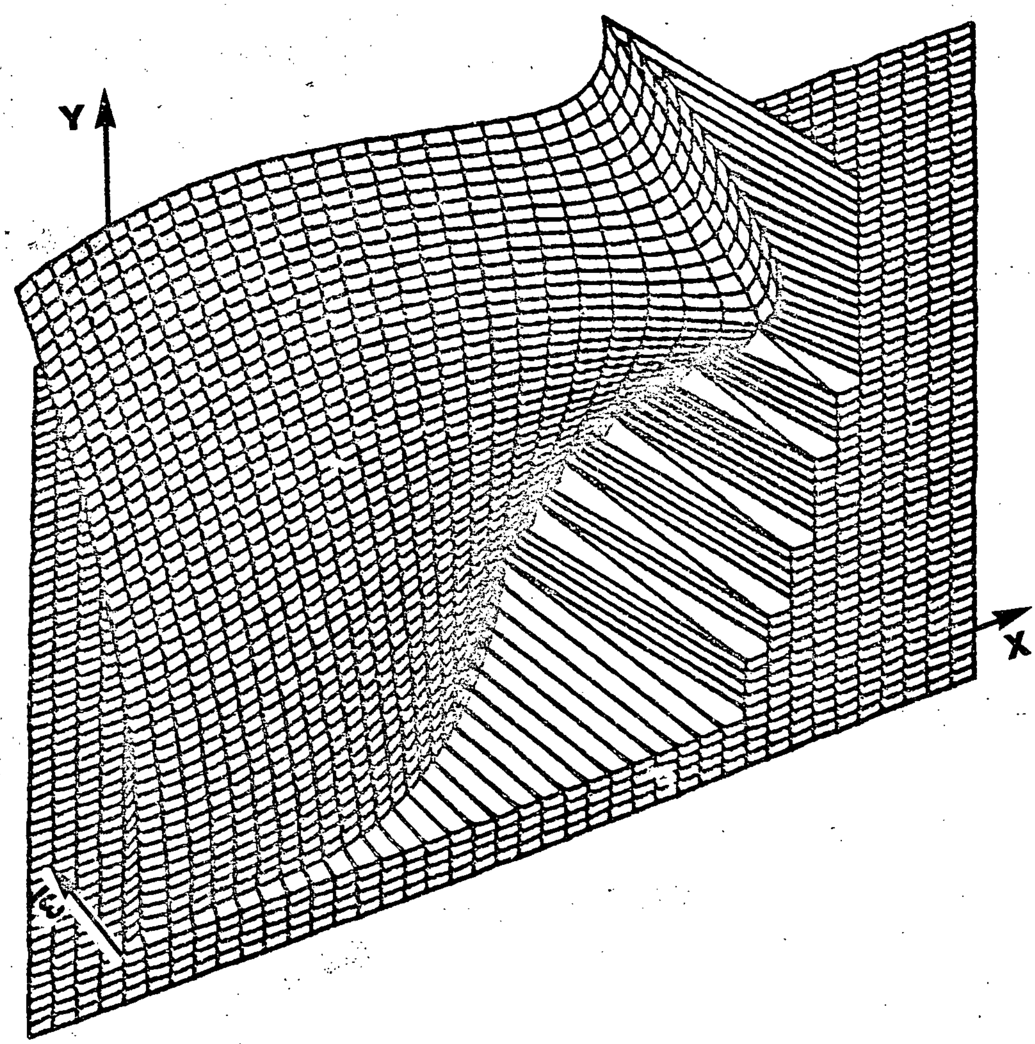

FIG.4.19 THREE DIMENSIONAL PLOT OF TOTAL EFFECTIVE STRAIN ($\bar{\varepsilon}$).
AS FUNCTION OF X AND Y FOR 15.7 FT./SEC DEFORMATION SPEED.

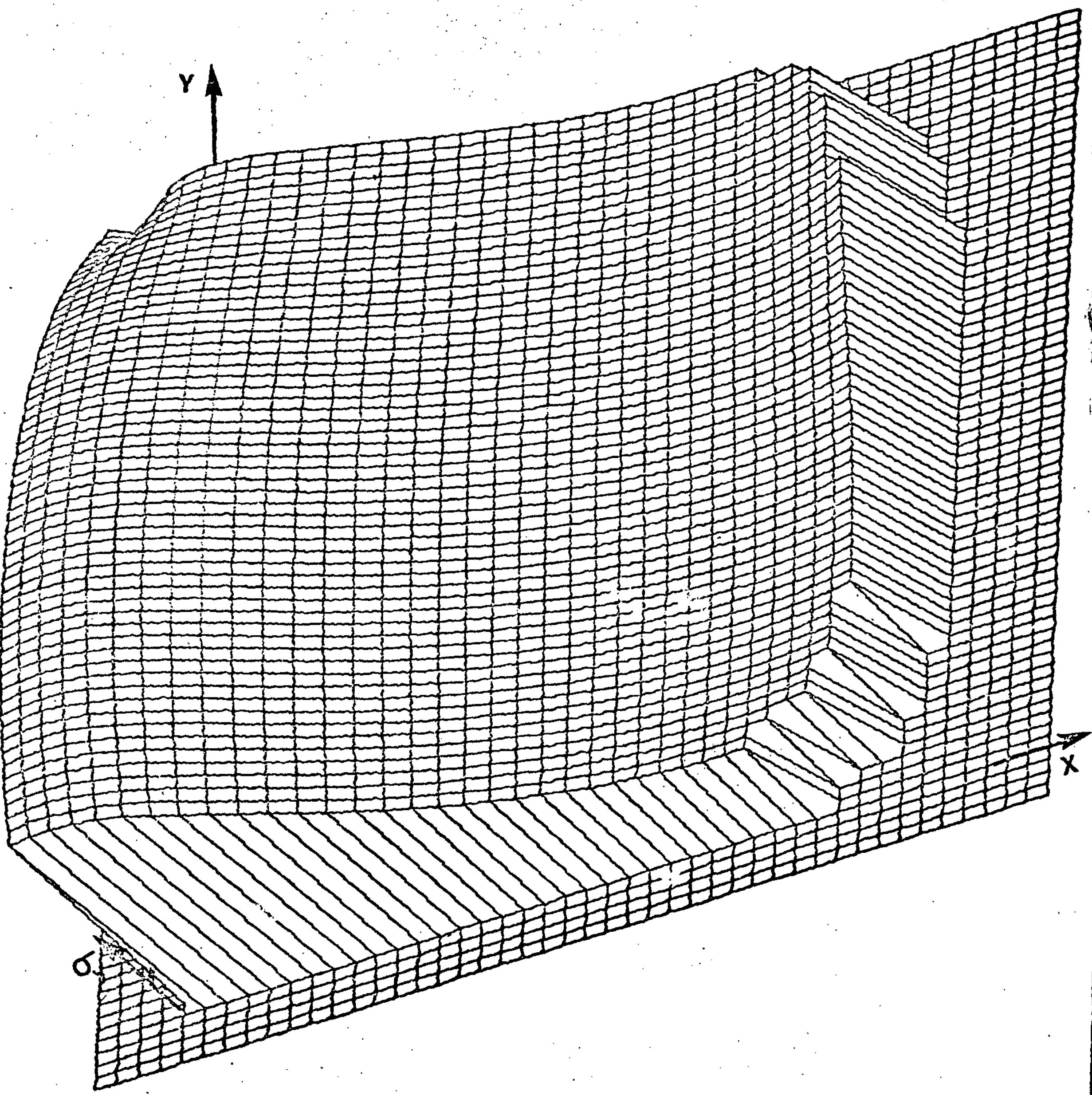

FIG. 4.20 THREE DIMENSIONAL PLOT OF NORMAL STRESS (σ_y) AS FUNCTION OF X AND Y FOR 0.02 FT./MIN DEFORMATION SPEED.

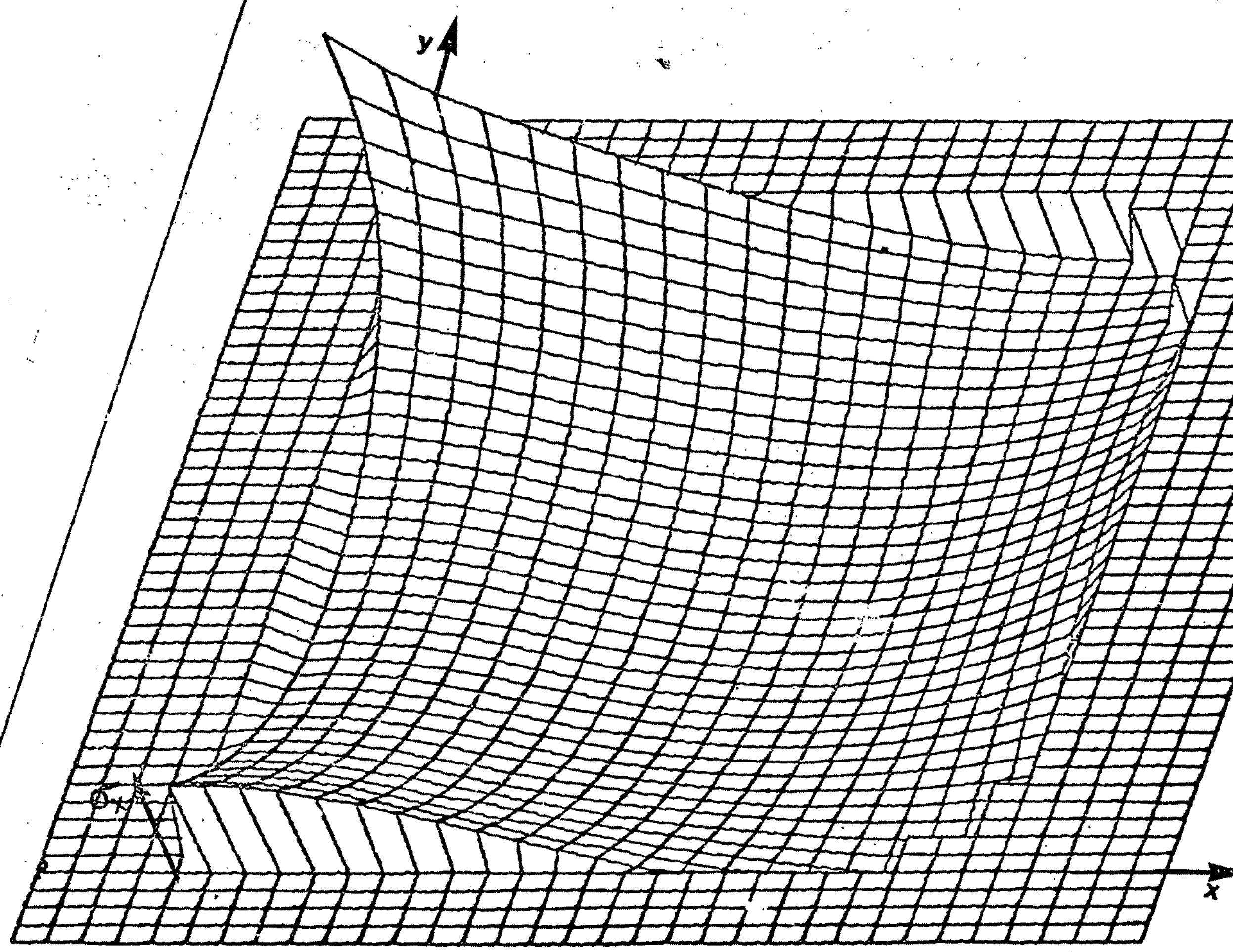

FIG.4.21 THREE DIMENSIONAL PLOT OF NORMAL STRESS (σ_x) AS FUNCTION OF X AND Y FOR DEFORMATION SPEED OF 0.02 FT./MIN.

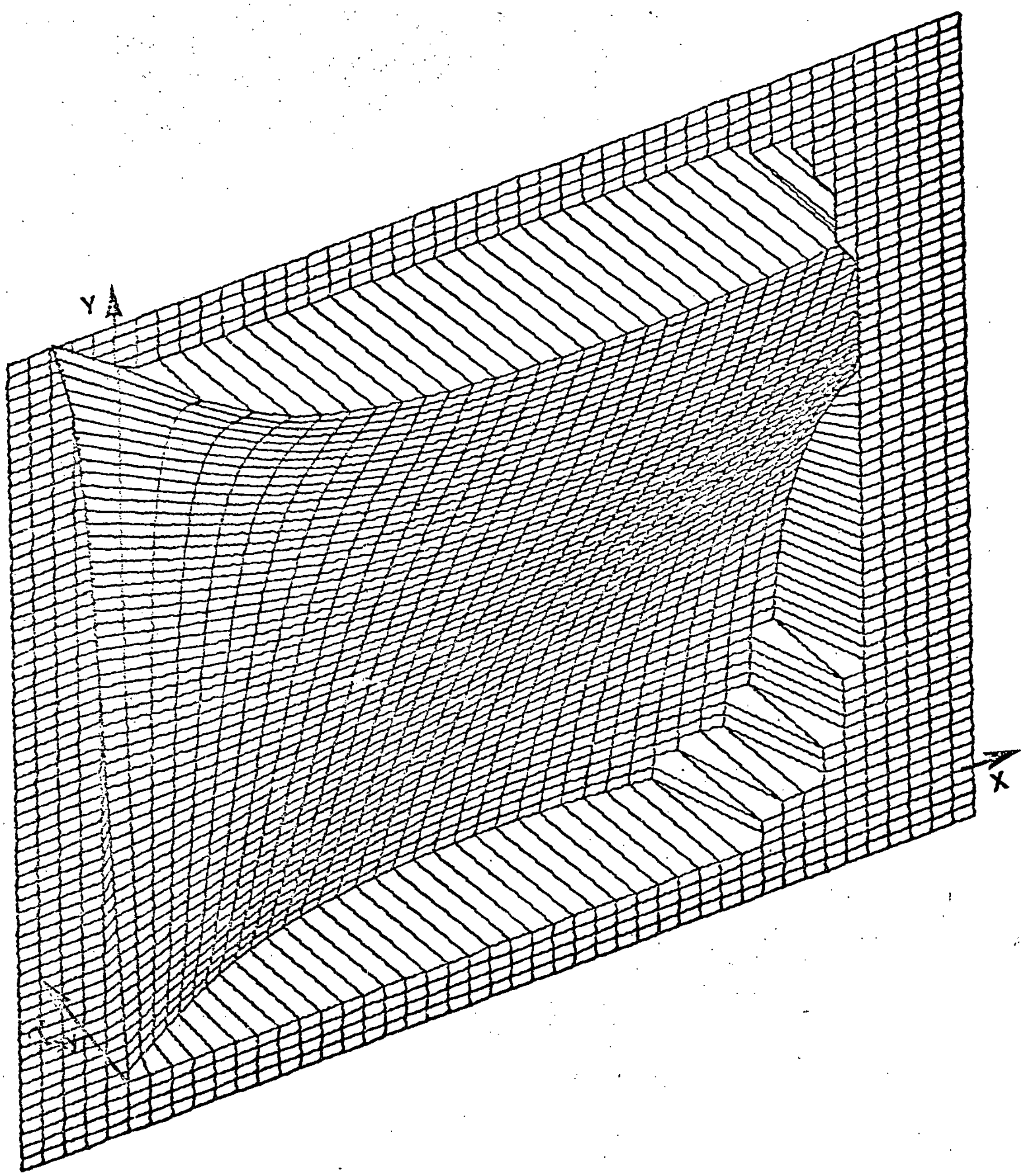

FIG.4.22 THREE DIMENSIONAL PLOT OF SHEAR STRESS (τ_{xy}) AS FUNCTION OF X AND Y FOR 0.02 FT./MIN DEFORMATION SPEED.

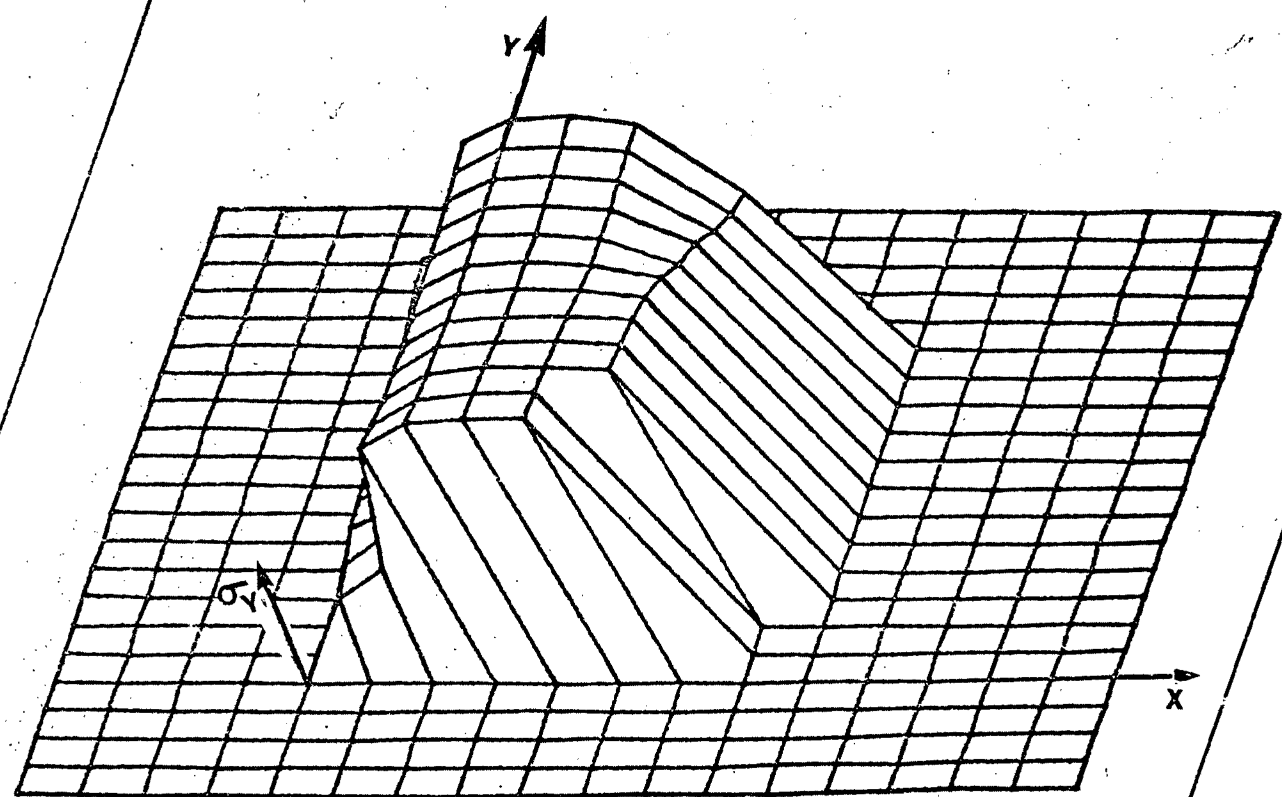

FIG 4.23 THREE DIMENSIONAL PLOT OF NORMAL STRESS (σ_Y) AS FUNCTION OF X AND Y FOR 15.7 FT./SEC. DEFORMATION SPEED.

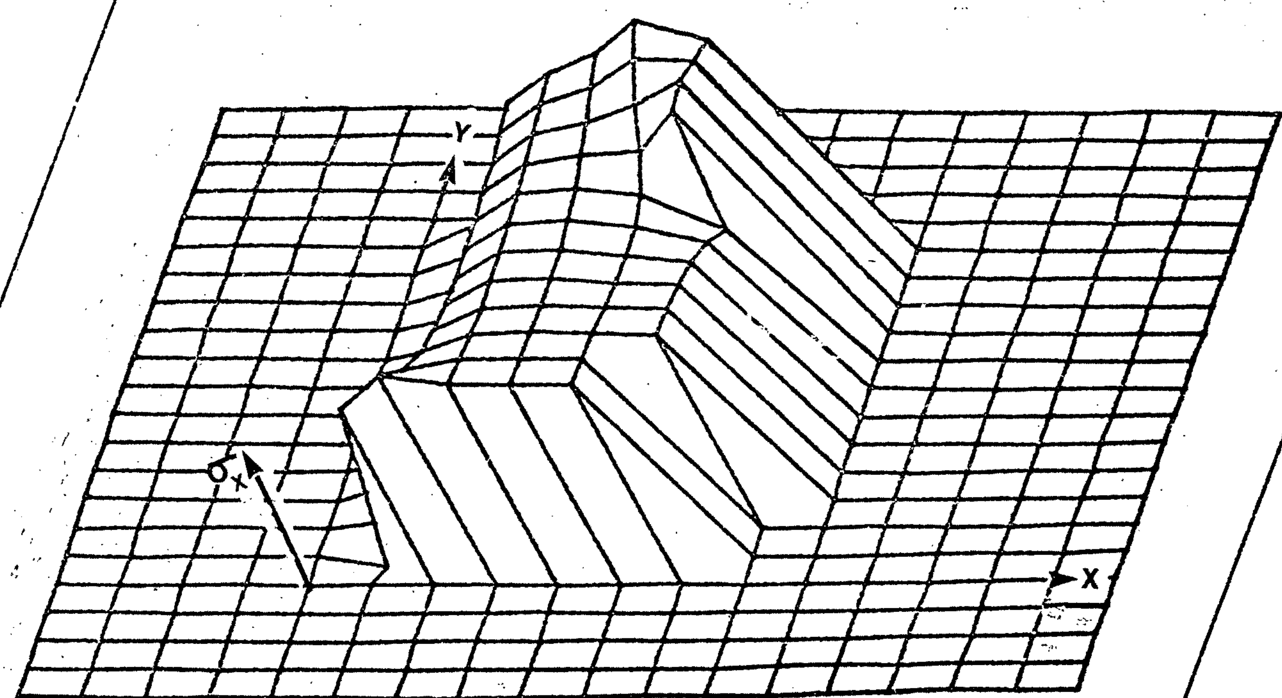

FIG.4.24 THREE DIMENSIONAL PLOT OF NORMAL STRESS (σ_x) AS FUNCTION OF X AND Y FOR 15.7 FT./SEC. DEFORMATION SPEED.

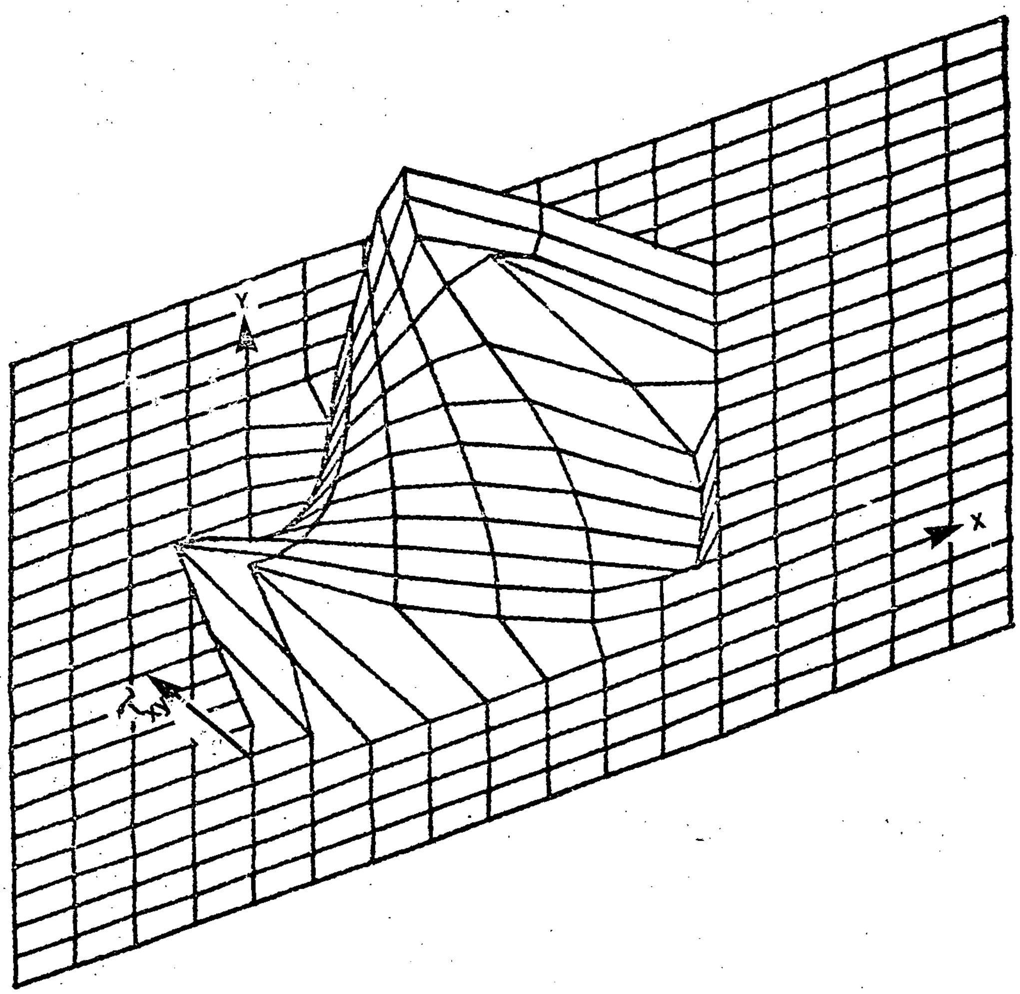

FIG.4.25 THREE DIMENSIONAL PLOT OF SHEAR STRESS (τ_{xy}) AS FUNCTION OF X AND Y FOR 15.7 FT./SEC DEFORMATION SPEED.

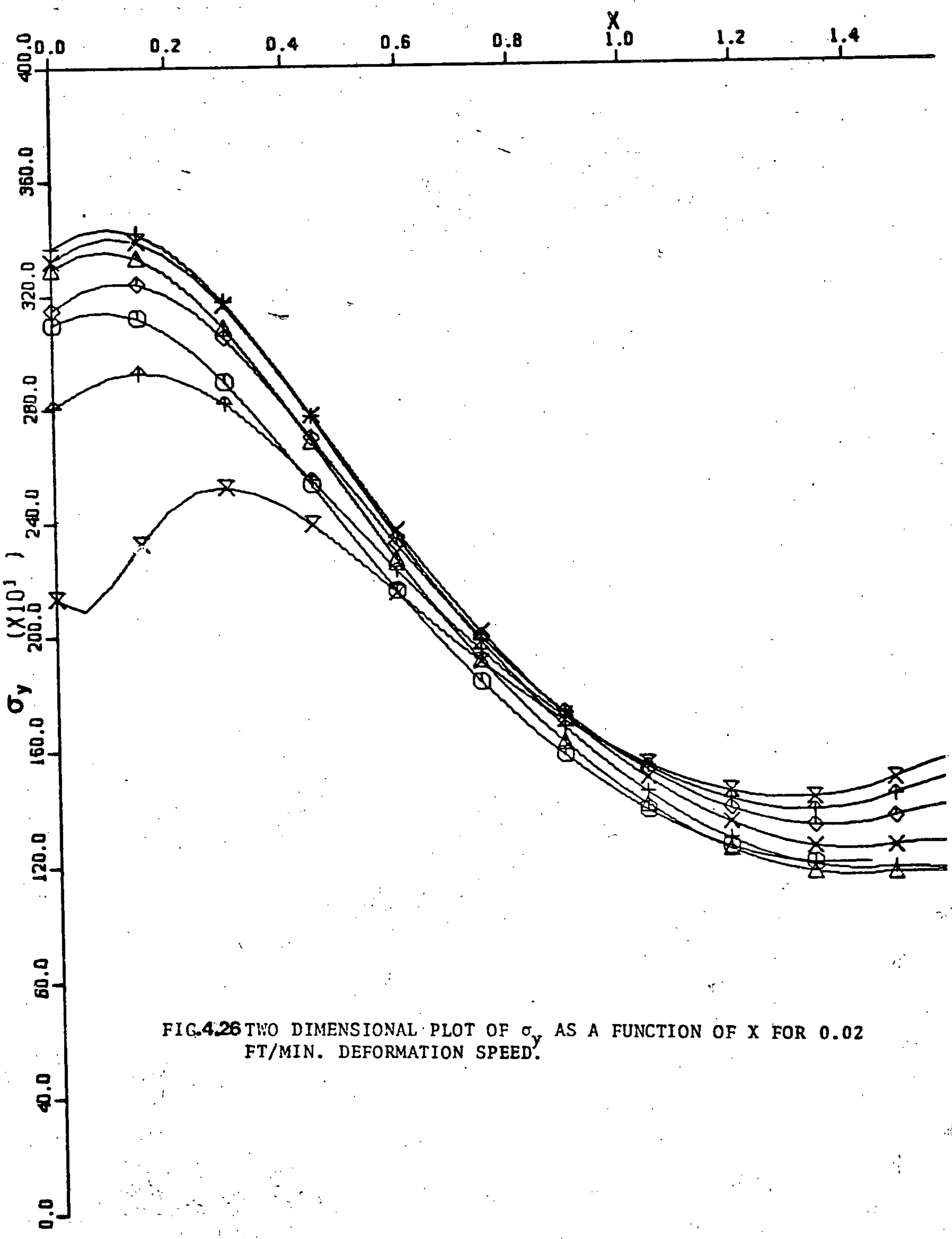

FIG.4.26 TWO DIMENSIONAL PLOT OF σ_y AS A FUNCTION OF X FOR 0.02 FT/MIN. DEFORMATION SPEED.

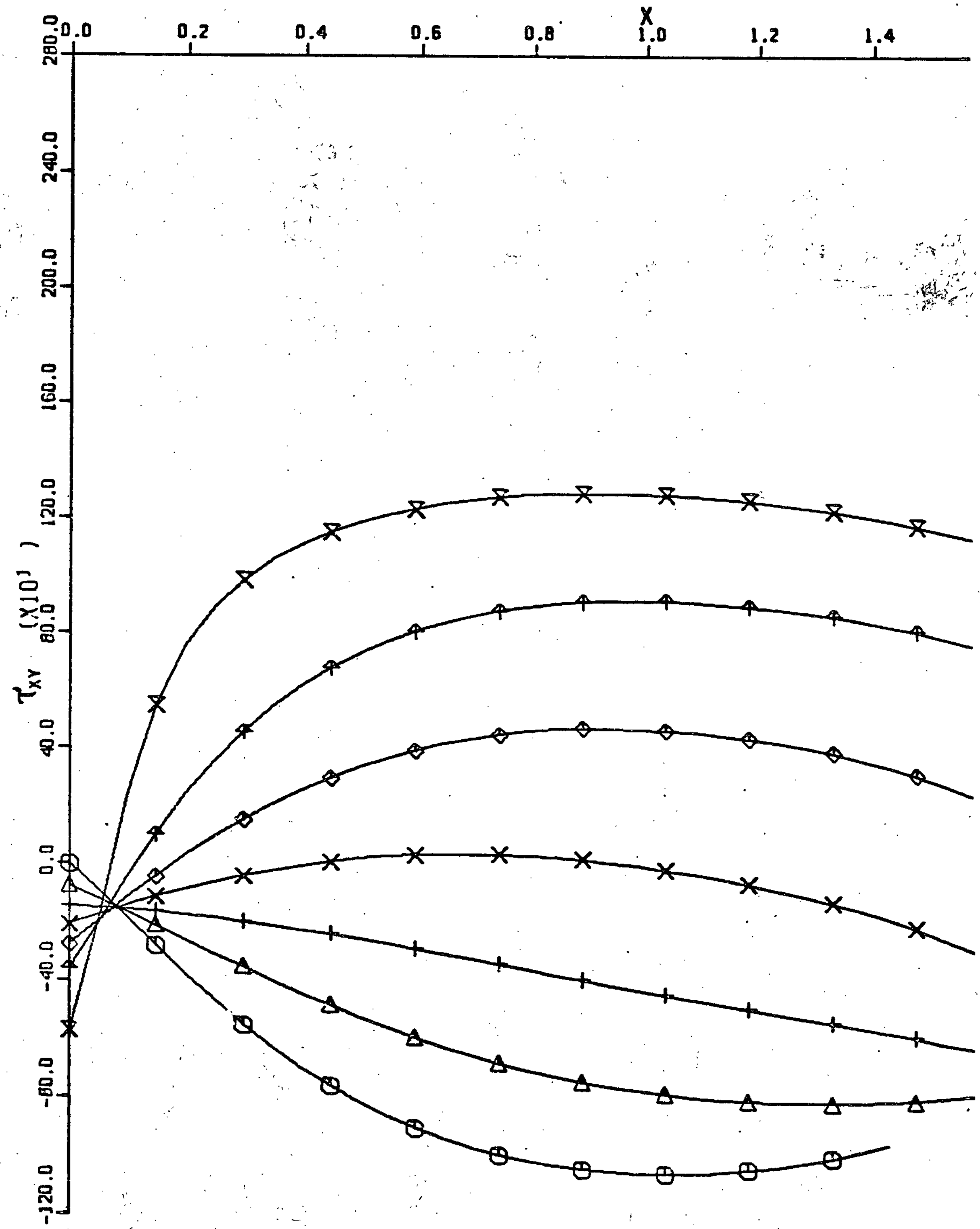

FIG. 4.27 TWO DIMENSIONAL PLOT OF 'τ_{xy}' AS A FUNCTION OF X FOR 0.02 FT./MIN. DEFORMATION SPEED.

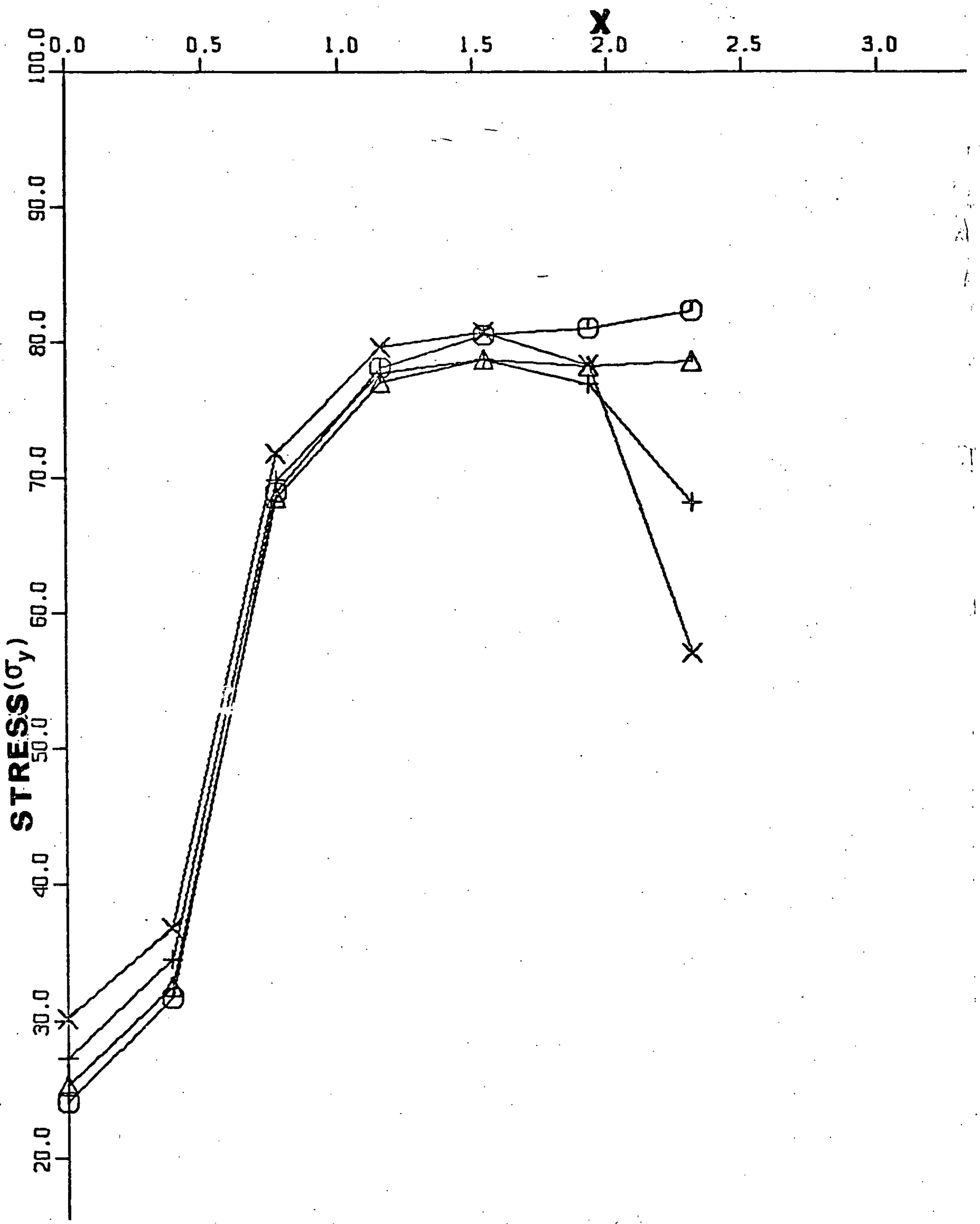

FIG.4.28 TWO DIMENSIONAL PLOT OF σ_y AS A FUNCTION OF X FOR 15.7 FT/SEC. DEFORMATION SPEED.

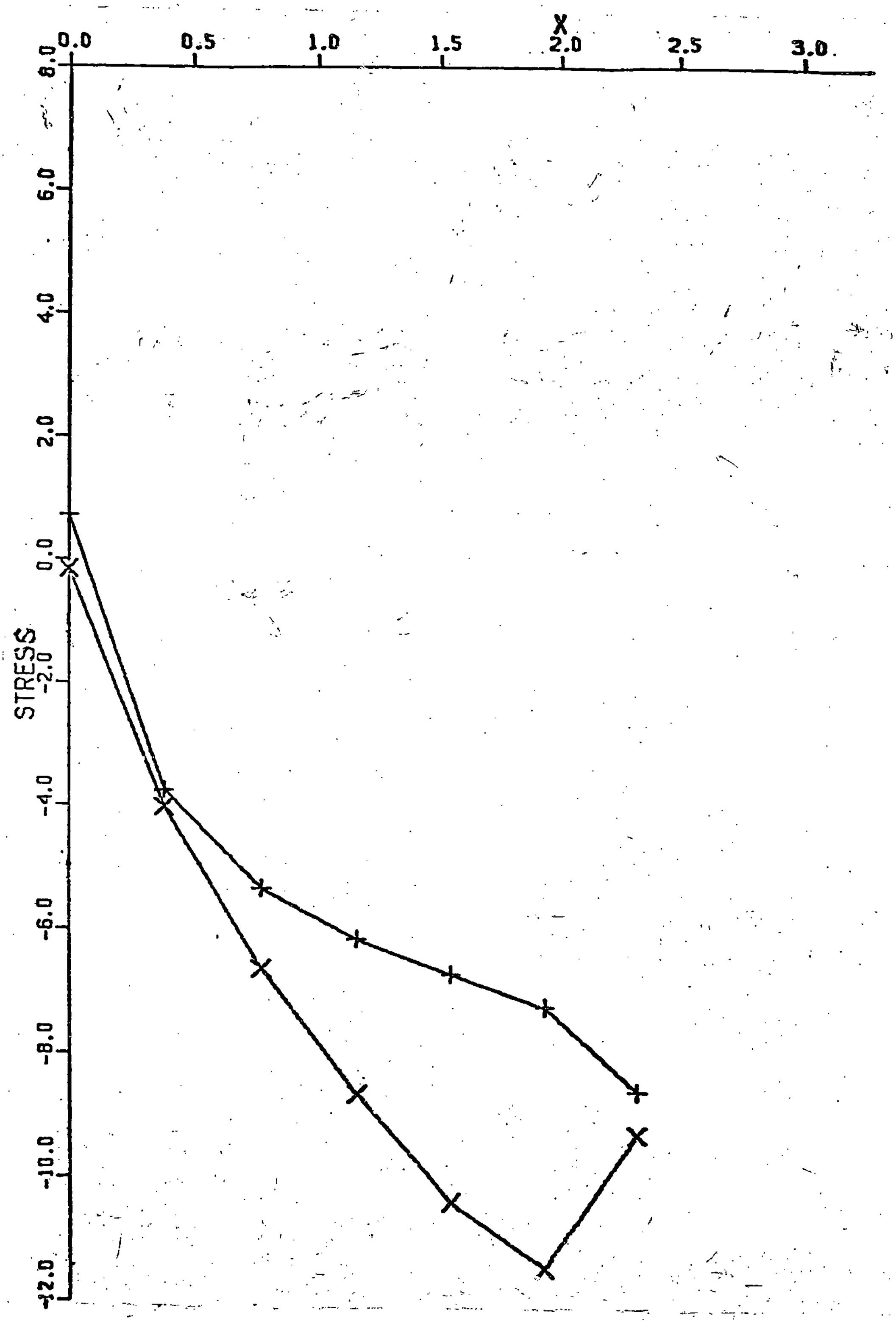

FIG.4.29 TWO DIMENSIONAL PLOT OF 'τ_{XY}' AS A FUNCTION OF X FOR 15.7 FT./SEC. DEFORMATION SPEED.

4.3. SOURCES OF ERROR

The quality of the grid node positional data used as input to the program is the most important single item affecting the results. Sparse or poorly digitized data is likely to cause inconsistencies in the output stress distributions. The surface fitting routines will smooth certain irregularities but there is a limit to their capabilities.

The velocity of the upper plater varies during the cycle, and during specimen deformation, according to the equations 3.4 and 3.9. A further fluctuation of platen velocity may occur as the drivewheel speed changes during the cycle. Initial energy balance calculations show this change is likely to be very small particularly with low strength projectiles. A prior knowledge of the actual upper-platen velocity profile during deformation is not required as this is obtained automatically from the digitised displacement data and a knowledge of the time increment between frames of the high speed photographs.

Plane-strain deformation was achieved using a Kudo apparatus. While this assured plane-strain condition it did introduce a frictional drag on the end faces of the specimen. The effect was minimized using silicon grease as a lubricant and from examination of deformed specimen it was concluded the effect was not important.

In the analysis the material was assumed to be strain-rate insensitive which is a common assumption and not unreasonable for many metal-forming materials. It is possible to relate effective stress, $\overline{\sigma}$, to both effective strain $\overline{\varepsilon}$ and effective strain rate $\dot{\overline{\varepsilon}}$. With modifications to the analysis strain-rate sensitive materials could be accommodated.

5. CONCLUSIONS

The visioplasticity approach have been developed for dynamic and quasi-static, steady or non-steady deformation processes.

The effect of impact velocity on the mechanism of deformation during different metal-working processes can be studied using this work. It is clear from the initial study of upsetting, that strain and stress distribution vary significantly with strain-rate.

6. SUGGESTIONS FOR FURTHER WORK

The method developed enables the stress distributions to be determined in many dynamic metal-forming operations. A starting point for this is to determine the change of stress distribution with strain rate (or impact velocity), material density and surface geometry for plane-strain upsetting operations.

Modifications can be made to the surface fitting routines to accommodate the constraints that the velocity gradient is zero along the y axis, and that the vertical component of velocity, v, is equal to the platen velocity for points on the platen-workpiece interface. It is likely that a 5th order polynomial would then be needed for surface fitting.

R E F E R E N C E S

References

1. Hoffmann, O., and Sachs, G.,"Introduction to the Theory of Plasticity for Engineers," McGraw Hill, New York, 1953.

2. Siebel, E., "Die Formgebung in bildsmen Zustande", Verlang Stahleissen, Dusseldorf, 1932.

3. Henky, H., "Uber einige statisch bestimmte Falle des Gleichgewichts in plastischen Korpern", Z. Angew. Math. Mech. 3, 241-251, 1923.

4. Prandtl, L., "Anwendungs beispiele zu einem Henckyschen Satz uber das Gleichgewicht", A. Angew. Math. Mech., 3, 401-406, 1923.

5. Caratheodory, C., and Schmidt, E., "Uber die Hencky-Prandtlschen Kurven", Z. Angew. Math. Mech., 3, 468-475, 1923.

6. Geiringer, H., "Beitrang zum vollstandingen ebenen Plastizitats - Problem," Proc. Third International Congress of Applied Mechanics, 1., 185-190, 1930.

7. Hill, R., The Mathematical Theory of Plasticity Clarendon Press, Oxford, 1950.

8. Prager, W. and Hodge, P.G. Jr., Theory of Perfectly Plastic Solids, Wiley, New York, 1951.

9. Lee, E.H., "The Theoretical Analysis of Metal Forming Problems in Plane Strain", J. Applied Mechanics, 19, 97-103, 1952.

10. Johnson, W. and Miller, P.B., Plasticity for Mechanical Engineers, D. Van Nustrand Co., Ltd., 1962.

11. Bishop, J.F., "On the Effect of Friction on Compression and Indentation Between Flat Dies", J. Mech. Phys. Solids, 6, 132-144, 1958.

12. Green, A.P., "On Unsymmetrical Extrusion in Plane Strain", J. Mech. Phys. Solids, 3, 189-196, 1955.

13. Oxley, P.L.B. and Farmer, L.E., "Slip-Line Field for Plane-Strain Extrusion of a Strain-Hardening Material", J. Mech. Phys. Solids, V19, N6 Nov. 1971, 369-388.

14. Chitkara, N.F. and Collins, I.F., "A Graphical Technique for Constructing Anisotropic Slip-Line Field", Int. J. Mech. Sc., 1974, pp. 241-248

15. Rice, J.R., "Plane Strain Slip-Line Theory for Anisotropic Rigid/Plastic Materials", J. Mech. Phys. Solids, V21 N2, March, 1973, 63-74.

16. Booker, J.R. and Davis, E.I., "A General Treatment of Plastic Anisotropy under conditions of Plane Strain", J. Mech. Phys. Solids, Vol. 20, 1972, pp. 239-250.

17. Shabaik, A., "Effect of Friction and Degree of Deformation on Buldge Profile During Compression", Proc. North American Metal-Working Conference, McMaster University, Canada, 1973, pp. 221-238.

18. Wilson, W.R.D., "Slip-Line Solutions for Strip Drawing with Arbitrary Friction Conditions", Proc. 5th. NAMRC, SME, 1977, pp. 80-86.

19. Ewing, D.J.F., "A Series Method for Constructing Plastic Fields," J. Mech. Phys. Solids, Vol. 15, 1967, pp. 105-114.

20. Collins, I.F., "The Algebraic-Geometry of Slip-Line Fields with Applications to Boundary Value Problems", Proc. Roy. Soc., Ser. A, Vol. 303, 1968, pp. 317-338.

21. Drucker, D.C., Prager, W. and Greenberg, H.J., "Extended Limit Design Theorems for Continuous Media", Quart. Appl. Math., 9, 1952, pp. 381-389.

22. Avitzer, B., Metal Forming: Process and Analysis, McGraw Hill, New York, 1968.

23. Johnson, W., "Estimate of Upper Bound Loads for Extrusion and Coining Operations", Proc. Inst. Mech. Engrs. (London), 173, pp. 61-72, 1957.

24. Kudo, H., "An Upper Bound Approach to Plane Strain Forging and Extrusion - I", Int. J. Mech. Science, 229-252, 1960.

25. Kudo, H., "An Upper Bound Approach to Plane Strain Forging and Extrusion - II", Int. J. Mech. Sci., 1: 229-252, 1960.

26. Kudo, H., "An Upper Bound Approach to Plane Strain and Extrusion - III", Int. J. Mech. Sci., 1: 366-368, 1960.

27. Kobayashi, S., "Upper Bound Solution of Axisymmetric Forming Problems - I", Presented at the Production Engineering Conference of ASME, May, 1963.

28. Kobayashi, S., "Upper Bound Solutions of Axisymmetric Forming Problems II", Trans. ASME, Series B, J. Eng. Ind., 86 No. 4, 1964.

29. Nagpal, V., Lahoti, G.D., Altan, T., "A Numerical Method for Simultaneous Production of Metal Flow and Temperatures in Upset Forging of Rings", ASME Paper No. 77-WA/Prod.-35.

30. Lahoti, G.D. and Altan, T., "Prediction of Temperature Distributions in Tube Extrusion using a Velocity Field without Discontinuities", Proc. 2nd. NAMRC, University of Wisconsin, Madison, 1974, pp. 207-224.

31. Lahoti, G.D. and Altan, T., "Computer-Aided Analysis of Metal Flow and Temperatures in Radial Forging of Tubes", Proc. Int. Prod. Eng. Res. Conference, New Delhi, 1977, pp. 323-339.

32. Vickers, G.W., Plumtree, A., Sowerby, R. and Duncan, J.L., "Simulation of the Heading Process", ASME Paper No. 74-WA/Prod-19.

33. Collins, I.F., "The Upper Bound Theorem for Rigid/Plastic Solids Generalized to Include Coloumb Friction", J. Mech. Phys. Solids, Vol. 17, 1969, pp. 323-338.

34. Sauerwine, F. and Avitzer, B., "Limit Analysis of Hollow Disk Forging, Part I: Upper Bound", ASME Paper No. 77-WA/Prod-2, 1977.

35. Sauerwine, F. and Avitzer, B., "Limit Analysis of Hollow Disk Forging, Part 2: Lower Bound", ASME Paper No. 77-WA/Prod-3, 1977.

36. Dwivedi, S.N., Sharan, R. and Mishra, C.B., "Plastic Deformation of Polygonal Disks under High Velocity Impact", Presented in 8th Conference of U.S. National Congress of Applied Mechanics, June, 1978.

37. Juneja, B.L. and Prakash, R., "An Analysis for Drawing and Extrusion of Polygonal Sections", Int. J. Mach. Tool Des. Res., Vol. 15, 1975, pp. 1-30.

38. Nagpal, N., "Analysis of Plane-Strain Extrusion through Arbitrarily Shaped Dies using Flow Function", J. Engg. Ind., Vol. 99, 1977, pp. 544-548.

39. Nagpal, N., "General Kinematically Admissible Velocity Field for some Axisymmetric Metal Forming Problems, "J. Engg. Ind., Vol. 96, 1974.

40. Zienkiewicz, O.C., The Finite Element Method, 3rd Edition, McGraw-Hill, 1977.

41. Lee, C.H. and Kobayashi, S., "New Solutions to Rigid-Plastic Deformation Problems using a Matrix Method," Trans. ASME, J. of Engrg. for Ind. Vol. 95, 1973, pp. 865-873.

42. Godbole, P.H. and Zienkiewicz, O.C., "A Penalty Function Approach to Problems of Plastic Flow of Metals with Large Surface Deformation", J. Strain Analysis, Vol. 10, 1975, pp. 180-183.

43. Huebner, K.H., The Finite Element Method for Engineers, John Wiley & Sons, 1975.

44. Strang, G. and Fix, G.J., An Analysis of the Finite Element Method, Prentice-Hall, Englewood Cliffs, N.J., 1973.

45. Rowe, G.W., "Recent Developments in the Theory and Practice of Metal Forming", Proc. Third North American Metal-Working Research Conference, Carnegie-Melton University, 1975, pp. 2-25.

46. Alexander, J.M. and Price, "Finite Element Analysis of Hot Metal Forming", Proc. 18th Int. Conf. Mach. Tool Design Research, 1977, pp. 267-274.

47. Lee, E.H., Mallet, R.L. and Yang, W.H., "Stress and Deformation Analysis of the Metal Extrusion Process", Computer Methods in Applied Mechanics and Engg., Vol. 10, 1977, pp. 339-353.

48. Lee, E. H., Mallet, R.L., and McMeeking, R.M., "Stress and Deformation Analysis of Metal Forming Processes, "Numerical Modelling of Manufacturing Processes", ASME Special Publication PVP-PB-025, 1977, pp. 19-34.

49. Odell, E.I., "A Study of Wall Ironing by the Finite Element Technique", ASME Paper No. 77-WA/Prod-8.

50. Wifi, A.S., "An Incremental Complete Solution of the Stretch Forming and Deep-Drawing of Circular Blank using a Hemispherical Punch", Int. J. Mech. Science, Vol. 18, 1976, pp. 23-31.

51. Wang, N.M. and Budiansky, B., "Analysis of Sheet Metal Stamping by Finite Element Method", General Motors Research Publication GMR-2423, Sept. 1977.

52. Shah, S.N. and Kobayashi, S., "A Theory of Metal Flow in Axisymmetric Piercing and Extrusion", J. Rud. Engrg., Vol. 1, 1977, pp. 73-103.

53. Kobayashi, S., "Rigid-Plastic Finite Element Analysis of Axisymmetric Metal Forming Processes, Numerical Modelling of Manufacturing Processes", ASME Special Publication PVP-PB-025, 1977, pp. 49-65.

54. Kobayashi, S. and Matsumoto, H., "A note on the Matrix Method for Rigid-Plastic Analysis of Ring Compression", Proc. 18th MT DR Conference, London, 1977, pp. 3-9.

55. Kobayashi, S. and Chen, C.H., "Deformation Analysis of Multi-Pass Bar Drawing and Extrusion", CIRP Annalus, 1978.

56. Price, J.W.H. and Alexander, J.M., "A study of Isothermal Forming or Creep Forming of a Titanium Alloy", 4th North American Metal-Working Research Conference, Battelle, Columbus, Ohio, 1976, pp. 46-57.

57. Lung, M. and Mahrenholtz, "A Finite Element Procedure for Analysis of Metal Forming Processes", Trans. of CSME, Vol. 2, No. 1, 1973-74.

58. Wilkins, M.L., "Calculation of Elastic-Plastic Flow", Lawrence Radiation Laboratory Report, UCRL-7322, Rev. 1, Livermore, University of California, 1969.

59. Gordon, P. and Karpp, R., "Application of a New Finite Difference Method of Metal Forming", Proc. Fourth NAMRC, Battelle, Columbus Lab., 1976, pp. 72-79.

60. Shabaik, A.H., "Computer Simulation of Metal Flow During Extrusion", Proc. 1976 Int. Conference on Computer Simulation for Materials Applications, Nuclear Metallurgy, Vol. 20, Part 2, 1976, pp. 752-765.

61. Woo, D.M., "On the Complete Solution of the Deep Drawing Problem", Int. J. Mech. Sci., 10, 1968, pp. 83-94.

62. Wang, N.M. and Shammamy, M.R., "On the Plastic Bulging of a Circular Diaphragm by Hydrostatic Pressure", J. Mech. Phys. Solids 17, 1969, pp. 43-61.

63. Wang, N.M., "Large Plastic Deformation of a Circular Sheet Caused by Punch Stretching", J. Appl. Mech. 1970, pp. 431-440.

64. Yamada, Y. and Yokochi, G., "Elastic-Plastic Analysis of the Hydraulic Bulge Test by the Membrane Theory", Manf. Res. 21, 1969.

65. Thomsen, E.G. and Lapslley, J.T., "Experimental Stress Determination within a metal during Plastic Flow", Proc. Soc. Exptl. Stress Analysis., 11, No. 2, 59-68, 1954.

66. Thomsen, E.G., Yang, C.T., and Bierbower, J.B., "An Experimental Investigation of the Mechanics of Plastic Deformation of Metals". University of California Press, Berkeley and Los Angeles, 1954, pp. 89-144.

67. Thomsen, E.G., "Visioplasticity", CIRP Conference, September, 1963.

68. Shabaik, A. Altan, T. and Thomsen, E.G., "Visioplasticity", Final Report Prepared for the U.S. Navy, Bureau of Naval Weapons, February, 1965.

69. Shabaik, A. and Kobayashi, S., "Investigation of the Application of Visioplasticity Methods of Analysis to Metal Deformation Processing", Final Report prepared for the U.S. Navy, Bureau of Naval Weapons, Feb. 1966.

70. Shabaik, A. and Thomsen, E.G., "Investigation of the Application of Visioplasticity Methods of Analysis to Metal Deformation Processing", Final Report prepared for the U. S. Navy, Bureau of Naval Weapons, Feb. 1967.

71. Shabaik, A. and Kobayashi, S., "Computer Application to the Visioplasticity Method", Journal of Engineering for Industry, Trans. ASME, Series B., Vol. 89, No. 2, May, 1967, pp. 339-346.

72. Lee, C.H., and Shiro Kubayashi, "Matrix Method of Analysis for Plastic Deformation Mechanics and its Application to Visioplasticity", Ann. CIRP, Volume 21, No. 1, pp. 71-72, 1972.

73. Medrano, R.E. and Gillis, P.P., "Visioplasticity Techniques in Axisymmetric Extrusion", Journal of Strain Analysis, Vol. 7, No. 3, 1972, pp. 170-177.

74. Shabaik, A.H., "Computer Aided Visioplasticity Solution to Axisymmetric Extrusion Through Curved Boundaries", Journal of Engineering for Industry, Nov., 1972, pp. 1225-1231.

75. Medrano, R.E., Gillies, P.P., Conrad, H. and Hinesley, C.P., "Use of Microstructure for Visioplasticity Analysis", Journal Strain Analysis, Volume 9, Number 3, pp. 146-151, July, 1974.

76. Brown, J.H. and P.F. Thomson, "Mechanics of Deformation During Cold Rolling", Australia's Conference on the Mechanics of Structures and Materials, pp. 415-422, 1977.

77. Robinson, J.N. and Shabaik, A.H., "Determination of the Relationship between Strain and Microhardness by means of Visioplasticity", Machine Design, Volume 4, Number 9, pp. 2091-2095, Sept. 1973.

78. Mohamed, S.A. and Tetelman, A.S., "Application of the Visioplasticity Technique for Derivation of the Criterion for Ductile Rapture Initiation in Fully Plastic Notched Bars", Engineering Fracture Mechanics, Vol. 7, No. 4, pp. 631-640, 1975.

79. Green,A.P.,"The Use of Plasticine Models to Simlate the Plastic Flow of Metals,"Phil. Mag. Ser. 7,Vol. 42,Page 365-373,1951.

APPENDIX

```
      IMPLICIT REAL*8(A-H,O-Z)
      COMMON XX(15),XI,YI,CC,CN,CA,Y(400,2),EBR(400,20)
      COMMON/C1/RHO,YOLD(15,2),DT
      DIMENSION XYT(2,20,20,2),U(20,20),V(20,20),XY(2,80,80
)
      DIMENSION X(15,400),ERROR(2),ISUB(80,80)
      REAL*4 Z1(90,90),Z2(90,90),TAUXY(80,80)
      LOGICAL REFINE
      DIMENSION EBRDT(80,80),EXDT(80,80),EYDT(80,80)
     1,GAMDT(80,80),LANDA(80,80)
      REAL*8 DEBR(80,80)
      REAL*8 XLS(10,800)
      REAL*8 LANDA
      REAL*8 X1(20,20,2),Y1(20,20,2)
         DIMENSION AINT2(80)
C
C                IX=NO PTS IN X
C                IY=NO PTS IN Y
C                IT=NO OF TIME STEPS
C                DT=TIME INTERVAL BETWEEN TIME STEPS
C                CC,CN ARE CONSTANTS WHERE SIGB=CC*EB**CN
C                CA IS LOWER INTERVAL OF INTEGRATION FOR SIG
Y
C                SIGYOA IS CONSTANT ADDED TO SIGY
C                XYT(L,I,J,K) CONTAINS: L=1 X-COORD; L=2 Y-C
OORD
C                   FOR I=1,IY J=1,IX L=1,2
C
      READ(5,10) IX,IY,IT
10    FORMAT(3I2)
      READ(5,20) DT
20    FORMAT(8F10.0)
      READ(5,20) CC,CN,CA,SIGYOA
C
C           NIX CONTAINS # GRID PTS IN X DIRECTION, NIY IN Y
DIRECTION FOR PLOTS
C
      READ(5,10) NIX,NIY
      READ(5,20) RHO
C
C                X & Y COORD READ FOR TIME=0
C
      READ(4,30) (((XYT(K,I,J,1),K=1,2),I=1,IY),J=1,IX)
      DO 25 II=1,IX
      DO 25 IJ=1,IY
      IF (II.EQ.1) XYT(1,IJ,II,1)=0.D0
                   XYT(2,IJ,II,1)=XYT(2,IJ,II,1)-1.0D0
25    CONTINUE
30    FORMAT(5X,2F6.3,1X,2F6.3,1X,2F6.3,1X,2F6.3,1X,2F6.3)
      LTM=2
      NTM=1
      IDIM=20
      IDIMP=80
      IXY=IX*IY
      CALL AXIS(0.,0.,'X',-1,10.,0.,0.,.2)
      CALL AXIS(0.,0.,'Y',1,10.,90.,0.,.2)
      CALL PLOT(XYT(1,IY,1,1)*5.,XYT(2,IY,1,1)*5.,3)
      CALLPLOT(XYT(1,IY,IX,1)*5.,XYT(2,IY,IX,1)*5.,2)
```

```
      CALL PLOT(XYT(1,1,IX,1)*5.,XYT(2,1,IX,1)*5.,2)
      DO 35 I=2,IX,2
      DO 35 J=2,IY,3
      X1(I,J,1)=XYT(1,J,I,1)
35    Y1(I,J,1)=XYT(2,J,I,1)
C
C                 INITIALIZE EBR TO ZERO
      DO 40 I=1,20
      DO 40 J=1,400
      EBR(J,I)=0.D0
40    CONTINUE
      FACT=1.D0
C
C                 FOR EACH TIME STEP EBR IS ACCUMULATED
      IT1=IT-1
      DO 80 K=1,IT1
C
C                 X&Y COORD ARE READ FOR NEXT TIME STEP
C
      NTM=3-NTM
      LTM=3-LTM
      READ(4,30) (((XYT(KK,I,J,NTM),KK=1,2),I=1,IY),J=1,IX)
      DO 45 I=1,IX
      DO 45 J=1,IY
      IF (I.EQ.1) XYT(1,J,I,NTM)=0.D0
           XYT(2,J,I,NTM)=XYT(2,J,I,NTM)-1.0D0
45    CONTINUE
C
C                 U,V CALCULATED FOR THIS TIME STEP
C                 U MUST BE >0, V MUST BE <0
C
48    DO 50 J=1,IX
      DO 50 I=1,IY
      U(I,J)=-(XYT(1,I,J,NTM)-XYT(1,I,J,LTM))/DT
      V(I,J)=-(XYT(2,I,J,NTM)-XYT(2,I,J,LTM))/DT
      IF (U(I,J).GT.0.D0) U(I,J)=0.D0
      IF (V(I,J).LT.0.D0) V(I,J)=0.D0
50    CONTINUE
C
C                 CURVE FITTING FOR U AND V USING DLSQHS
C                 SET UP INDEPENDENT VARIABLES IN X
C                 DEPENDENT VARIABLES IN Y
C
      DO 60 J=1,IX
      IL=IY*(J-1)
      DO 60 I=1,IY
      L=I+IL
      CALL AUX(XYT(1,I,J,NTM),XYT(2,I,J,NTM),X(1,L))
      XLS(1,L)=-X(2,L)
      XLS(2,L)=-2.D0*X(10,L)
      XLS(3,L)=-3.D0*X(11,L)
      XLS(4,L)=-4.D0*X(12,L)
      XLS(5,L)=-.5D0*X(3,L)
      XLS(6,L)=-X(13,L)
      XLS(7,L)=-1.5D0*X(14,L)
      XLS(8,L)=-1.D0/3.D0*X(4,L)
      XLS(9,L)=-2.D0/3.D0*X(15,L)
      XLS(10,L)=-.25D0*X(5,L)
```

```
         DO 55 IK=1,10
   55    XLS(IK,IXY+L)=X(IK+5,L)
         Y(L,1)=U(I,J)
   60    Y(IXY+L,1)=V(I,J)
         CALL DLSQHS(Y,XLS,2*IXY,10,1,800,10,ERROR,.FALSE.,IER
 ,&200)
         DO 62 IK=1,5
   62    Y(IK,2)=0.D0
         DO 63 IK=6,15
   63    Y(IK,2)=Y(IK-5,1)
         Y(1,1)=0.D0
         Y(2,1)=-Y(6,2)
         Y(3,1)=-.5D0*Y(10,2)
         Y(4,1)=-1.D0/3.D0*Y(13,2)
         Y(5,1)=-.25D0*Y(15,2)
         DO 64 IK=6,9
   64    Y(IK,1)=0.D0
         Y(10,1)=-2.D0*Y(7,2)
         Y(11,1)=-3.D0*Y(8,2)
         Y(12,1)=-4.D0*Y(9,2)
         Y(13,1)=-Y(11,2)
         Y(14,1)=-1.5D0*Y(12,2)
         Y(15,1)=-2.D0/3.D0*Y(14,2)
 C
 C           U&V COEFF SAVED FOR DU/DT,DV/DT
 C
         IF (K.NE.(IT1-1)) GO TO 410
         DO 400 I=1,15
         DO 400 J=1,2
  400    YOLD(I,J)=Y(I,J)
  410    CONTINUE
 C
 C                    THE VALUES OF EDTX,EDTY,GAMXY,EBRDT,AND EBR
  ARE CALCULATED
 C                      AT EACH TIME STEP
 C
         DO 52 I=2,IX,2
         DO 52 J=2,IY,3
         X1(I,J,NTM)=XYT(1,J,I,LTM)-DT*AUX2(XYT(1,J,I,NTM),
        1  XYT(2,J,I,NTM),Y(1,1),.TRUE.)
         Y1(I,J,NTM)=XYT(2,J,I,LTM) - DT*AUX2(XYT(1,J,I,NTM),
        1  XYT(2,J,I,NTM),Y(1,2),.FALSE.)
         CALL PLOT(X1(I,J,LTM)*5.,Y1(I,J,LTM)*5.,3)
         CALL PLOT(X1(I,J,NTM)*5.,Y1(I,J,NTM)*5.,2)
         CALL SYMBOL(X1(I,J,NTM)*5.,Y1(I,J,NTM)*5.,.14,5,0.,-1
 )
   52    CONTINUE
         IF (K.NE.IT1)GO TO 53
         CALL PLOT(0.,XYT(2,IY,1,NTM)*5.,3)
         CALL PLOT(XYT(1,IY,IX,NTM)*5.,XYT(2,IY,IX,NTM)*5.,2)
         DO 49 I=2,IY
         CALL PLOT(XYT(1,IY-I+1,IX,NTM)*5.,XYT(2,IY-I+1,IX,NTM
 )*5.,2)
   49    CONTINUE
         CALL PLOT(12.,0.,-3)
   53    CONTINUE
         DO 70 J=1,IX
         IL=IY*(J-1)
```

```
            DO 70 I=1,IY
            IJ=I+IL
            CALL AUX(XYT(1,I,J,NTM),XYT(2,I,J,NTM),XX)
            CALL DERIV(Y(1,1),XYT(1,I,J,NTM),XYT(2,I,J,NTM),DUDX,
      DUDY,3)
            CALL DERIV(Y(1,2),XYT(1,I,J,NTM),XYT(2,I,J,NTM),DVDX,
      DVDY,1)
            GAMXY=DUDY+DVDX
            DFACT=(DUDX**2)/3.D0+(GAMXY)**2/12.D0
      65    EBRDT(I,J)=2.D0*DSQRT(DFACT)
            IF (K.EQ.IT1) FACT=.5D0
            EBR(IJ,1)=EBR(IJ,1)+FACT*DT*EBRDT(I,J)
      70    CONTINUE
      80    CONTINUE
      C
      C                 4TH DEGREE POLY FIT TO EBR
      C
            CALL DLSQHS(EBR,X,IX*IY,15,2,400,15,ERROR,.FALSE.,IER
      ,&200)
      C
      C     MASTER GRID IS SET FOR FINAL PLOTS
      C
      C                 XY(2,I,J) CONTAINS THE MASTER GRID ST XY(1,
      I,J) IS
      C                  THE X-COORD, XY(2,I,J) IS THE Y-COORD FOR
      I=1,IX J=1,IY
            XMAX=0.D0
            DO 90 I=1,IY
            IF (XYT(1,I,IX,NTM).LT.XMAX) GO TO 90
            XMAX=XYT(1,I,IX,NTM)
            IMY=I
      90    CONTINUE
            YMAX=XYT(2,IY,IX,NTM)
      100   CONTINUE
            DY=YMAX/(NIY-1)
            DO 110 I=1,NIX
            XY(2,I,1)=0.D0
            DO 110 J=2,NIY
            XY(2,I,J)=XY(2,I,J-1)+DY
      110   CONTINUE
            DX=XMAX/(NIX-1)
            DO 120 I=1,NIY
            XY(1,1,I)=0.D0
            DO 120 J=2,NIX
            XY(1,J,I)=XY(1,J-1,I)+DX
      120   CONTINUE
      C
      C                 TO FIND ZERO FILLS ON PLOTS
      C
            CALL FILL(XYT,IX,IY,ISUB,XY,NIX,NIY,IMY,NTM,IDIM,IDIM
      P)
      C
      C                 TO PLOT U,V,EBRDT, AND TAUXY
      C
            DO 125 J=1,NIY
            DO 125 I=1,NIX
            EBRDT(I,J)=0.D0
            DEBR(I,J)=0.D0
```

```
125   TAUXY(I,J)=0.D0
      NIY10=NIY+10
      NIX10=NIX+10
      DO 126 J=1,NIY10
      DO 126 I=1,NIX10
      Z1(I,J)=0.D0
126   Z2(I,J)=0.D0
      DO 130 J=1,NIY
      DO 135 I=1,NIX
      IF (ISUB(I,J).EQ.0) GO TO 130
      Z1(I+5,J+5)=-AUX2(XY(1,I,J),XY(2,I,J),Y(1,1),.TRUE.)
      Z2(I+5,J+5)=AUX2(XY(1,I,J),XY(2,I,J),Y(1,2),.FALSE.)
      CALL DERIV(Y,XY(1,I,J),XY(2,I,J),EXDT(I,J),GAMDT(I,J)
     ,3)
      CALL DERIV(Y(1,2),XY(1,I,J),XY(2,I,J),EBRDT(I,J),EYDT
     (I,J),3)
      GAMDT(I,J)=GAMDT(I,J)+EBRDT(I,J)
      DFACT=(3.D0*EXDT(I,J)**2+.75D0*GAMDT(I,J)**2)
131   EBRDT(I,J)=2.D0/3.D0*DSQRT(DFACT)
      DEBR(I,J)=AUX2(XY(1,I,J),XY(2,I,J),EBR,.FALSE.)
      LANDA(I,J)=1.5D0*EBRDT(I,J)/(CC*DEBR(I,J)**CN)
      TAUXY(I,J)=GAMDT(I,J)/(2.D0*LANDA(I,J))
135   CONTINUE
130   CONTINUE
C
C                PLOT U,V,EBRDT,TAUXY
C
      DXY=XY(2,NIX,NIY)/XY(1,NIX,NIY)
      CALL PERS(Z1,IDIMP+10,NIX+10,NIY+10,DXY,.333,45.,45.,
     10.,10.)
      CALL PLOT(12.,0.,-3)
      CALL PERS(Z2,IDIMP+10,NIX+10,NIY+10,DXY,.333,45.,45.,
     10.,10.)
      CALL PLOT(12.,0.,-3)
      DO 137 J=1,NIY10
      DO 137 I=1,NIX10
      Z1(I,J)=0.
137   Z2(I,J)=0.
      DO 138 J=1,NIY
      DO 138 I=1,NIX
138   Z1(I+5,J+5)=DEBR(I,J)
      CALL PERS(Z1,IDIMP+10,NIX+10,NIY+10,DXY,.333,45.,45.,
     10.,10.)
      CALL PLOT(12.,0.,-3)
      DO 139 J=1,NIY10
      DO 139 I=1,NIX10
139   Z1(I,J)=0.
      DO 140 J=1,NIY
      DO 140 I=1,NIX
      Z1(I+5,J+5)=EBRDT(I,J)
140   Z2(I+5,J+5)=-TAUXY(I,J)
      CALL PERS(Z1,IDIMP+10,NIX+10,NIY+10,DXY,.333,45.,45.,
     10.,10.)
      CALL PLOT(12.,0.,-3)
      CALL PERS(Z2,IDIMP+10,NIX+10,NIY+10,DXY,.333,45.,45.,
     10.,10.)
      CALL PLOT(12.,0.,-3)
C
```

```
C                  CALC SIGY
C
         EXTERNAL DF1,DF2
         DO 141 J=1,NIY10
         DO 141 I=1,NIX10
         Z1(I,J)=0.
141      Z2(I,J)=0.
            DGRID=(XY(2,1,2)-XY(2,1,1))/2
            JGRID=1
1000        IF(CA.GT.XY(2,1,JGRID)+DGRID) GO TO 1010
            GO TO 1020
1010        JGRID=JGRID+1
            IF (JGRID.EQ.NIY) GO TO 1020
            GO TO 1000
1020        AINT2(1)=0.D0
            DO 1030 I=2,NIX
            AINT2(I)=AINT2(I-1)
            IF (ISUB(I,JGRID).EQ.0) GO TO 1030
            AINT2(I)=AINT2(I)+DQUANK(DF2,XY(1,I-1,JGRID),
        1XY(1,I,JGRID),.001D0,TOL,FIFTH)
1030     CONTINUE
         DO 150 J=1,NIY
         DO 150 I=1,NIX
         IF (ISUB(I,J).EQ.0) GO TO 150
         XI=XY(1,I,J)
         YI=XY(2,I,J)
         AINT1=0.D0
         IF (JGRID .EQ. J) GO TO 1060
         JADD=0
         IF (ISUB(I,JGRID).EQ.1) GO TO 1050
         JINC=1
         IF (JGRID.GT.J) JINC=-1
1040     JADD=JADD+JINC
         IF (JGRID+JADD.EQ.J) GO TO 1060
         IF (ISUB(I,JGRID+JADD).EQ.1) GO TO 1050
         GO TO 1040
1050     AINT1=DQUANK(DF1,XY(2,I,JGRID+JADD),XY(2,I,J),.001D0,
TOL,FIFTH)
1060     Z1(I+5,J+5)=SIGYOA-AINT1-AINT2(I)
         Z2(I+5,J+5)=Z1(I+5,J+5)+(EXDT(I,J)-EYDT(I,J))/LANDA(I
,J)
150      CONTINUE
         CALL PERS(Z1,IDIMP+10,NIX+10,NIY+10,DXY,.333,45.,45.,
10.,10.)
         CALL PLOT(12.,0.,-3)
         CALL PERS(Z2,IDIMP+10,NIX+10,NIY+10,DXY,.333,45.,45.,
10.,10.)
         CALL PLOTND
         STOP
200      STOP 1
         END
         SUBROUTINE AUX(X,Y,XX)
         IMPLICIT REAL*8(A-H,O-Z)
         DIMENSION XX(15)
         XX(1)=1.D0
         XX(2)=X
         XX(3)=X*X
         XX(4)=X*XX(3)
```

```
            XX(5)=X*XX(4)
            XX(6)=Y
            XX(7)=Y*Y
            XX(8)=Y*XX(7)
            XX(9)=Y*XX(8)
            XX(10)=X*Y
            XX(11)=XX(10)*Y
            XX(12)=XX(11)*Y
            XX(13)=XX(10)*X
            XX(14)=XX(13)*Y
            XX(15)=XX(13)*X
            RETURN
            END
            FUNCTION AUX2(XX,YY,P,LL)
            IMPLICIT REAL*8(A-H,O-Z)
      C
      C                EVALUATE THE FITTED FUNCTION AT XX,YY
      C                P CONTAINS THE FITTED PARAMETERS
      C                LL IS TRUE IF THE INDEPENDENT VARIABLE MUST
         BE EVALUATED BY AUX
      C
            LOGICAL LL
            COMMON X
            DIMENSION X(15),P(1)
            IF (LL) CALL AUX(XX,YY,X(1))
            AUX2=0.D0
            DO 10 I=1,15
            AUX2=AUX2+P(I)*X(I)
      10    CONTINUE
            RETURN
            END
            FUNCTION DF1(YC)
            IMPLICIT REAL*8(A-H,O-Z)
            COMMON XX(15),XI,YI,C1,C2,CA,Y(400,2),PEBR(20,20)
            COMMON/C1/RHO,YOLD(15,2),DT
      C
      C                THE INTEGRAND DTAU/DX IS EVALUATED
      C
            EBR=AUX2(XI,YC,PEBR,.TRUE.)
            CALL DERIV(Y(1,1),XI,YC,EXDT,DUDY,3)
            CALL DERIV(Y(1,2),XI,YC,DVDX,DVDY,3)
            GAMDT=DUDY+DVDX
            EBRDT=2.D0/3.D0*DSQRT(3.D0*EXDT**2+.75D0*GAMDT**2)
            CALL DERIV(PEBR,XI,YC,DEBRDX,DUM,1)
            CALL DERIV2(Y(1,1),XI,YC,DUDXY,3)
            CALL DERIV2(Y(1,2),XI,YC,DVDXX,1)
            DGAMDX=DUDXY+DVDXX
            CALL DERIV2(Y(1,1),XI,YC,DEXDX,1)
            DEBRDT=(4.D0*EXDT*DEXDX+GAMDT*DGAMDX)/(3.D0*EBRDT)
            DF1=C1*EBR**C2/(3.D0*EBRDT)*(C2*DEBRDX*GAMDT/EBR
           1 +DGAMDX - DEBRDT*GAMDT/EBRDT)
            U=AUX2(XI,YC,Y(1,1),.FALSE.)
            V=AUX2(XI,YC,Y(1,2),.FALSE.)
            VOLD=AUX2(XI,YC,YOLD(1,2),.FALSE.)
                        FACT=RHO*((V-VOLD)/DT)
            DF1=DF1+FACT
            RETURN
            END
```

```
      FUNCTION DF2(X)
      IMPLICIT REAL*8(A-H,O-Z)
      COMMON XX(15),XI,YI,C1,C2,CA,Y(400,2),PEBR(20,20)
      COMMON/C1/RHO,YOLD(15,2),DT
      REAL*8 LAMBDA
C
C                THE INTEGRAND DTAU/DY IS EVALUATED
C
      EBR=AUX2(X,CA,PEBR,.TRUE.)
      CALL DERIV(Y(1,1),X,CA,EXDT,DUDY,3)
      CALL DERIV(Y(1,2),X,CA,DVDX,EYDT,3)
      GAMDT=DUDY+DVDX
      EBRDT=2.D0/3.D0*DSQRT(3.D0*EXDT**2+.75D0*GAMDT**2)
      CALL DERIV(PEBR,X,CA,DUM,DEBRDY,2)
      CALL DERIV2(Y(1,1),X,CA,DUDYY,2)
      CALL DERIV2(Y(1,2),X,CA,DVDXY,3)
      DGAMDY=DUDYY+DVDXY
      CALL DERIV2(Y(1,1),X,CA,DEXDY,3)
      YEBRDT=(4.D0*EXDT*DEXDY+GAMDT*DGAMDY)/(3.D0*EBRDT)
      CALL DERIV2(Y(1,1),X,CA,DEXDX,1)
      CALL DERIV2(Y(1,2),X,CA,DEYDX,3)
      LAMBDA=(2.D0*C1*EBR**C2)/(3.D0*EBRDT)
      CALL DERIV(PEBR,X,CA,DEBRDX,DUM,1)
      CALL DERIV2(Y(1,2),X,CA,DVDXX,1)
      DGAMDX=DEXDY+DVDXX
      DEBRDT=(4.D0*EXDT*DEXDX+GAMDT*DGAMDX)/(3.D0*EBRDT)
      DF2=LAMBDA*(((EYDT-EXDT)*(-C2*DEBRDX/EBR
     1 +DEBRDT/EBRDT)+DEXDX-DEYDX)
     1 +.5D0*(C2*DEBRDY*GAMDT/EBR + DGAMDY - YEBRDT*GAMDT/E
BRDT))
      U=AUX2(X,CA,Y(1,1),.FALSE.)
      V=AUX2(X,CA,Y(1,2),.FALSE.)
      UOLD=AUX2(X,CA,YOLD(1,1),.FALSE.)
                 FACT=RHO*((U-UOLD)/DT)
      DF2=DF2 + FACT
      RETURN
      END
      SUBROUTINE DERIV(A,X,Y,DUDX,DUDY,N)
C
C                EVALUATE DERIV WRT X AND Y
C                IF N=1 DUDX, IF N=2 DUDY, OTHERWISE DUDX AN
D DUDY
C
      IMPLICIT REAL*8(A-H,O-Z)
      COMMON XX(15)
      DIMENSION A(1)
      IF (N .EQ. 2) GO TO 10
      DUDX=A(2)+2.D0*A(3)*X + 3.D0*A(4)*XX(3) + 4.D0*A(5)*X
X(4)
     1 +A(10)*Y+A(11)*XX(7) + A(12)*XX(8) + 2.D0*A(13)*XX(1
0)
     1 +2.D0*A(14)*XX(11) + 3.D0*A(15)*XX(13)
      IF (N.EQ.1) RETURN
10    DUDY=A(6) + 2.D0*A(7)*Y +3.D0*A(8)*XX(7) + 4.D0*A(9)*
XX(8)
     1 +A(10)*X + 2.D0*A(11)*XX(10) +3.D0*A(12)*XX(11)
     1 + A(13)*XX(3) +2.D0*A(14)*XX(13) + A(15)*XX(4)
      RETURN
```

```
              END
              SUBROUTINE DERIV2(A,X,Y,DUDD,N)
              IMPLICIT REAL*8(A-H,O-Z)
        C
        C               EVALUATE 2ND ORDER DERIV WRT X AND Y
        C               N=1 DXDX; N=2 DYDY; N=3 DXDY
        C
              DIMENSION A(1)
              GO TO (10,20,30),N
        10    DUDD=2.D0*A(3) + 6.D0*A(4)*X + 12.D0*A(5)*X*X
             1 +2.D0*A(13)*Y +2.D0*A(14)*Y*Y + 6.D0*A(15)*X*Y
              RETURN
        20     DUDD=2.D0*A(7) + 6.D0*A(8)*Y + 12.D0*A(9)*Y*Y +
             1 2.D0*A(11)*X + 6.D0*A(12)*X*Y + 2.D0*A(14)*X*X
              RETURN
        30    DUDD=A(10) + 2.D0*A(11)*Y + 3.D0*A(12)*Y*Y
             1 + 2.D0*A(13)*X + 4.D0*A(14)*X*Y + 3.D0*A(15)*X*X
              RETURN
              END
              SUBROUTINE FILL(XYT,IX,IY,ISUB,XY,NIX,NIY,IMY,NTM,IDI
        M,IDIMP)
              IMPLICIT REAL*8(A-H,O-Z)
              DIMENSION XYT(2,IDIM,IDIM,2),ISUB(IDIMP,1),XY(2,IDIMP
        ,1)
        C
        C               ISUB CONTAINS 1 WHERE A FUNCTION VALUE IS
        C               PLOTTED, 0 IF OUTSIDE BOUNDARY
        C
              DO 10 I=1,NIX
              DO 10 J=1,NIY
        10    ISUB(I,J)=1
              XMIN=XYT(1,IMY,IX,NTM)
              DO 15 I=1,IY
              IF (XYT(1,I,IX,NTM).GT.XMIN) GO TO 15
              XMIN=XYT(1,I,IX,NTM)
              IMYMIN=I
        15    CONTINUE
              DO 110 J=1,NIY
              DO 100 I=1,NIX
              IF (XY(1,I,J).LT.XYT(1,IMYMIN,IX,NTM)) GO TO 100
              IF (XY(1,I,J).GT.XYT(1,IMY,IX,NTM)) GO TO 80
              LB=1
              NB=2
        20    IF(XY(2,I,J).LT.XYT(2,NB,IX,NTM)) GO TO 30
              LB=LB+1
              NB=NB+1
              IF (NB.LT.IY) GO TO 20
        30    IF(XY(1,I,J).LT.XYT(1,LB,IX,NTM).AND.
             1  XY(1,I,J).LT.XYT(1,NB,IX,NTM)) GO TO 100
              IF (XY(1,I,J).GT.XYT(1,LB,IX,NTM).AND.
             1  XY(1,I,J).GT.XYT(1,NB,IX,NTM)) GO TO 80
              YN=XYT(2,LB,IX,NTM)+(XYT(2,NB,IX,NTM)-XYT(2,LB,IX,NTM
        ))
             1 /(XYT(1,NB,IX,NTM)-XYT(1,LB,IX,NTM))*
             1 (XY(1,I,J)-XYT(1,LB,IX,NTM))
              IF (YN.GT.XY(2,I,J).AND.XYT(1,LB,IX,NTM).GE.
             1  XYT(1,NB,IX,NTM)) GO TO 100
              IF (YN.LT.XY(2,I,J).AND. XYT(1,LB,IX,NTM).LE.
```

```
             1  XYT(1,NB,IX,NTM)) GO TO 100
      80     DO 90 II=I,NIX
      90     ISUB(II,J)=0
             GO TO 110
     100     CONTINUE
     110     CONTINUE
             RETURN
             END
```

PROGRAM FOR TWO DIMENSIONAL PLOT


```
                IMPLICIT REAL*8(A-H,O-Z)
                COMMON XX(15),XI,YI,CC,CN,CA,Y(400,2),EBR(400,20)
                COMMON/C1/RHO,YOLD(15,2),DT
                DIMENSION XYT(2,20,20,2),U(20,20),V(20,20),XY(2,80,80
      )
                DIMENSION X(15,400),ERROR(2),ISUB(80,80)
                REAL*4 Z1(90,90),Z2(90,90),TAUXY(80,80)
                LOGICAL REFINE
                DIMENSION EBRDT(80,80),EXDT(80,80),EYDT(80,80)
               1,GAMDT(80,80),LANDA(80,80)
                REAL*8 DEBR(80,80)
                REAL*8 XLS(10,800)
                REAL*8 LANDA
                   DIMENSION AINT2(80)
      C
      C                   IX=NO PTS IN X
      C                   IY=NO PTS IN Y
      C                   IT=NO OF TIME STEPS
      C                   DT=TIME INTERVAL BETWEEN TIME STEPS
      C                   CC,CN ARE CONSTANTS WHERE SIGB=CC*EB**CN
      C                   CA IS LOWER INTERVAL OF INTEGRATION FOR SIG
      Y
      C                   SIGYOA IS CONSTANT ADDED TO SIGY
      C                   XYT(L,I,J,K) CONTAINS: L=1 X-COORD: L=2 Y-C
      OORD
      C                      FOR I=1,IY J=1,IX L=1,2
      C
                READ(5,10) IX,IY,IT
      10        FORMAT(3I2)
                READ(5,20) DT
      20        FORMAT(8F10.0)
                READ(5,20) CC,CN,CA,SIGYOA,CB
      C
      C              NIX CONTAINS # GRID PTS IN X DIRECTION, NIY IN Y
      DIRECTION FOR PLOTS
      C
                READ(5,10) NIX,NIY
                READ(5,20) RHO
      C
      C                   X & Y COORD READ FOR TIME=0
      C
                READ(4,30) (((XYT(K,I,J,1),K=1,2),I=1,IY),J=1,IX)
                DO 25 II=1,IX
                DO 25 IJ=1,IY
                IF (II.EQ.1) XYT(1,IJ,II,1)=0.D0
                IF(IJ.EQ.1) XYT(2,IJ,II,1)=0.D0
                DO 25 IK=1,2
                IF (XYT(IK,IJ,II,1).LT.0.D0) XYT(IK,IJ,II,1)=0.D0
      25        CONTINUE
      30        FORMAT(5X,2F6.3,1X,2F6.3,1X,2F6.3,1X,2F6.3,1X,2F6.3)
                CALL PLOTIT (XYT(1,1,1,1),IX,IY)
                LTM=2
                NTM=1
                IDIM=20
                IDIMP=80
                IXY=IX*IY
      C
      C                   INITIALIZE EBR TO ZERO
```

```
          DO 40 I=1,20
          DO 40 J=1,400
          EBR(J,I)=0.D0
   40     CONTINUE
          FACT=1.D0
C
C                    FOR EACH TIME STEP EBR IS ACCUMULATED
          IT1=IT-1
          DO 80 K=1,IT1
C
C                    X&Y COORD ARE READ FOR NEXT TIME STEP
C
          NTM=3-NTM
          LTM=3-LTM
          READ(4,30) (((XYT(KK,I,J,NTM),KK=1,2),I=1,IY),J=1,IX)
          DO 45 I=1,IX
          DO 45 J=1,IY
          IF (I.EQ.1) XYT(1,J,I,NTM)=0.D0
          IF (J.EQ.1) XYT(2,J,I,NTM)=0.D0
          DO 45 IK=1,2
          IF (XYT(IK,J,I,NTM).LT.0.) XYT(IK,J,I,NTM)=0.D0
   45     CONTINUE
          CALL PLOTIT (XYT(1,1,1,NTM),IX,IY)
C
C                    U,V CALCULATED FOR THIS TIME STEP
C                    U MUST BE >0, V MUST BE <0
C
          DO 50 J=1,IX
          DO 50 I=1,IY
          U(I,J)=-(XYT(1,I,J,NTM)-XYT(1,I,J,LTM))/DT
          V(I,J)=-(XYT(2,I,J,NTM)-XYT(2,I,J,LTM))/DT
          IF (U(I,J).GT.0.D0) U(I,J)=0.D0
          IF (V(I,J).LT.0.D0) V(I,J)=0.D0
   50     CONTINUE
C
C                    CURVE FITTING FOR U AND V USING DLSQHS
C                    SET UP INDEPENDENT VARIABLES IN X
C                    DEPENDENT VARIABLES IN Y
C
          DO 60 J=1,IX
          IL=IY*(J-1)
          DO 60 I=1,IY
          L=I+IL
          CALL AUX(XYT(1,I,J,NTM),XYT(2,I,J,NTM),X(1,L))
          XLS(1,L)=-X(2,L)
          XLS(2,L)=-2.D0*X(10,L)
          XLS(3,L)=-3.D0*X(11,L)
          XLS(4,L)=-4.D0*X(12,L)
          XLS(5,L)=-.5D0*X(3,L)
          XLS(6,L)=-X(13,L)
          XLS(7,L)=-1.5D0*X(14,L)
          XLS(8,L)=-1.D0/3.D0*X(4,L)
          XLS(9,L)=-2.D0/3.D0*X(15,L)
          XLS(10,L)=-.25D0*X(5,L)
          DO 55 IK=1,10
   55     XLS(IK,IXY+L)=X(IK+5,L)
          Y(L,1)=U(I,J)
   60     Y(IXY+L,1)=V(I,J)
```

```
        CALL DLSQHS(Y,XLS,2*IXY,10,1,800,10,ERROR,.FALSE.,IER
     ,&200)
        DO 62 IK=1,5
 62     Y(IK,2)=0.D0
        DO 63 IK=6,15
 63     Y(IK,2)=Y(IK-5,1)
        Y(1,1)=0.D0
        Y(2,1)=-Y(6,2)
        Y(3,1)=-.5D0*Y(10,2)
        Y(4,1)=-1.D0/3.D0*Y(13,2)
        Y(5,1)=-.25D0*Y(15,2)
        DO 64 IK=6,9
 64     Y(IK,1)=0.D0
        Y(10,1)=-2.D0*Y(7,2)
        Y(11,1)=-3.D0*Y(8,2)
        Y(12,1)=-4.D0*Y(9,2)
        Y(13,1)=-Y(11,2)
        Y(14,1)=-1.5D0*Y(12,2)
        Y(15,1)=-2.D0/3.D0*Y(14,2)
 C
 C           U&V COEFF SAVED FOR DU/DT,DV/DT
 C
        IF (K.NE.(IT1-1)) GO TO 410
        DO 400 I=1,15
        DO 400 J=1,2
 400    YOLD(I,J)=Y(I,J)
 410    CONTINUE
 C
 C                THE VALUES OF EDTX,EDTY,GAMXY,EBRDT,AND EBR
  ARE CALCULATED
 C                   AT EACH TIME STEP
 C
        DO 70 J=1,IX
        IL=IY*(J-1)
        DO 70 I=1,IY
        IJ=I+IL
        CALL AUX(XYT(1,I,J,NTM),XYT(2,I,J,NTM),XX)
        CALL DERIV(Y(1,1),XYT(1,I,J,NTM),XYT(2,I,J,NTM),DUDX,
     DUDY,3)
        CALL DERIV(Y(1,2),XYT(1,I,J,NTM),XYT(2,I,J,NTM),DVDX,
     DVDY,1)
        GAMXY=DUDY+DVDX
        DFACT=(DUDX**2)/3.D0+(GAMXY)**2/12.D0
 65     EBRDT(I,J)=2.D0*DSQRT(DFACT)
        IF (K.EQ.IT1) FACT=.5D0
        EBR(IJ,1)=EBR(IJ,1)+FACT*DT*EBRDT(I,J)
 70     CONTINUE
 80     CONTINUE
 C
 C                4TH DEGREE POLY FIT TO EBR
 C
        CALL DLSQHS(EBR,X,IX*IY,15,2,400,15,ERROR,.FALSE.,IER
     ,&200)
 C
 C      MASTER GRID IS SET FOR FINAL PLOTS
 C
 C                XY(2,I,J) CONTAINS THE MASTER GRID ST XY(1,
     I,J) IS
```

```
C                 THE X-COORD, XY(2,I,J) IS THE Y-COORD FOR
I=1,IX J=1,IY
          XMAX=0.D0
          DO 90 I=1,IY
          IF (XYT(1,I,IX,NTM).LT.XMAX) GO TO 90
          XMAX=XYT(1,I,IX,NTM)
          IMY=I
90        CONTINUE
          YMAX=XYT(2,IY,IX,NTM)
100       CONTINUE
          DY=YMAX/(NIY-1)
          DO 110 I=1,NIX
          XY(2,I,1)=0.D0
          DO 110 J=2,NIY
          XY(2,I,J)=XY(2,I,J-1)+DY
110       CONTINUE
          DX=XMAX/(NIX-1)
          DO 120 I=1,NIY
          XY(1,1,I)=0.D0
          DO 120 J=2,NIX
          XY(1,J,I)=XY(1,J-1,I)+DX
120       CONTINUE
C
C                 TO FIND ZERO FILLS ON PLOTS
C
          CALL FILL(XYT,IX,IY,ISUB,XY,NIX,NIY,IMY,NTM,IDIM,IDIM
P)
C
C                 TO PLOT U,V,EBRDT, AND TAUXY
C
          DO 125 J=1,NIY
          DO 125 I=1,NIX
          EBRDT(I,J)=0.D0
          DEBR(I,J)=0.D0
125       TAUXY(I,J)=0.D0
          NIY10=NIY+10
          NIX10=NIX+10
          DO 126 J=1,NIY10
          DO 126 I=1,NIX10
          Z1(I,J)=0.D0
126       Z2(I,J)=0.D0
          DO 130 J=1,NIY
          DO 135 I=1,NIX
          IF (ISUB(I,J).EQ.0) GO TO 130
          Z1(I+5,J+5)=-AUX2(XY(1,I,J),XY(2,I,J),Y(1,1),.TRUE.)
          Z2(I+5,J+5)=AUX2(XY(1,I,J),XY(2,I,J),Y(1,2),.FALSE.)
          CALL DERIV(Y,XY(1,I,J),XY(2,I,J),EXDT(I,J),GAMDT(I,J)
,3)
          CALL DERIV(Y(1,2),XY(1,I,J),XY(2,I,J),EBRDT(I,J),EYDT
(I,J),3)
          GAMDT(I,J)=GAMDT(I,J)+EBRDT(I,J)
          DFACT=(3.D0*EXDT(I,J)**2+.75D0*GAMDT(I,J)**2)
131       EBRDT(I,J)=2.D0/3.D0*DSQRT(DFACT)
          DEBR(I,J)=AUX2(XY(1,I,J),XY(2,I,J),EBR,.FALSE.)
          LANDA(I,J)=1.5D0*EBRDT(I,J)/(CC*DEBR(I,J)**CN)
          TAUXY(I,J)=GAMDT(I,J)/(2.D0*LANDA(I,J))
135       CONTINUE
130       CONTINUE
```

```
C
C                           PLOT U,V,EBRDT,TAUXY
C
              CALL PLOT2(TAUXY,XY,IX,IY,ISUB,NIX,NIY)
              CALL PLOT(12.,0.,-3)
              DXY=XY(2,NIX,NIY)/XY(1,NIX,NIY)
C             CALL PERS(Z1,IDIMP+10,NIX+10,NIY+10,DXY,.333,45.,45.,
         10.,10.)
C             CALL PLOT(12.,0.,-3)
C             CALL PERS(Z2,IDIMP+10,NIX+10,NIY+10,DXY,.333,45.,45.,
         10.,10.)
C             CALL PLOT(12.,0.,-3)
              DO 137 J=1,NIY10
              DO 137 I=1,NIX10
              Z1(I,J)=0.
     137      Z2(I,J)=0.
              DO 138 J=1,NIY
              DO 138 I=1,NIX
     138      Z1(I+5,J+5)=DEBR(I,J)
C             CALL PERS(Z1,IDIMP+10,NIX+10,NIY+10,DXY,.333,45.,45.,
         10.,10.)
C             CALL PLOT(12.,0.,-3)
              DO 139 J=1,NIY10
              DO 139 I=1,NIX10
     139      Z1(I,J)=0.
              DO 140 J=1,NIY
              DO 140 I=1,NIX
              Z1(I+5,J+5)=EBRDT(I,J)
     140      Z2(I+5,J+5)=-TAUXY(I,J)
C             CALL PERS(Z1,IDIMP+10,NIX+10,NIY+10,DXY,.333,45.,45.,
         10.,10.)
C             CALL PLOT(12.,0.,-3)
C             CALL PERS(Z2,IDIMP+10,NIX+10,NIY+10,DXY,.333,45.,45.,
         10.,10.)
C             CALL PLOT(12.,0.,-3)
C
C                           CALC SIGY
C
              EXTERNAL DF1,DF2
              DO 141 J=1,NIY10
              DO 141 I=1,NIX10
              Z1(I,J)=0.
     141      Z2(I,J)=0.
                 DGRID=(XY(2,1,2)-XY(2,1,1))/2
                 JGRID=1
     1000        IF(CA.GT.XY(2,1,JGRID)+DGRID) GO TO 1010
                 GO TO 1018
     1010        JGRID=JGRID+1
                 IF (JGRID.EQ.NIY) GO TO 1018
                 GO TO 1000
     1018     IGRID=1
     1015     IF (ISUB(IGRID+1,JGRID).EQ.0) GO TO 1020
              IGRID=IGRID+1
              IF (IGRID.EQ.NIX) GO TO 1020
              GO TO 1015
     1020     DO 1030 I=1,NIX
              XI=XY(1,I,1)
              IF (XI.LE.CB) GO TO 1025
```

```
      IF (XI .GT. CB .AND. ISUB(I,JGRID) .NE. 0) GO TO 1025
      XI=XY(1,IGRID,JGRID)
1025  IF (XI .EQ. CB) GO TO 1027
      AINT2(I)=DQUANK(DF2,CB,XI,.001D0,TOL,FIFTH)
      GO TO 1030
1027  AINT2(I)=0.D0
1030  CONTINUE
      DO 150 J=1,NIY
      DO 150 I=1,NIX
      IF (ISUB(I,J).EQ.0) GO TO 150
      XI=XY(1,I,J)
      YI=XY(2,I,J)
      AINT1=0.D0
      IF (JGRID .EQ. J) GO TO 1060
      JADD=0
      IF (ISUB(I,JGRID).EQ.1) GO TO 1050
      JINC=1
      IF (JGRID.GT.J) JINC=-1
1040  JADD=JADD+JINC
      IF (JGRID+JADD.EQ.J) GO TO 1060
      IF (ISUB(I,JGRID+JADD).EQ.1) GO TO 1050
      GO TO 1040
1050  AINT1=DQUANK(DF1,XY(2,I,JGRID+JADD),XY(2,I,J),.001D0,
TOL,FIFTH)
1060  Z1(I+5,J+5)=SIGYOA-AINT1-AINT2(I)
      TAUXY(I,J)=Z1(I+5,J+5)
      Z2(I+5,J+5)=Z1(I+5,J+5)+(EXDT(I,J)-EYDT(I,J))/LANDA(I
,J)
150   CONTINUE
      CALL PLOT2(TAUXY,XY,IX,IY,ISUB,NIX,NIY)
      CALL PLOTND
      STOP
      CALL PERS(Z1,IDIMP+10,NIX+10,NIY+10,DXY,.333,45.,45.,
10.,10.)
      CALL PLOT(12.,0.,-3)
      CALL PERS(Z2,IDIMP+10,NIX+10,NIY+10,DXY,.333,45.,45.,
10.,10.)
      CALL PLOTND
      STOP
200   STOP 1
      END
      SUBROUTINE AUX(X,Y,XX)
      IMPLICIT REAL*8(A-H,O-Z)
      DIMENSION XX(15)
      XX(1)=1.D0
      XX(2)=X
      XX(3)=X*X
      XX(4)=X*XX(3)
      XX(5)=X*XX(4)
      XX(6)=Y
      XX(7)=Y*Y
      XX(8)=Y*XX(7)
      XX(9)=Y*XX(8)
      XX(10)=X*Y
      XX(11)=XX(10)*Y
      XX(12)=XX(11)*Y
      XX(13)=XX(10)*X
      XX(14)=XX(13)*Y
```

```
            XX(15)=XX(13)*X
            RETURN
            END
            FUNCTION AUX2(XX,YY,P,LL)
            IMPLICIT REAL*8(A-H,O-Z)
      C
      C               EVALUATE THE FITTED FUNCTION AT XX,YY
      C               P CONTAINS THE FITTED PARAMETERS
      C               LL IS TRUE IF THE INDEPENDENT VARIABLE MUST
       BE EVALUATED BY AUX
      C
            LOGICAL LL
            COMMON X
            DIMENSION X(15),P(1)
            IF (LL) CALL AUX(XX,YY,X(1))
            AUX2=0.D0
            DO 10 I=1,15
            AUX2=AUX2+P(I)*X(I)
       10   CONTINUE
            RETURN
            END
            FUNCTION DF1(YC)
            IMPLICIT REAL*8(A-H,O-Z)
            COMMON XX(15),XI,YI,C1,C2,CA,Y(400,2),PEBR(20,20)
            COMMON/C1/RHO,YOLD(15,2),DT
      C
      C               THE INTEGRAND DTAU/DX IS EVALUATED
      C
            EBR=AUX2(XI,YC,PEBR,.TRUE.)
            CALL DERIV(Y(1,1),XI,YC,EXDT,DUDY,3)
            CALL DERIV(Y(1,2),XI,YC,DVDX,DVDY,3)
            GAMDT=DUDY+DVDX
            EBRDT=2.D0/3.D0*DSQRT(3.D0*EXDT**2+.75D0*GAMDT**2)
            CALL DERIV(PEBR,XI,YC,DEBRDX,DUM,1)
            CALL DERIV2(Y(1,1),XI,YC,DUDXY,3)
            CALL DERIV2(Y(1,2),XI,YC,DVDXX,1)
            DGAMDX=DUDXY+DVDXX
            CALL DERIV2(Y(1,1),XI,YC,DEXDX,1)
            DEBRDT=(4.D0*EXDT*DEXDX+GAMDT*DGAMDX)/(3.D0*EBRDT)
            DF1=C1*EBR**C2/(3.D0*EBRDT)*(C2*DEBRDX*GAMDT/EBR
           1 +DGAMDX - DEBRDT*GAMDT/EBRDT)
            U=AUX2(XI,YC,Y(1,1),.FALSE.)
            V=AUX2(XI,YC,Y(1,2),.FALSE.)
            VOLD=AUX2(XI,YC,YOLD(1,2),.FALSE.)
            FACT=RHO*(V-VOLD)/DT
            DF1=DF1+FACT
            RETURN
            END
            FUNCTION DF2(X)
            IMPLICIT REAL*8(A-H,O-Z)
            COMMON XX(15),XI,YI,C1,C2,CA,Y(400,2),PEBR(20,20)
            COMMON/C1/RHO,YOLD(15,2),DT
            REAL*8 LAMBDA
      C
      C               THE INTEGRAND DTAU/DY IS EVALUATED
      C
            EBR=AUX2(X,CA,PEBR,.TRUE.)
            CALL DERIV(Y(1,1),X,CA,EXDT,DUDY,3)
```

```
      CALL DERIV(Y(1,2),X,CA,DVDX,EYDT,3)
      GAMDT=DUDY+DVDX
      EBRDT=2.D0/3.D0*DSQRT(3.D0*EXDT**2+.75D0*GAMDT**2)
      CALL DERIV(PEBR,X,CA,DUM,DEBRDY,2)
      CALL DERIV2(Y(1,1),X,CA,DUDYY,2)
      CALL DERIV2(Y(1,2),X,CA,DVDXY,3)
      DGAMDY=DUDYY+DVDXY
      CALL DERIV2(Y(1,1),X,CA,DEXDY,3)
      YEBRDT=(4.D0*EXDT*DEXDY+GAMDT*DGAMDY)/(3.D0*EBRDT)
      CALL DERIV2(Y(1,1),X,CA,DEXDX,1)
      CALL DERIV2(Y(1,2),X,CA,DEYDX,3)
      LAMBDA=(2.D0*C1*EBR**C2)/(3.D0*EBRDT)
      CALL DERIV(PEBR,X,CA,DEBRDX,DUM,1)
      CALL DERIV2(Y(1,2),X,CA,DVDXX,1)
      DGAMDX=DEXDY+DVDXX
      DEBRDT=(4.D0*EXDT*DEXDX+GAMDT*DGAMDX)/(3.D0*EBRDT)
      DF2=LAMBDA*(((EYDT-EXDT)*(-C2*DEBRDX/EBR
     1 +DEBRDT/EBRDT)+DEXDX-DEYDX)
     1 +.5D0*(C2*DEBRDY*GAMDT/EBR + DGAMDY - YEBRDT*GAMDT/E
BRDT))
      U=AUX2(X,CA,Y(1,1),.FALSE.)
      V=AUX2(X,CA,Y(1,2),.FALSE.)
      UOLD=AUX2(X,CA,YOLD(1,1),.FALSE.)
      FACT=RHO*((U-UOLD)/DT
      DF2=DF2 + FACT
      RETURN
      END
      SUBROUTINE DERIV(A,X,Y,DUDX,DUDY,N)
C
C                  EVALUATE DERIV WRT X AND Y
C                  IF N=1 DUDX, IF N=2 DUDY, OTHERWISE DUDX AN
D DUDY
C
      IMPLICIT REAL*8(A-H,O-Z)
      COMMON XX(15)
      DIMENSION A(1)
      IF (N .EQ. 2) GO TO 10
      DUDX=A(2)+2.D0*A(3)*X + 3.D0*A(4)*XX(3) + 4.D0*A(5)*X
X(4)
     1 +A(10)*Y+A(11)*XX(7) + A(12)*XX(8) + 2.D0*A(13)*XX(1
0)
     1 +2.D0*A(14)*XX(11) + 3.D0*A(15)*XX(13)
      IF (N.EQ.1) RETURN
10    DUDY=A(6) + 2.D0*A(7)*Y +3.D0*A(8)*XX(7) + 4.D0*A(9)*
XX(8)
     1 +A(10)*X + 2.D0*A(11)*XX(10) +3.D0*A(12)*XX(11)
     1 + A(13)*XX(3) +2.D0*A(14)*XX(13) + A(15)*XX(4)
      RETURN
      END
      SUBROUTINE DERIV2(A,X,Y,DUDD,N)
      IMPLICIT REAL*8(A-H,O-Z)
C
C                  EVALUATE 2ND ORDER DERIV WRT X AND Y
C                  N=1 DXDX; N=2 DYDY; N=3 DXDY
C
      DIMENSION A(1)
      GO TO (10,20,30),N
10    DUDD=2.D0*A(3) + 6.D0*A(4)*X + 12.D0*A(5)*X*X
```

```
          1 +2.D0*A(13)*Y +2.D0*A(14)*Y*Y + 6.D0*A(15)*X*Y
            RETURN
   20        DUDD=2.D0*A(7) + 6.D0*A(8)*Y + 12.D0*A(9)*Y*Y +
          1 2.D0*A(11)*X + 6.D0*A(12)*X*Y + 2.D0*A(14)*X*X
            RETURN
   30       DUDD=A(10) + 2.D0*A(11)*Y + 3.D0*A(12)*Y*Y
          1 + 2.D0*A(13)*X + 4.D0*A(14)*X*Y + 3.D0*A(15)*X*X
            RETURN
            END
            SUBROUTINE FILL(XYT,IX,IY,ISUB,XY,NIX,NIY,IMY,NTM,IDI
  M,IDIMP)
            IMPLICIT REAL*8(A-H,O-Z)
            DIMENSION XYT(2,IDIM,IDIM,2),ISUB(IDIMP,1),XY(2,IDIMP
  ,1)
  C
  C                 ISUB CONTAINS 1 WHERE A FUNCTION VALUE IS
  C                 PLOTTED, 0 IF OUTSIDE BOUNDARY
  C
            DO 10 I=1,NIX
            DO 10 J=1,NIY
   10       ISUB(I,J)=1
            XMIN=XYT(1,IMY,IX,NTM)
            DO 15 I=1,IY
            IF (XYT(1,I,IX,NTM).GT.XMIN) GO TO 15
            XMIN=XYT(1,I,IX,NTM)
            IMYMIN=I
   15       CONTINUE
            DO 110 J=1,NIY
            DO 100 I=1,NIX
            IF (XY(1,I,J).LT.XYT(1,IMYMIN,IX,NTM)) GO TO 100
            IF (XY(1,I,J).GT.XYT(1,IMY,IX,NTM)) GO TO 80
            LB=1
            NB=2
   20       IF(XY(2,I,J).LT.XYT(2,NB,IX,NTM)) GO TO 30
            LB=LB+1
            NB=NB+1
            IF (NB.LT.IY) GO TO 20
   30       IF(XY(1,I,J).LT.XYT(1,LB,IX,NTM).AND.
          1  XY(1,I,J).LT.XYT(1,NB,IX,NTM)) GO TO 100
            IF (XY(1,I,J).GT.XYT(1,LB,IX,NTM).AND.
          1  XY(1,I,J).GT.XYT(1,NB,IX,NTM)) GO TO 80
            YN=XYT(2,LB,IX,NTM)+(XYT(2,NB,IX,NTM)-XYT(2,LB,IX,NTM
  ))
          1 /(XYT(1,NB,IX,NTM)-XYT(1,LB,IX,NTM))*
          1 (XY(1,I,J)-XYT(1,LB,IX,NTM))
            IF (YN.GT.XY(2,I,J).AND.XYT(1,LB,IX,NTM).GE.
          1  XYT(1,NB,IX,NTM)) GO TO 100
            IF (YN.LT.XY(2,I,J).AND. XYT(1,LB,IX,NTM).LE.
          1  XYT(1,NB,IX,NTM)) GO TO 100
   80       DO 90 II=I,NIX
   90       ISUB(II,J)=0
            GO TO 110
  100       CONTINUE
  110       CONTINUE
            RETURN
            END
            SUBROUTINE PLOTIT(XYT,IX,IY)
            IMPLICIT REAL*8(A-H,O-Z)
```

```
      DIMENSION XYT(2,20,20)
      CALL AXIS(0.,0.,'X',-1,10.,0.,0.,.2)
      CALL AXIS(0.,0.,'Y',1,10.,90.,0.,.2)
      DO 10 J=1,IY
      CALL PLOT(XYT(1,J,1)*5.,XYT(2,J,1)*5.,3)
      CALL SYMBOL(XYT(1,J,1)*5.,XYT(2,J,1)*5.,.14,4,0.,-1)
      DO 10 I=2,IX
      CALL PLOT(XYT(1,J,I)*5.,XYT(2,J,I)*5.,2)
      CALL SYMBOL(XYT(1,J,I)*5.,XYT(2,J,I)*5.,.14,4,0.,-1)
10    CONTINUE
      DO 20 J=1,IX
      CALL PLOT(XYT(1,1,J)*5.,XYT(2,1,J)*5.,3)
      DO 20 I=1,IY
      CALL PLOT(XYT(1,I,J)*5.,XYT(2,I,J)*5.,2)
20    CONTINUE
      CALL PLOT(12.,0.,-3)
      RETURN
      END
      SUBROUTINE PLOT2(TXY,XY,IX,IY,ISUB,NIX,NIY)
      REAL*8 XY(2,80,80)
      DIMENSION TXY(80,80),ISUB(80,80),TAUXY(80,80),X(80)
      DO 5 I=1,80
      DO 5 J=1,80
5     TAUXY(I,J)=0.D0
      DO 10 I=1,NIX
      DO 10 J=1,NIY
10    TAUXY(I,J)=TXY(I,J)
      CALL SCALE(TAUXY,6400,10.,YMIN,DY,1)
      CALL AXIS(0.,10.,'X',1,10.,0.,0.,.2)
      CALL AXIS(0.,0.,'      ',5,10.,90.,YMIN,DY)
      NY=NIY/IY*3
      KK=0
      DO 50 J=1,NIY,NY
      L=NIX
15    IF(ISUB(L,J).EQ.1) GO TO 20
      L=L-1
      GO TO 15
20    DO 30 I=1,L
30    X(I)=XY(1,I,J)*5.
      CALL LINE(X,TAUXY(1,J),L,1)
      NX=NIX/IX
      KK=KK+1
      DO 40 K=1,L,NX
      CALL SYMBOL(X(K),TAUXY(K,J),.14,KK,0.,-1)
40    CONTINUE
50    CONTINUE
      END
```